

Dissertation zur Erlangung des Doktorgrades  
der Fakultät für Biologie  
der Ludwig-Maximilians-Universität München

# **Screening anti-prion compounds and diagnosing prion diseases by amplifying PrP<sup>Sc</sup> *in vitro***



**Shi, Song**

from

Chongqing, P. R. China

October, 2014



Diese Dissertation wurde angefertigt  
unter der Leitung von Prof. Thomas Cremer  
am Institut für Neuropathologie und Prionforschung  
an der Ludwig-Maximilians-Universität München

Erstgutachter:	Prof. Thomas Cremer
Zweitgutachter:	Prof. Ruth Brack-Werner

Tag der Abgabe:	09.10.2014
-----------------	------------

Tag der mündlichen Prüfung:	24.02.2015
-----------------------------	------------



## **Eidesstattliche Erklärung**

Ich versichere hiermit an Eides statt, dass die vorgelegte Dissertation von mir selbständig und ohne unerlaubte Hilfe angefertigt wurde. Die aus anderen Quellen direkt oder indirekt übernommenen Daten und Konzepte sind unter Angaben der entsprechenden Literatur gekennzeichnet.

Die vorliegende Dissertation wurde weder in gleicher noch in ähnlicher Form einer anderen Prüfungsbehörde vorgelegt.

München, den 01.10.2014

## **Affidavit**

I hereby declare that the submitted dissertation was made by me independently and without unauthorized assistance. The either sources directly or indirectly acquired data and concepts are identified by quoting the relevant literatures.

This dissertation was presented neither in the same nor in a similar form of test elsewhere.

München, den 01.10.2014



# Contents

<b>1</b>	<b>Summary.....</b>	<b>1</b>
<b>2</b>	<b>Introduction.....</b>	<b>3</b>
2.1	Prion diseases and prion propagation <i>in vivo</i> .....	3
2.2	Cell-free conversion models of prions <i>in vitro</i> .....	5
2.2.1	Necessity of establishing prion propagation model <i>in vitro</i> .....	5
2.2.2	Protein misfolding cyclic amplification (PMCA).....	5
2.2.3	Real-time quaking-induced conversion (RT-QulC).....	10
2.2.4	Quantitative RT-QulC (qRT-QulC).....	12
2.3	Development of anti-prion compound anle138b.....	14
2.4	Monitoring anle138b treatment with qRT-QulC.....	15
<b>3</b>	<b>Materials and Methods.....</b>	<b>17</b>
3.1	Preparing brain homogenates for screening anti-prion compounds with PMCA.....	17
3.2	Screening anti-prion compounds with PMCA reaction.....	17
3.3	Western blotting for testing PMCA product.....	18
3.4	Experiments in prion-infected mice for screening anti-prion compounds.....	18
3.5	Histology and immunohistochemistry for screening anti-prion compounds.....	20
3.6	Quantifying the PrPSc of anti-prion treated and untreated mice.....	20
3.7	sucrose-gradient assay.....	21
3.8	rPrP expression and purification for RT-QulC and qRT-QulC.....	21
3.9	Brain preparation for RT-QulC.....	22
3.10	Human CSF samples for RT-QulC.....	23
3.11	RT-QulC reaction.....	23
3.12	Tissue preparation for qRT-QulC.....	24
3.13	PrPres purification for qRT-QulC.....	24
3.14	PrP <sup>C</sup> purification for qRT-QulC.....	25
3.15	Performing qRT-QulC.....	26
3.16	PK-digestion and Western blotting for establishing qRT-QulC.....	26
3.17	Purifying PrPres from urine and brain for monitoring anti-prion therapy.....	27
<b>4</b>	<b>Results.....</b>	<b>30</b>
4.1	Screening compounds of inhibiting prion formation.....	30
4.1.1	Discovery of anle138b by screening for anti-prion compounds.....	30

4.1.2	Efficacy of treatment started after the onset of disease .....	35
4.1.3	Targeting of pathological PrP <sup>Sc</sup> aggregation by anle138b .....	37
4.2	Establishment of RT-QulC for prion diagnosis .....	42
4.2.1	Minimum component for prion propagation .....	42
4.2.2	Technique evolution from QulC to RT-QulC .....	44
4.2.3	Establishment of RT-QulC for diagnosing human CJD in CSF .....	45
4.2.4	International collaboration of diagnosing human CJD in CSF .....	49
4.2.5	Determining optimal substrates for detection of various prions .....	56
4.3	Establishing qRT-QulC for quantification of PrP <sup>Sc</sup> in prion-infected tissues .....	59
4.3.1	Establishing quantitative RT-QulC .....	59
4.3.2	Quantification of PrPres in peripheral organs .....	67
4.4	Monitoring anti-prion treatment by quantifying PrP <sup>Sc</sup> in the urine .....	73
4.4.1	Testing the reliability of quantifying PrPres with qRT-QulC .....	73
4.4.2	Quantifying PrPres in the urine monitors anti-prion treatment .....	76
<b>5</b>	<b>Discussion .....</b>	<b>79</b>
5.1	Utilizing PMCA for screening anti-prion compounds .....	79
5.2	Tests of inhibiting prion propagation <i>in vivo</i> are essential .....	79
5.3	RT-QulC for diagnosing prion diseases .....	80
5.4	qRT-QulC for quantifying PrP <sup>Sc</sup> in prion-infected tissues .....	81
5.5	Monitoring anti-prion treatment by quantifying PrP <sup>Sc</sup> in the urine .....	82
5.6	Perspectives .....	85
<b>6</b>	<b>References .....</b>	<b>87</b>
<b>7</b>	<b>Abbreviations .....</b>	<b>97</b>
<b>8</b>	<b>Acknowledgements .....</b>	<b>99</b>
<b>9</b>	<b>Curriculum Vitae .....</b>	<b>101</b>



# 1 Summary

Prion diseases, a group of fatal infectious neurodegenerative diseases causing Creutzfeldt-Jakob disease (CJD) in humans, bovine spongiform encephalopathy (BSE) in cattle, scrapie in sheep and goat and other prion diseases in animals affecting public health, are characterized by the accumulation of the pathogenic prion protein PrP<sup>Sc</sup> in the brain. Inhibiting the propagation of PrP<sup>Sc</sup>, the only known part of the infectious particle, the prion, is believed to cure prion diseases.

Small molecules that inhibit PrP<sup>Sc</sup> aggregation, therefore, may provide a disease-modifying therapy for these diseases, for which only symptomatic treatment is expected to be available so far. We have developed anle138b, a novel aggregation inhibitor strongly inhibited disease progression in prion-infected mouse. *In vitro*, I utilized the protein misfolding cyclic amplification (PMCA) to indicate that anle138b effectively blocked the formation as well as propagation of PrP<sup>Sc</sup>. Furthermore, anle138b strongly inhibited all prion strains tested including BSE-derived and human prions. *In vivo*, anle138b inhibited PrP<sup>Sc</sup> accumulation in prion-infected mice, blocked neuronal cell death and significantly prolonged survival without showing detectable toxicity at therapeutic doses. These data suggest that anle138b may hold promise for the anti-prion therapy.

However, I have noticed that monitoring the therapeutic efficacy of anti-prion agents *in vivo* requires large numbers of experimental animals for measuring the levels of Proteinase K (PK)-digested PrP<sup>Sc</sup>, termed PrPres, in the harvested brain at different stages of the entire incubation period. This strategy causes high experimental costs, suffering of experimental animals, and is not applicable to clinical trials in humans. Therefore, I firstly established a technique termed real-time quaking-induced conversion (RT-QuIC) that is reported to reliably diagnose prion disease by amplifying tiny amount of PrP<sup>Sc</sup> *in vitro*. I had performed several rounds of both pilot studies and blind tests that detect PrP<sup>Sc</sup> in cerebrospinal fluid (CSF) of human CJD patients and successfully discriminate CJD case from other neurodegenerative diseases. Remarkably, I obtained 100% sensitivity and 100% specificity of diagnosing human CJD with

RT-QulC. Thereafter, I took this approach one further step to establish a system termed quantitative RT-QulC (qRT-QulC) that allows sensitively monitoring the therapeutic efficacy of anle138b by quantifying the PrPres in both brain and urine of treated and untreated mice after prion-infection. I found that variations of levels of PrPres in the urine corresponded to those in the brain. These findings indicate that directly quantifying PrPres in the urine with qRT-QulC can track prion progression for monitoring the efficacy of anti-prion treatment. This suggests that using qRT-QulC to assess therapeutic efficiency of anti-prion compounds by quantifying PrPres in urine is feasible.

## 2 Introduction

### 2.1 Prion diseases and prion propagation *in vivo*

Transmissible spongiform encephalopathies (TSEs), or prion diseases, are a group of infectious and lethal neurodegenerative disorders including sporadic Creutzfeldt-Jakob disease (CJD) and variant Creutzfeldt-Jakob disease (vCJD) in human, bovine spongiform encephalopathy (BSE) in cattle, scrapie in sheep and chronic wasting disease (CWD) in deer (Prusiner, 1982). Prion diseases are characterized by the accumulation in the central nervous system (CNS) of a  $\beta$ -sheet rich and pathogenic protein,  $\text{PrP}^{\text{Sc}}$ , which is the only known constituent of prions. Prion propagation seems to rely on autocatalytic amplification of  $\text{PrP}^{\text{Sc}}$  by converting the cellular prion protein ( $\text{PrP}^{\text{C}}$ ), a normal protein that is host-encoded, glycosylated and poor of  $\beta$ -sheet, to the pathogenic  $\text{PrP}^{\text{Sc}}$  form without the participation of nucleic acids (Prusiner 1998; Bieschke et al, 2004). The conversion of  $\text{PrP}^{\text{C}}$  to  $\text{PrP}^{\text{Sc}}$  is a post-translational event and involves a conformational change of the protein (Caughey et al, 1997; Pan et al, 1993). To distinguish the  $\text{PrP}^{\text{Sc}}$  isolated from infectious tissue and is *per definitionem* associated with the TSE agent on the one hand and structurally altered PrP, which has been converted into a relatively Proteinase K (PK)-resistant form *in vitro*, on the other, I refer to the latter as 'PrPres'. After PK-treatment, fully digested  $\text{PrP}^{\text{C}}$  is undetectable in immunodetection. But the  $\text{PrP}^{\text{Sc}}$  is partial digested to remain PrPres part that is detectable by showing band shift in Western blotting. Thus, PK-digestion and followed immunodetection are the most commonly used approach to distinguish  $\text{PrP}^{\text{Sc}}$  from  $\text{PrP}^{\text{C}}$  when analyzing infected tissues (**Figure 1**).

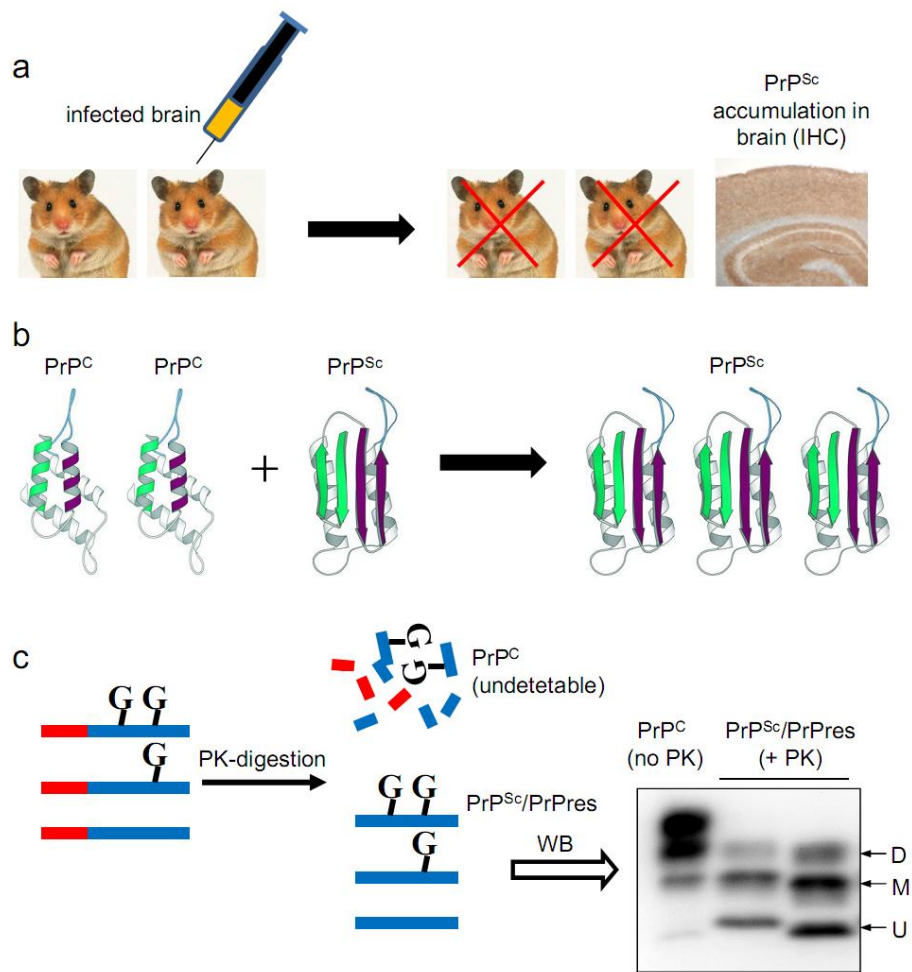


**Figure 1. Prion disease is characterized by the accumulation of partially PK-resistant PrP<sup>Sc</sup> in the brain.** (a) Susceptible animals, e.g., hamster, can be infected by the brain samples of prion-infected individuals. Large amount of PrP<sup>Sc</sup> accumulations can be found in the brain by immunohistochemistry (IHC). (b) Prion transmission is based on the propagation of an abnormal protein PrP<sup>Sc</sup>. This protein shares the identical primary structure (amino acid sequence) with the normal cellular prion protein PrP<sup>C</sup> that is expressed by the host *PRNP* gene. However, PrP<sup>Sc</sup> is conformationally different from PrP<sup>C</sup>, especially the  $\beta$ -sheet which structure is rich in PrP<sup>Sc</sup> but poor in PrP<sup>C</sup>. PrP<sup>C</sup> is converted into abnormal and infectious conformation by using PrP<sup>Sc</sup> as the template. (c) PK treatment can digest entire PrP<sup>C</sup> but only part of PrP<sup>Sc</sup>. After PK-digestion, the treated PrP<sup>Sc</sup>, termed PrPres, shows band shifts on Western blots thus helps to find the prion-contaminated samples. Subject key: G, glycosylation on PrP; PK, Proteinase K; D, diglycosylated pattern of PrP; M, M,

monoglycosylated pattern of PrP; U, unglycosylated PrP.

## **2.2 Cell-free conversion models of prions *in vitro***

### **2.2.1 Necessity of establishing prion propagation model *in vitro***

Since the misfolding of PrP<sup>C</sup> into a PK-resistant form PrP<sup>Sc</sup> causing lethal prion disease is widely accepted, the demands of curing prion disease, preventing prion transmission and risk assessment of prion contamination in surgery (such as transplant), transfusion and food-safety are essential. Investigating prion transmission in susceptible animals should be ideal for the mechanism of prion propagation. However, *in vivo* assay is time-consuming and expensive. For example, studies of prion diseases invariably demonstrate that the prolonged and silent duration of incubation may exceed 50 years in human (Collinge et al, 2006) and 15 years in cattle (Casalone et al, 2004) before developing clinical features. Although rodent and primate models have already been well established, the issue of time-consume is still remaining, e.g., 150 – 190 days post inoculation (dpi) in mouse (Castilla et al, 2008). In other words, supporting the works of screening anti-prion drug condidates from a huge library (may exceed 10 000 types of structure) or diagnosing prion disease with several months is unacceptable. Thus, establishment of techniques to examine the prion propagation with shorter incubation time is essential.

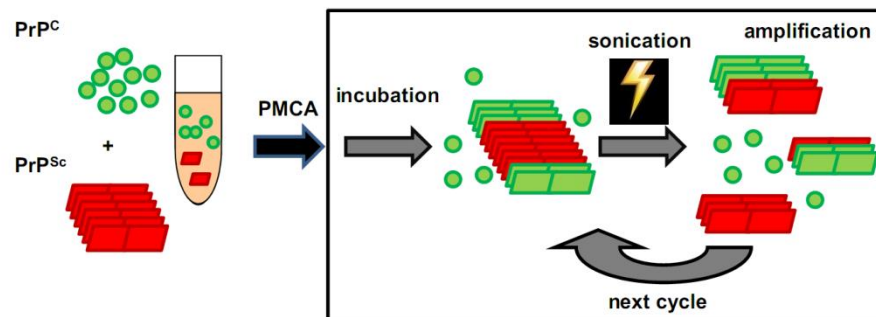
### **2.2.2 Protein misfolding cyclic amplification (PMCA)**

One theoretical consideration of solving the matter of costs is the *in vitro* generation of prions. The possibility of using cell-free conversion to amplify PrP<sup>Sc</sup> *in vitro* has been shown (Caughey, 2000; Wong et al, 2001). Further, a more rapid and efficient technique termed protein misfolding cyclic amplification (PMCA), was established by Soto's group (Saborio et al, 2001) to amplify prions *in vitro*. PMCA technique is characterized by spiking samples containing PrP<sup>Sc</sup> seed into normal brain

homogenate substrate followed by subjecting this mix to periodic ultra-wave sonication and incubation. In PMCA reaction,  $\text{PrP}^{\text{Sc}}$  seed works as a template to convert  $\text{PrP}^{\text{C}}$  of normal brain homogenate into new  $\text{PrP}^{\text{Sc}}$  to realize a PCR-like amplification. The PMCA product can be PK-digested for detecting newly formed  $\text{PrP}^{\text{Sc}}$  with immunodetection. But repeated sonication and incubation will cause the activity loss of  $\text{PrP}^{\text{C}}$  substrate before the low amount of  $\text{PrP}^{\text{Sc}}$  seed reaches detectable level. In this case, PMCA products can be subsequently spiked into fresh brain homogenates for the next round of PMCA reaction. If this procedure is repeated serially, it is termed serial PMCA (sPMCA) (**Figure 2**). The principle of sPMCA is similar to passaging virus in cell culture, except that brain homogenate substrates are used in every round. Proceeding sPMCA with fresh brain substrate can retain the efficiency of  $\text{PrP}^{\text{Sc}}$  amplification. The product of each round should be harvested for detecting  $\text{PrP}^{\text{Sc}}$  till obtaining a reliable amplification. With sPMCA, tiny amount of  $\text{PrP}^{\text{Sc}}$  can be amplified to reach the high level. This technique can facilitate to detect  $\text{PrP}^{\text{Sc}}$  in those samples such as blood and urine (Castilla et al, 2005; Gonzalez-Romero et al, 2008) containing low amount of  $\text{PrP}^{\text{Sc}}$  that cannot be found by direct immunodetection or a single round of PMCA. More importantly, due to the use of healthy brain homogenates of susceptible animals as the substrates that contain most of the brain components, e.g.,  $\text{PrP}^{\text{C}}$ , lipids and other cofactors, sPMCA is effective to mimic the prion propagation in the brain. Inoculating susceptible animals with sick brain and sPMCA products respectively, the comparable infectivity, clinical signs and pathological features were observed (Bieschke et al, 2004; Castilla et al, 2005). Regarding the comparison of sensitivities, the half lethal dose ( $\text{LD}_{50}$ ) of the diluted brain from terminal ill animal is commonly  $10^{-7}$ - $10^{-8}$  g (Saá et al, 2006; Browning et al, 2011), but sPMCA can allow  $\text{PrP}^{\text{Sc}}$  propagating even the originally seeded brain is highly diluted, e.g.,  $10^{-40}$ -fold (Castilla et al, 2005). Normally, 1 g of brain from terminal ill animal contains  $10^{-5}$  to  $10^{-6}$  g of  $\text{PrP}^{\text{Sc}}$ , and the weight of 1  $\text{PrP}$  molecule is  $\sim 10^{-19.42}$  g (molecular weight of  $\text{PrP}$  is  $\sim 23$  kDa). Thus, 1 g of brain contains  $10^{13.42}$  to  $10^{14.42}$   $\text{PrP}^{\text{Sc}}$  molecules. Mathematically, only one  $\text{PrP}^{\text{Sc}}$  molecule is left in  $10^{-13.42}$  to  $10^{-14.42}$  g of brain. The sPMCA samples containing sick brain lower than  $10^{-14.42}$  g does not have any brain-derived  $\text{PrP}^{\text{Sc}}$ . The biological properties of  $\text{PrP}^{\text{Sc}}$  in such sPMCA product, including infectivity, PK-resistance and conformational feature are from *in vitro* formed but not brain-derived  $\text{PrP}^{\text{Sc}}$  (Castilla et al, 2005; Saá et al, 2006), indicating that the  $\text{PrP}^{\text{Sc}}$  amplification in PMCA (also in sPMCA) is a good

model to study the  $\text{PrP}^{\text{Sc}}$  propagation *in vivo* (Figure 3).

### Protein Misfolding Cyclic Amplification (PMCA)



### Serial PMCA

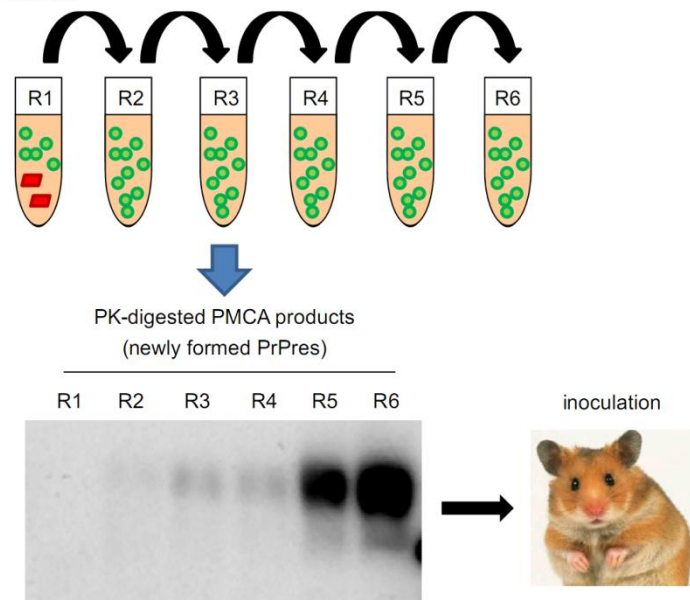


**Figure 2. The PCR-like amplification of  $\text{PrP}^{\text{Sc}}$  in PMCA and the cell culture-like passage in sPMCA.**  $\text{PrP}^{\text{Sc}}$  can amplify itself by using brain homogenates containing  $\text{PrP}^{\text{C}}$  substrate. PMCA products are spiked into fresh preparations for serially generating  $\text{PrP}^{\text{Sc}}$  in sPMCA. Final products of sPMCA lacking of brain-derived  $\text{PrP}^{\text{Sc}}$  can still infect susceptible animal, e.g., hamster. Thus, PMCA and sPMCA are both effective tools of investigating prion propagation *in vitro*. The amplification of  $\text{PrP}^{\text{Sc}}$  in PMCA is estimated by detecting PrPres in Western blotting after PK-digestion. Subject key: R, round, one PMCA reaction before spiking products into a fresh substrate for the next PMCA is called one round.

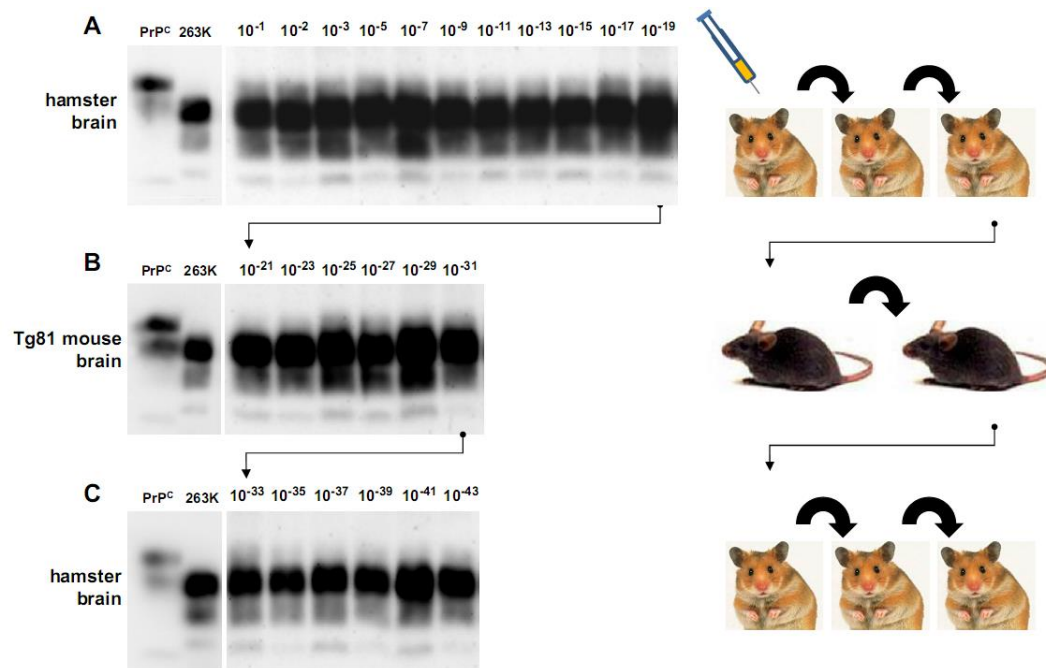


**Figure 3. sPMCA mimics prion propagation and transmission *in vitro*.** **(A)** 10% brain homogenates (brain weight divided by homogenate volume, w/v) of terminal ill hamster infected by prion-strain 263K was 10-fold diluted into 10% normal hamster brain homogenates (w/v) for the first round of PMCA. One reaction was 100  $\mu$ l containing 10  $\mu$ l of 263K brain homogenate and 90  $\mu$ l of normal brain homogenate. One round of PMCA was performed at 37°C for 48 h. Thereafter, 10  $\mu$ l was spiked into 90  $\mu$ l of freshly prepared normal hamster brain homogenates. From the round 4, 1  $\mu$ l of product of the last round was 100-fold diluted into 99  $\mu$ l of fresh normal brain homogenate followed by performing PMCA at 37°C for 48 h. This step is repeated several times till the original 263K brain reaching 10<sup>19</sup>-fold dilution. **(B)** The products (10<sup>19</sup>-fold dilution) are spiked 100-fold into brain homogenates of Tg81 mouse, a transgenic model expressing hamster PrP<sup>C</sup>, for a new round of PMCA. This is repeated several times till the original hamster 263K brain is 10<sup>31</sup>-fold diluted. **(C)** This product is 100-fold diluted in normal hamster brain homogenates to perform several rounds of PMCA till the original hamster 263K brain is 10<sup>43</sup>-fold diluted. In every round of PMCA shown in **A**, **B** and **C**, PrPres is consistently detected in 10  $\mu$ l of product after PK-digestion and Western blotting, indicating 263K PrP<sup>Sc</sup> can endlessly amplify in either hamster or Tg81 brain. These results are similar to *in vivo* transmission of 263K



prion from infected hamster to either the healthy hamsters or Tg81 mice (right panels). Therefore, sPMCA mimics the transmission of prions *in vitro* (figures are unpublished results).

By using PMCA technique, prion researchers can apply various conditions to study the crucial hypothesis about prions, the 'Protein-only' hypothesis (Prusiner, 1998), which means PrP<sup>Sc</sup> of mammalian is the only infectious component during prion transmission, was demonstrated by serial studies. This means, PMCA can be utilized to not only investigate potential factors that can enhance the prion propagation (Deleault et al, 2003; Deleault et al, 2007; Wang et al, 2010), but also find those factors that can disturb amplification, suggesting a possibility of using PMCA to screen anti-prion drug-like candidates. Given these advantages, my lab chose PMCA to select anti-prion compounds by testing their abilities to inhibit PrP<sup>Sc</sup> amplification *in vitro* before estimating their therapeutic efficacies in bioassays.

Another important part in prion field is the sensitive detection and quantification of prions during the incubation period of prion infection. The outcomes are able to suggest suitable diagnostic systems for medicine and biosafety. Despite authentic ability of amplifying PrP<sup>Sc</sup>, PMCA does not fulfill the requirement of rapid diagnosis of prions. This technique is still limited by its sensitivity, time-span and source of substrate, which factors affect the validation of clinical diagnosis. For example, PMCA of 72 h can sensitively detect PrP<sup>Sc</sup> in  $10^{-6}$  to  $10^{-8}$  g of brain from terminally ill animals (Chen et al, 2010), but PMCA reaction exceeding 72 h may induce the spontaneous conversion of PrP<sup>C</sup> into PK-resistant and infectious agent thus generates *de novo* prions (Barria et al, 2009). One possible solution for this '72 h cut-off' is to use sPMCA but it also shows the obvious shortages for prion diagnosis. For performing sPMCA by rounds, the repeated pipetting from one passage to another is essential (Morales et al, 2012). However, this procedure may require continuous amplification of several weeks with repeatedly opening caps and pipetting liquids. This increases the risk of generating aerosol that may cause cross-contamination, and decreases the applicability of estimating large-scale of suspected samples while treating PMCA products with PK and detecting PrPres with immunodetection (Western blotting, dot blotting and ELISA). In addition, the source of PMCA substrate must be from the brain

of the same species or transgenic models so that PMCA is only performed in special lab but not packed in a kit for the validation of clinical prion diagnosis.

### 2.2.3 Real-time quaking-induced conversion (RT-QulC)

To address the requirement of detecting prion with a rapid and high-throughput assay, a novel technique, termed Real-time quaking-induced conversion (RT-QulC), was established. RT-QulC can detect prions with very high sensitivity from diluted brain (Wilham et al, 2010), from cerebrospinal fluid (CSF) of end-stage disease containing only very low levels of infectivity (Atarashi et al, 2011; McGuire et al, 2012; Peden et al, 2012), and from CSF during the incubation period (Orrù et al, 2012). The mechanism of RT-QulC is based upon the seeded  $\text{PrP}^{\text{Sc}}$  converting PK-sensitive recombinant prion protein (rPrP) into a PK-resistant rPrP (rPrPres) form, which is rich in  $\beta$ -sheet structures. This reaction is performed with periodic shaking (**Figure 4**) and the result of amplified  $\text{PrP}^{\text{Sc}}$  is shown with the increased fluorescence that is caused by the  $\beta$ -sheet of newly formed rPrPres bound with Thioflavin T (ThT), a dye that efficiently binds to the  $\beta$ -sheet structure on the proteins (**Figure 5**). The correlation between ThT fluorescence and rPrPres has been shown and is used to monitor the conversion in a real-time curve (Atarashi et al, 2011).

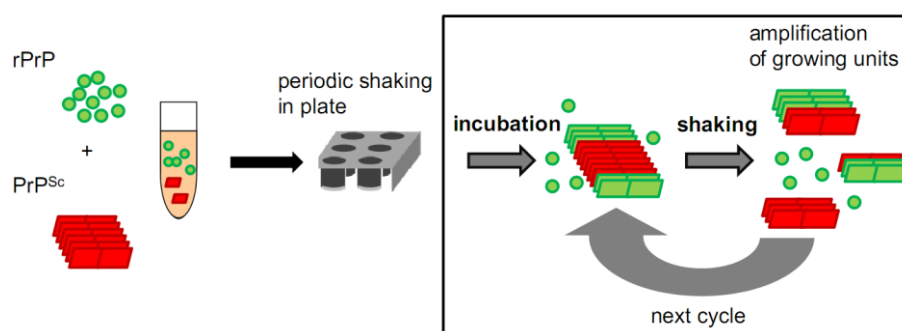


**Figure 4.  $\text{PrP}^{\text{Sc}}$  amplifies in RT-QulC system.**  $\text{PrP}^{\text{Sc}}$  is spiked into a preparation containing rPrP substrate followed by subjecting to RT-QulC for periodic shaking. rPrP is converted by  $\text{PrP}^{\text{Sc}}$  into rPrPres so that  $\text{PrP}^{\text{Sc}}$  is amplified.

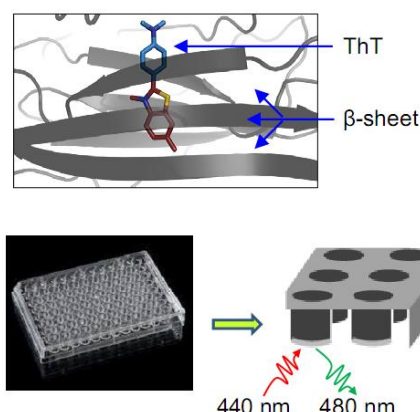


**Figure 5. Thioflavin T (ThT) binds the  $\beta$ -sheet of protein.** ThT dye binding to the  $\beta$ -sheet of protein can be detected by fluorescence with 440 nm of excitation and 480 nm of emission. Thus, newly formed rPrPres that is  $\beta$ -sheet rich can be detected by ThT-binding in RT-QuIC reaction.

RT-QuIC overcomes the problems of PMCA/sPMCA. First, comparing the sensitivity of a single round of PMCA that detects  $10^{-6}$  to  $10^{-8}$  g of prion-infected brain, the single round of RT-QuIC has higher sensitivity that can detect minimal  $10^{-15.5}$  g of PrP<sup>Sc</sup>/PrPres (Shi et al, 2013) coming from  $10^{-10}$  g of brain. Second, RT-QuIC is performed in a plate, e.g., 96-well, with tape-seal on each well, and the read-out is displayed directly by monitoring the ThT-fluorescence with automated processing and software analysis. Thus, it is no longer necessary to harvest the products for further PK-digestion and immunodetection, minimizing the risk of aerosol cross-contamination and decreasing the intensity of work, fulfilling the requirement of high-throughput screening. Third, RT-QuIC applies bacterially expressed rPrP as the substrate which is easily obtained, optimized and packed, suggesting the availabilities of spreading RT-QuIC to common clinical validation, food-safety assay, assessment of blood product and scale-up industrialization. Given these advantages above, RT-QuIC is superior to PMCA for prion diagnosis.

ThT-binding fluorescence directly indicates  $\beta$ -sheet structure in the solution. For keeping both efficiencies of excitation and emission, the tested solution should be clean and transparent. Therefore, RT-QuIC cannot be performed in a muddy solution

such as brain homogenate containing potential cofactor that may play roles in the misfolding of brain-derived PrP<sup>C</sup> to PrP<sup>Sc</sup>, indicating that RT-QulC is not an authentic *in vitro* model to mimic prion propagation in the brain. Here we chose RT-QulC only for sensitive detection of PrP<sup>Sc</sup> but not for selecting anti-prion candidates.

#### 2.2.4 Quantitative RT-QulC (qRT-QulC)

Although protease-resistant PrPres is often used as a definitive biological marker for TSE infection, the titer of infectivity measured by inoculation in experimental animals does not always fully correlate with the amount of PrPres detected by Western blotting. The correlation of seeding activity on rPrP conversion into rPrPres measured by RT-QulC with the amount of PrPres is also a complex issue. For example, it has been shown that vCJD prions have less seeding activity than sCJD prions despite the relatively high PrPres concentration (Peden et al, 2012), and that prions from brains of hamster prion-strain 263K-affected mice with little western blotting-detectable PrPres have a seeding activity comparable to that associated with the high-PrP<sup>Sc</sup> strain, mouse prion 139A (Vascellari et al, 2012). In previous studies, it has been shown that the complex correlation between amounts of PrPres and infectivity *in vivo* and seeding activity *in vitro* can be explained at least in part by differences in size distribution of PrP aggregates (Weber et al, 2008). Consequently, RT-QulC seeding activity may correlate more closely with prion infectivity than with PrPres levels, which can be considered an advantage in regard to the development of assays for prions detection.

I observed that in the RT-QulC reaction, adding small amounts of PrP<sup>Sc</sup>, or PrPres, resulted in a delayed initiation of conversion detected by ThT fluorescence (**Figure 6**). These lag-phases and the shape of the resulting ThT fluorescence curve appeared similar to the kinetics of amplification of DNA that is used for quantitative RT-PCR analysis (Schmittgen et al, 2000; Radonić et al, 2004) (**Figure 7**). Thus I investigated whether real-time protein amplification was quantitative and established a highly sensitive assay for the quantification of prion infectivity in a high-throughput system based on measuring lag time of detectable conversion. I termed this approach quantitative RT-QulC (qRT-QulC) and showed that it allows quantitation of prions in

various tissues with a detection limit corresponding to 0.001 LD<sub>50</sub> units.

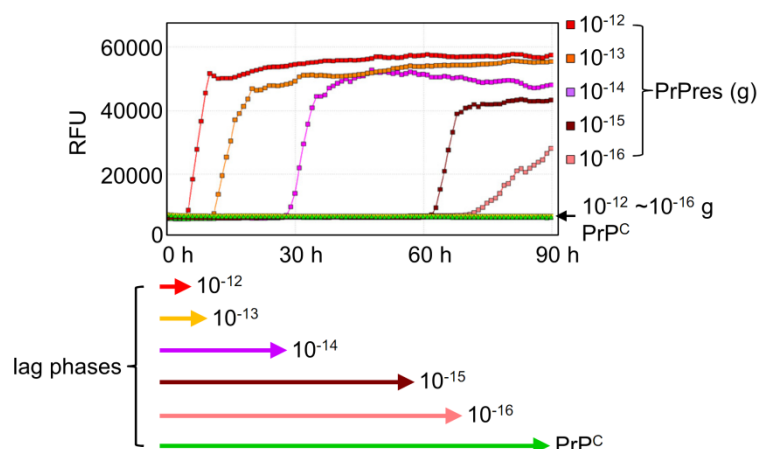


**Figure 6. Lag phases of RT-QuIC reactions are correlated with the seeded amounts of PrPres.** RT-QuIC reactions spiked with  $10^{-12}$  to  $10^{-16}$  g of PrPres show different lag phases of amplification detected by ThT fluorescence in 90 h of process. PrP<sup>C</sup> seeded as controls does not induce positive reaction in 90 h.

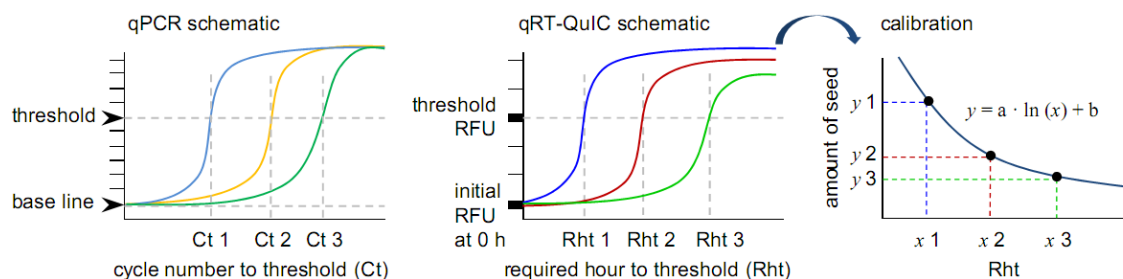


**Figure 7. Schematic illustrations of qPCR, qRT-QuIC and calibration.** The colorful lines represent the amplification profiles of DNA (qPCR) and prions (qRT-QuIC). In both techniques, the required times (Ct of qPCR and Rht of qRT-QuIC) are recorded as the dependent variables  $x$  while the fluorescence of amplification reach the threshold (represented by intersecting lines). Taking the Rhts and the known amount of seeds ( $y$ ) together can harvest the quantitative calibration. Ct, cycle number to threshold in qPCR; Rht, required hours to threshold in qRT-QuIC; RFU, relative fluorescence unit

## 2.3 Development of anti-prion compound anle138b

As mentioned above, prion diseases are a group of fatal neurodegenerative disorders in humans, cattle, sheep, elk, mink and experimental animals. These diseases are characterized by neuronal death and the accumulation of pathological disease-associated prion protein (PrP<sup>Sc</sup>) in the central nervous system (Prusiner, 1998). A recent large-scale epidemiological study indicates that the potential hosts of variant CJD (vCJD) are far more than the count of previous survey (1 out of 2000 in UK) (Gill et al, 2013), suggesting that prion diseases remain the threats of public health.

Developing drug-like candidates for curing prion diseases remains to be the major task in the field of prion researches (Mallucci and Collinge, 2005; Harrison, 2013). A crucial role of PrP<sup>Sc</sup> aggregates in disease pathogenesis is suggested by abundant evidence including i) the consistent detection of PrP<sup>Sc</sup> deposits in affected brain areas of human and animals, ii) pathogenic mutations on the *PRNP* gene that encodes cellular PrP (PrP<sup>C</sup>) affecting the human familial prion diseases and association of the PrP<sup>Sc</sup> locus with idiopathic prion diseases, such as fatal familial insomnia (FFI) and familial Creutzfeldt-Jakob disease (fCJD), iii) the epidemiological studies of the transmissions of Kuru and BSE, iv) experimental evidence *in vitro*, in cell culture, and in animal models that PrP<sup>Sc</sup> acts both as a template for this conversion and as a neurotoxic agent causing neuronal dysfunction and cell death (Prusiner, 1998; Collinge, 2001). Therefore, PrP<sup>Sc</sup> is not simply the biomarker of diagnosing prion diseases, more importantly, it is also the target for anti-prion therapy. Targeting neurotoxic protein aggregates may thus provide a therapeutic strategy for causal treatment of these devastating diseases and other protein aggregation disorders.

PMCA is a technique developed for investigating prion propagation *in vitro*. Due to the similarities of biochemical and infectious features of PMCA-derived PrP<sup>Sc</sup> and brain brain-derived PrP<sup>Sc</sup> (Castilla et al, 2005), we chose PMCA to characterize available candidates for *in vivo* anti-prion therapy.

Recently, we have introduced an efficient and non-toxic anti-prion compound, named anle138b, which was capable of significantly prolonging the survival time by inhibiting prion propagation and aggregation (Wagner et al, 2013). In this study, I applied PMCA to investigate the anti-prion abilities of inhibiting PrP<sup>Sc</sup> amplification by performing the reactions containing normal brain homogenate substrates, prion-infected brains and different synthetic compounds. By using PMCA, I found that anle138b compound effectively inhibited the propagation of mouse prion-strain RML. Further *in vivo* tests by feeding RML-infected C57BL/6 mice with anle138b starting at 80 dpi (days post inoculation) resulted in 250 dpi of prion incubation period, which was 80 days longer than 170 dpi of untreated controls. To assess the anti-prion therapeutic efficacy of anle138b, the brains of both treated and untreated mice were harvested at different time points of prion infection for detecting the levels of PrPres using immunohistochemistry, PK-digestion and Western blotting. I found that brain PrPres of anle138b-treated mice at 80, 120 and 170 dpi was much less than those in untreated mice. Furthermore, I found that anle138b inhibited propagation of not only the mouse scrapie prion strains RML and ME7, but also the mouse-adapted BSE strain 301C. More importantly, anle138b was found to inhibit the propagation of human brain-derived sCJD and vCJD in PMCA, suggesting the clinical validation of treating human CJD cases with anle138b. Given the comparability between *in vitro* amplifying prions with PMCA and *in vivo* assay with animal models, anle138b performs as an ideal anti-prion candidate for neutralizing prion diseases.

## 2.4 Monitoring anle138b treatment with qRT-QulC

Detecting PrPres (PK-resistant PrP<sup>Sc</sup> fragments after proteolysis) in the brains of different stages of prion disease is widely accepted for estimating anti-prion therapeutic treatment in experimental animals. This is applied not only in the study about anle138b compounds, but also in many studies which also investigated anti-prion through developing compounds and antibodies (Korth et al, 2001; White et al, 2003; Doh-ura et al, 2004; Mallucci and Collinge, 2005; Kawasaki et al, 2007; Wagner et al, 2013). Although all of these studies are impressive and compelling, it should be noticed that monitoring anti-prion therapy by detecting PrP<sup>Sc</sup> or PrPres in those harvested brains is

laborious with highly costs, e.g., for testing one compound, we applied at least 12 mice for the treated group and additional 12 mice for the untreated at each dpi, even though the library of compounds could be narrowed down as much as possible by using PMCA. Moreover, harvesting brains is not applicable for further clinical tests in humans. It is noteworthy that infectious prions in CNS affect the use of normal clinical diagnostic techniques, e.g., radiography and biopsy, due to either biohazard risk or irreversible injury to the patients. Monitoring the disease progression and the efficacy of treatment with competent molecular technique has not been achieved. Therefore, I aimed at finding a better way, which should facilitate tracking prion progress in living experimental animals and humans. RT-QuIC has been shown to have both high sensitivity and specificity for detecting PrP<sup>Sc</sup> in brain and CSF. In particular, RT-QuIC can be used to rapidly diagnose human CJD in the CSF (Atarashi et al, 2011; McGuire et al, 2012), although PrP<sup>Sc</sup> in human CSF is very low and the CSF is only weakly infectious (Brown et al, 1994). Given both sensitivity and specificity of RT-QuIC of detecting PrP<sup>Sc</sup> *in vitro*, as well as the high-throughput qRT-QuIC of quantifying PrPres in peripheral tissues (Shi et al, 2013), I chose qRT-QuIC to quantify the PrPres in easy-obtainable biological material, e.g., urine, to monitor the efficacy of anti-prion therapy.



### **3 Materials and Methods**

#### **3.1 Preparing brain homogenates for screening anti-prion compounds with PMCA**

Frozen mouse-adapted BSE (strain type: 301C) and mouse-adapted scrapie (strain type: RML and ME7) brains and human sporadic CJD (sCJD) and variant CJD (vCJD) brain samples were homogenized in pre-chilled PMCA conversion buffer, containing 1-fold PBS, 1% Triton X-100, 5 mM EDTA, 150 mM NaCl and protease inhibitor cocktail tablets (Roche, Basel, Switzerland). Crude 10% (w/v) homogenates were centrifuged with 2,000 x g at 4°C for 10 s. Aliquots of the supernatant were immediately frozen at -80°C for subsequent experiments. Whole normal mouse brains were obtained from 10-week-old C57BL/6 mice. After homogenization in pre-chilled PMCA conversion buffer, 10% (w/v) normal brain homogenates were centrifuged at 2,000 x g for 10 s, and aliquots of the supernatant were frozen at -80°C till used as the substrate for amplifying mouse-adapted prions. Frozen cortex harvested from non-CJD human brain was homogenized and stored as above for amplifying human CJDs.

#### **3.2 Screening anti-prion compounds with PMCA reaction**

PMCA was performed in a water-bath sonicator (Misonix sonicator 3000, Misonix, Farmingdale, NY, USA), which had a microplate horn for PCR tubes. Normal brain homogenate was spiked with infected brain homogenate (100:1, v/v) and 99 µl of this mixture was transferred into 0.2-ml PCR tubes which contained 1 µl of DMSO or compound solved in DMSO. Eighteen PMCA cycles for mouse substrates and 40 cycles for human substrates were performed. Each cycle consisted of sonication at 60% potency (~209 W) for 20 sec followed by incubation at 37 °C for 59 min 40 sec.

### 3.3 Western blotting for testing PMCA product

PMCA product was digested with 50 µg/ml proteinase K (PK) at 37 °C for 1 h. After adding an equal volume of 2×SDS loading buffer and boiling for 10 min, samples were separated by SDS-PAGE of 15% gel followed by transferring to PVDF membranes (Immobilon-P, Millipore, MA, USA) at 12 V for 2 h. For western blotting, the membrane was blocked with 5% nonfat milk in PBST. Mouse-derived PrP was detected by 1:5000 diluted 4H11 monoclonal antibody (Herms et al, 1999) and human-derived PrP was detected by 1:5000 diluted 3F4 monoclonal antibody (Dako, Glostrup, Denmark) in 1 fold PBST at room temperature for 2 h. After three washes in 1 fold PBST, the membrane was immersed in a 1:5000 diluted alkaline phosphatase conjugated goat-anti-mouse IgG (Dako) in 1 fold PBST and incubated at room temperature for 2 h. Detection was performed with CDP-Star solution (Roche, Mannheim, Germany). Western blottings were scanned and quantified by a Diana III luminescence imaging system along with the AIDA software package (Raytest, Straubenhardt, Germany).

In Western blots shown in results section, “start” indicates the sample taken from the PMCA reaction mixture at time point 0 after mixing normal brain homogenate with a minute amount of PrP<sup>Sc</sup> that acts as a seed for the subsequent PMCA reaction. Thus, this sample provides the reference for screening drug-like candidates which following PMCA incubation contain different amounts of newly formed PK-resistant PrPres depending on the different efficacy of prion amplification during PMCA. Thus, this assay design (comparison of time points before and after PMCA amplification) does not require a “loading control”. Due to load identical volumes of 10% brain homogenates after PK-digestion, this assay does not need a house-keeping gene encoded protein control such as  $\alpha$ -tubulin and  $\beta$ -actin.

### 3.4 Experiments in prion-infected mice for screening anti-prion compounds

For screening and structure-activity analysis, compounds were tested in regard to their inhibitory effect on PrP<sup>Sc</sup> accumulation in vivo by three experimental protocols:

a) Seven-week-old female C57BL/6 mice were inoculated intracerebrally (i.c.) with

30 µl of 1 % (w/v) brain homogenate (RML scrapie). Treatment was started at 80 days post infection (dpi) with 1 mg compound per day mixed with 10 µl of DMSO + 200 µl of peanut butter applied orally. PrP<sup>Sc</sup> level in the brain was measured at 120 dpi by western blotting analysis.

- b) Seven-week-old female C57BL/6 mice were inoculated intraperitoneally (i.p.) with 100 µl of 1 % (w/v) brain homogenate (RML scrapie). PrP<sup>Sc</sup> level in the spleen was determined at 35 dpi following 34 days of treatment with 1 mg compound mixed with 10 µl of DMSO + 200 µl of peanut butter per day.
- c) Seven-week-old female C57BL/6 mice were inoculated i.c. with 30 µl of 1 % (w/v) brain homogenate (RML scrapie). Treatment was started at 80 dpi with 0.84 mg compound (in 25 µl of DMSO) per day applied by intraperitoneal injection for 14 days followed by 2 x 5 days (with 2 days without treatment in between) of 1 mg compound (in 10 µl of DMSO + 40 µl of vegetable oil) applied orally by gavage. PrP<sup>Sc</sup> level in brain was measured at 106 dpi.

For long-term survival experiments, anle138b was administered orally in DMSO/peanut butter as described above. In a first set of experiments, 5 mg anle138b were given once daily starting either at day 80 or day 120 post i.c. infection. Animals of each treatment group were monitored daily for signs of disease by trained animal caretakers from day 80 post infection. The animals were sacrificed, when they had reached the terminal stage of the disease based on clinical signs (ataxia, tremor, difficulty in righting up from a position lying on its back, and tail stiffness). Typically the disease progress through the terminal stage will lead to the death of the animal within one or two days. From all animals one brain hemisphere and one half of the spleen were freshly frozen at -80 °C for biochemical analysis. The other hemisphere and the remaining half of the spleen as well as all inner organs were fixed in 4% formaldehyde solution for histological analysis. In a further experiment, treatment with anle138b was started on the day of i.c. infection with a dose of 5 mg anle138b twice daily. The *in vivo* experiments used for comparison with PMCA results were mainly performed by Dr. Jens Wagner as a part of his doctoral thesis.

### **3.5 Histology and immunohistochemistry for screening anti-prion compounds**

Prion infectivity was inactivated by immersion in 100% formic acid (Brown et al, 1990). Paraffin-fixed sections (2.5 µm) of brain tissue were stained with H&E. For PrP<sup>Sc</sup> detection using monoclonal antibody CDC1 (Pfeifer et al, 2006), sections were immunostained on a Ventana automated staining apparatus. To assess neuronal degeneration, neurons with pyknotic nuclei were counted in blinded slides in the cerebellar granule cell layer. This approach has been validated previously as an efficient measure for apoptotic neuronal cell death (Giese et al, 1995). For each animal, 30 randomly chosen high power visual fields were analyzed.

### **3.6 Quantifying the PrP<sup>Sc</sup> of anti-prion treated and untreated mice**

For quantification of PrP<sup>Sc</sup>, brain homogenates were homogenized 10 % (w/v) in lysis buffer (100 mM NaCl, 10 mM EDTA, 0.5 % (v/v) NP-40, 0.5 % (w/v) deoxycholate, 10 mM Tris/HCl pH 7.4) and subjected to dot blot analysis using 6H4 monoclonal antibody (Prionics, Switzerland) at a dilution of 1:5000. For PrPres western blotting, infected brain homogenates were treated with PK (100 µg/ml, 1h, 37°C) prior to dot blot analysis. Spleens were homogenized in Dulbecco's PBS 10 % (w/v) and PrP<sup>Sc</sup> was precipitated from 500 µl of homogenates using sodium phosphotungstic acid (NaPTA) as previously described (Wadsworth et al, 2001). Pellets were resuspended in 20 µl of 0.1 % sarkosyl buffer and treated with PK (50 µg/ml, 1 h, 37 °C). PrPres was visualized with CDP-Star detection reagent (Roche, Mannheim, Germany). Quantification was performed using a Diana III luminescence imaging system along with the AIDA software package (Raytest, Straubenhardt, Germany). The relative inhibition of PrP<sup>Sc</sup> accumulation compared to DMSO-treated groups was calculated as follows:

$$\% \text{ inhibition} = (1 - (x-s)/(c-s)) * 100$$

x = amount of PrPres in compound-treated group at end of treatment period

s = amount of PrPres in control group at start of treatment period

c = amount of PrPres in control group at end of treatment period

### 3.7 Sucrose-gradient assay

Sucrose-gradient assay was performed as described elsewhere (Tzaban et al, 2002) with minor modifications. Briefly, 10% brain homogenates (w/v) were prepared using 1xPBS (pH 7.2) containing 0.1% NP-40 with protease inhibitor cocktail EDTA-free (Roche, Switzerland) and were stored at -80°C without centrifugation. Before further processing, samples were thawed on ice. To obtain a 1% (w/v) brain homogenate 1xPBS containing 0.5% sodium deoxycholate and 1% sarcosyl was added. Then samples were agitated with 1200 rpm at 4°C for 30 min (Thermomixer Comfort, Eppendorf, Germany). To discard debris, samples were centrifuged with 20,000 × g at 4°C for 1 min. To prepare a sucrose-gradient solutions containing 10 mM Tris (pH 7.2), 1% sarcosyl and sucrose (10%, 20%, 30%, 40%, 50% and 60%, respectively) were filled into a 4 ml 11×60 mm polyallomer tube (Beckman coulter, USA) beginning with 200 µl of 60% sucrose solution loaded to the bottom, followed by adding 400 µl of 50% to 10% sucrose, respectively. For the last loading, 200 µl brain homogenate was gently tiled on the top of the 10% sucrose. Ultracentrifugation with 100,000 × g at 4°C for 1 h was performed using a Sw60Ti rotor (Beckman coulter, USA). Samples for Western blotting were harvested after centrifugation from the top to the bottom of the sucrose-gradient in 200 µl of fractions (i.e. fraction 1 represents the top of the gradient and fraction 12 the bottom fraction). For analyzing size-distribution of PrPres, fractions from the sucrose-gradient were digested by 50 µg/ml PK at 37°C for 1 h. Reaction was stopped by adding 2x SDS loading buffer and boiling at 100°C for 15 min for Western blot assays as described in section 3.3.

### 3.8 rPrP expression and purification for RT-QuIC and qRT-QuIC

BL21 (DE3) E.coli. and pET41a system (Merk, Germany) were used to express full-length rPrPs of human, hamster, mouse and sheep. Bacteria were cultured in LB medium at 37°C with 220 rpm shaking and were added 1 mM of IPTG (final concentration) when OD reached 0.7 to 0.9. The cell pellet was harvested by 10,000 g

centrifugation at 4°C for 10 min after 4 hours of induction. Thereafter, cells were resuspended in BugBuster Master Mix (Novagen, Germany) containing rLysozyme and Benzonase to extract inclusion bodies (manual for BugBuster, Novagen, Germany). Extracted inclusion bodies were denatured with 8 M Guanidine hydrochloride at 25°C for 1 hour. The denatured protein solution was centrifuged at 16,000 g at 4°C for 20 min to remove the debris.

I chose Ni<sup>2+</sup>-NTA superflow (Qiagen, Germany) resin for protein purification. NTA resin was prepared by following the manufacturer's manual. The denatured protein was loaded onto prepared resin followed by binding with inversion on the rotor at 25°C for 1 hour. After that, the resin was loaded into the column (GE Healthcare, USA) followed by connecting to the AKTA prime (GE healthcare, USA). Purification procedures including refolding and elution for preparing hamster, mouse and sheep rPrP were followed the methods described elsewhere (Atarashi et al, 2008). Purification of human rPrP was a novel method that has been filed a patent application (Song Shi, Armin Giese and Hans Kretzschmar, Method for the isolation of recombinant prion protein and the use thereof, EP 13182421.1).

After elution, the rPrP solution was loaded into 6 kDa Cellu Sep dialysis tubing (Interchim, France) followed by immersion in pre-chilled dialysis buffer (9 mM NaH<sub>2</sub>PO<sub>4</sub>, 1 mM Na<sub>2</sub>HPO<sub>4</sub>, pH 5.9) at 4°C. The dialysis was done in 2 successive steps, which were 2 hours and 18 hours, respectively. 100 volumes of dialysis buffer were used for each step. The dialyzed solutions were sterilized with a 0.22 µm filter (Millipore, USA) and the absorption was measured at 280 nm for calculating the concentration of rPrP. The concentration of each fraction was adjusted to 0.5 mg/ml by adding sterilized and chilled dialysis buffer. The rPrP solution was aliquoted and frozen in liquid nitrogen, followed by transfer to a freezer (-80°C) for long-term storage.

### **3.9 Brain preparation for RT-QuIC**

Brain samples of human sCJD and vCJD, cattle classic type BSE (C-BSE) and low-type BSE (L-BSE), normal human and normal cattle were prepared as 10% brain

homogenates as described in section 3.2.1. Thereafter, these brain homogenates were serially 10-fold diluted by using 1×QuIC-PBS (pH 7.2) containing 130 mM NaCl, 5 mM NaH<sub>2</sub>PO<sub>4</sub>, 5 mM Na<sub>2</sub>HPO<sub>4</sub> and 1 mM EDTA. Preparations were aliquoted and frozen at -80°C till being used as the seeds.

### 3.10 Human CSF samples for RT-QuIC

For the pilot study, human CSF samples were collected in our institute within the framework of the German national CJD surveillance study. Coded CSF samples were obtained from both definite CJD and non-CJD patients with confirmatory assays of detecting pathological changes and PrP<sup>Sc</sup> deposits in the brains by histology and immunochemistry, as well as PrPres by Western blotting. Within an international collaboration, blindly prepared human CSF samples were sent from Dr. Alison Green's group (National Creutzfeldt-Jakob Disease Research & Surveillance Unit, NCJDRSU, Western General Hospital, University of Edinburgh, UK).

### 3.11 RT-QuIC reaction

The RT-QuIC reactions were performed in the volume of 100 µl containing (final concentrations after seeding) 400 mM NaCl, 5 mM NaH<sub>2</sub>PO<sub>4</sub>, 5 mM Na<sub>2</sub>HPO<sub>4</sub>, 1 mM EDTA, 100 µM thioflavin T and 100 µg/ml rPrP (pH 7.2) in a Nunc 96-well plate (Thermo Scientific, USA). These ingredients were first prepared as a master mix preparation (90 µl for each reaction) before adding 10 µl of seeds (brain and CSF). Before incubation, the plate was sealed carefully with transparent tape for avoiding cross-contamination and aerosol formation. Reactions were performed on a FLUOstar Optima (BMG Labtech, Germany) at 42°C for 90 hours with 1 min shaking at 600 rpm followed by 1 min stationary incubation. The fluorescence was measured with bottom optic every hour. The excitation was 440 nm, emission was 480 nm and the gain setting was 2000. The whole procedure was controlled by a programmed Script Mode (this edited mode is a gift from Dr. Byron Caughey, NIAID, NIH). Curves were directly shown by the provided functions of BMG Optima Data Analysis software.

### 3.12 Tissue preparation for qRT-QulC

6-week old C57BL/6 mice were inoculated with mouse-adapted RML and ME7 scrapie (i.c). 10  $\mu$ l of 10% brain homogenate in 1 $\times$ PBS (pH 7.2) was used for each inoculum. 7 time-points (30, 60, 90, 120, 135, 150 and 170 dpi, days post inoculation) were set for RML-infection and 6 time-points (30, 60, 90, 120, 135 and 150 dpi) were for ME7-infection. At each dpi, five mice were sacrificed with CO<sub>2</sub>. To harvest the tissues (brain, heart, liver, spleen, lung, kidney and hindlimb muscle) they were washed with chilled 1 $\times$ PBS containing 5% sodium citrate to remove the blood. Then tissues were weighed and stored in liquid nitrogen. The tissues of age-related control C57BL/6 mice were prepared following the same procedure.

### 3.13 PrPres purification for qRT-QulC

I followed a published protocol (Polymenidou et al, 2002) to purify PrPres. RML- and ME7-infected mouse tissue was prepared to 10% homogenate (w/v) with lysis buffer (pH 7.2) containing 130 mM NaCl, 10 mM NaH<sub>2</sub>PO<sub>4</sub>, 10 mM Na<sub>2</sub>HPO<sub>4</sub>, 0.5% Triton X-100, 0.5% sodium deoxycholate, 2 mM MgCl<sub>2</sub>, 2.5 U/ml of Benzonase (Merck, Germany) and EDTA-free protease inhibitor cocktail (Roche, Switzerland). Homogenate was incubated at 25°C for 30 min for digesting nucleic acids followed by 1,000 g centrifugation at 4°C for 5 min for removing debris. Thereafter, 100  $\mu$ l of supernatant were doubly diluted with lysis buffer to reach 200  $\mu$ l of total volume followed by 20  $\mu$ g/ml of PK-digestion at 37°C for 1 h. The digestion was stopped by adding 5 mM PMSF (Sigma-Aldrich, Switzerland) and the PK-treated supernatants were transferred into 300  $\mu$ l of 1 $\times$ QulC buffer (130 mM NaCl, 5 mM NaH<sub>2</sub>PO<sub>4</sub>, 5 mM Na<sub>2</sub>HPO<sub>4</sub> and 1 mM EDTA, pH 7.4). The total volume reached 500  $\mu$ l.

The preparations were then brought to equal volume of buffer containing 20% NaCl and 0.1% sarkosyl. These solutions were vortexed vigorously followed by incubating on ice with gentle shaking for 10 min. After centrifugation at 16,000 g at 4°C for 10 min, the pellets were washed by 500  $\mu$ l of 20 mM Tris-HCl containing 0.05% sarkosyl followed by 16,000 g of centrifugation at 4°C for 10 min. This washing step was repeated twice. The pellet was stored at -80°C till being used as the seed.



For preparing the prion seeds, the frozen pellets were thawed at 4°C followed by washing with 500 µl of ddH<sub>2</sub>O. The resuspended solutions were precipitated by centrifugation at 16,000 g for 10 min at 4°C. This step was repeated twice. The last pellets were resuspended thoroughly by 50 µl of ddH<sub>2</sub>O followed by 1,000 g of centrifugation at 4°C for 1 min. 45 µl of supernatant from peripheral tissues (tissue extract) was brought to qRT-QuIC to be both the seed and required water. Ten µl of PrPres with known concentration quantified by WB was used as the seed for obtaining a standard calibration curve.

### 3.14 PrP<sup>C</sup> purification for qRT-QuIC

We referred to a published protocol (Deleault et al, 2007) to purify mouse PrP<sup>C</sup>. The brain from a healthy 20-week old C57BL/6 mouse was homogenized in chilled 1×PBS (pH 7.2) containing EDTA-free protease inhibitor cocktail (Roche, Switzerland) to make a 10% homogenate (w/v). After centrifugation at 3,000 g at 4°C for 30 min, the pellet was resuspended with an equal volume of chilled buffer (pH 7.2) containing 130 mM NaCl, 10 mM NaH<sub>2</sub>PO<sub>4</sub>, 10 mM Na<sub>2</sub>HPO<sub>4</sub>, 2% NP-40, 1% sodium deoxycholate and EDTA-free protease inhibitor cocktail (Roche, Switzerland). After incubation on ice for 30 min, the homogenate was subjected to 100,000 g centrifugation at 4°C for 30 min to remove the debris. The supernatant was filtrated with a 0.22 µm filter (Millipore, USA) followed by pouring over the ImmunoPure Immobilized Protein A column (Pierce, USA) to remove the endogenous immunoglobulins. The filtrated solution was incubated with 1 ml of Protein A resin cross-link to mouse-PrP specific monoclonal 4H11 antibody at 4°C over night. Then the resin was washed with 10 volumes of washing buffer (20 mM Tris-HCl, 500 mM NaCl and 5 mM EDTA, pH 8.0) followed by washing with 10 volumes of 1×PBS containing 0.5% NP-40. PrP<sup>C</sup> was eluted with 5 ml of 200 mM glycine. The solution was loaded into 10 kDa filter centrifugal tubes (Millipore, USA) to centrifuge at 3,000 g at 4°C for 1 h for desalting and buffer exchanging. Then the protein was resuspended with 5 ml of 1×QuIC buffer and subjected to gel filtration by passing over the Superdex 75 column (GE lifescience, USA). The harvested protein in the peak was concentrated with a 10 kDa filter centrifugal tube (Millipore, USA) followed by estimating protein concentration with

quantitative immunoblot. The yield of mouse PrP<sup>C</sup> was approx. 3 µg/brain.

### **3.15 Performing qRT-QulC**

The qRT-QulC reactions were performed in the volume of 100 µl containing (final concentrations after seeding) 400 mM NaCl, 5 mM NaH<sub>2</sub>PO<sub>4</sub>, 5 mM Na<sub>2</sub>HPO<sub>4</sub>, 1 mM EDTA, 100 µM thioflavin T and 100 µg/ml rPrP (pH 7.2) in a Nunc 96-well plate (Thermo Scientific, USA). These ingredients were firstly prepared as a master mix preparation (90 µl for each reaction) before seeding 10 µl of seeds (purified PrPres and PrP<sup>C</sup>). Before reaction, the plate was sealed carefully with transparent tape for avoiding cross-contamination and aerosol. Reactions were performed on a FLUOstar Optima (BMG Labtech, Germany) at 37°C for 90 hours with 1 min shaking at 600 rpm followed by 1 min stationary incubation. The fluorescence was measured with bottom optic every hour. The excitation was 440 nm, emission was 480 nm and the gain setting was 2000. Curves and intersecting lines (for indicating both the threshold and required hour) were directly shown by the provided functions of BMG Optima Data Analysis software.

### **3.16 PK-digestion and Western blotting for establishing qRT-QulC**

Ten percent (w/v) brain homogenates of RML- and ME7-infected mice and purified RML- and ME7-PrPres were digested with 100 µg/ml of proteinase-K (Roche, Switzerland) at 37°C for 1 h. The digestions were stopped by heating at 100°C for 10 min with 2xloading buffer. The proteins were separated in a 15% SDS-PAGE followed by transfer to a PVDF membrane (Millipore, USA). The membrane was blocked with 5% non-fat milk for 1 h at room temperature. The proteins were detected with mouse-PrP specific 4H11 monoclonal antibody. Signals were measured on a Diana III luminescence imaging system (Raytest, Germany).

### **3.17 Purifying PrPres from urine and brain for monitoring anti-prion therapy**

Urine was harvested from anle138b treated mice with Pasteur pipets. Mouse urine of 200  $\mu$ l was treated by 1  $\mu$ g/ml of PK at 37°C for 1 h followed by stopping digestion with 5 mM PMSF (final concentration). The PK-treated urine was transferred into 300  $\mu$ l of 1  $\times$  QuIC buffer (130 mM NaCl, 5 mM NaH<sub>2</sub>PO<sub>4</sub>, 5 mM Na<sub>2</sub>HPO<sub>4</sub> and 1 mM EDTA, pH 7.4). The total volume reached 500  $\mu$ l. The followed steps of purifying urinary PrPres and the protocol of preparing brain-derived PrPres for qRT-QuIC were the same as the description in section 3.13. The normal mouse urine and brain were treated with the protocols of purifying PrPres from infected urine and brain.





## 4 Results

### 4.1 Screening compounds of inhibiting prion formation

#### 4.1.1 Discovery of anle138b by screening for anti-prion compounds

Before the start of my dissertation, the research group of Prof. Armin Giese had tested a compound collection of 20,000 chemically diverse drug-like compounds both for inhibition of prion protein aggregation using both molecular SIFT assay (Bertsch et al, 2005; Bieschke et al, 2000) and anti-prion cell culture assay (Leidel et al, 2011; Geissen et al, 2011). Structure-activity and cluster analysis of the data obtained with two assays identified a cluster of highly active compounds belonging to the chemical class of 3,5-diphenyl-pyrazole (DPP) derivatives (This part of work was done by Uwe Bertsch, Thomas Hirschberger, and Armin Giese, see ref. Wagner et al, 2013). Therefore, in collaboration with the group of Christian Griesinger at the Max-Planck Institute for biophysical chemistry in Göttingen, a focussed library of ~150 DPP-related compounds was designed, synthesized and tested *in vitro* for inhibition formation of pathological PrP<sup>Sc</sup>, in cell-culture, and *in vivo* for therapeutic effects on disease progression and oligomer formation in a range of animal models. A detailed account of our experimental drug discovery strategy is provided (**Figure 8**). An evaluation of the DPP leader structure according to medicinal chemistry criteria (Clark, 2003; Lipinski et al, 2001; Veber et al, 2002) indicated good metabolic stability and oral bioavailability required for long term therapy. *In vivo* experiments were done in the prion-infected mouse model, as this provides an authentic neurodegenerative disease model with a well-defined and relatively rapid time course. Compounds were given orally and, in addition to therapeutic efficacy, brain levels were investigated for a number of compounds (**Table 1**).

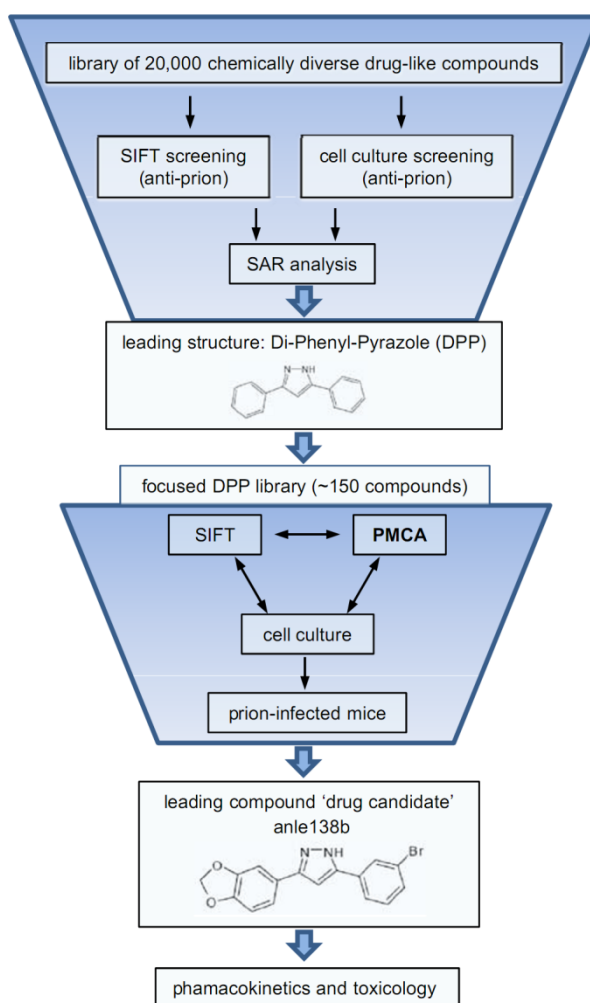


**Figure 8. Summary of experimental strategy.** In a first project phase, a library of 10,000 chemically diverse drug-like compounds was tested in regard to inhibition of prion protein aggregation in a molecular SIFT screening assay. Based on this data in combination with testing of primary hits in a cellular anti-prion assay, N-benzylidene-benzohydrazide (NBB) derivatives were identified as a new lead structure with anti-prion activity providing a proof of principle of the experimental strategy. However, NBB's contain a Schiff's base like  $=N-NH-CO-$  structure that can result in rapid metabolism *in vivo*. In order to identify further lead structures with favorable medicinal chemical properties, the project was continued by screening of 10,000 additional compounds and a parallel analysis of all these 20,000 compounds in a microtiter plate based high-throughput anti-prion cell culture assay followed by structure-activity and cluster analysis of the data obtained with these two independent

approaches. This analysis identified a cluster of highly active compounds belonging to the chemical compound class of 3,5-diphenyl-pyrazole (DPP) derivatives. Thereafter, we synthesized a focused library of ~150 DPP-related compounds for further testing in PMCA, in cell-culture, and *in vivo* in regard to therapeutic effects on prion aggregation and disease progression in animal models. Based on results from these anti-prion assays, 38 compounds were selected for *in vivo* testing in prion-infected mice. In these experiments, the compound anle138b [3-(1,3-benzodioxol-5-yl)-5-(3-bromophenyl)-1H-pyrazole] showed the highest anti-prion activity.



Table 1. Structure-activity relationship for various DPP-derivatives.

compound	R1	R2	R3	% inhibition		
				PrP <sup>Sc</sup> PMCA <sup>#</sup>	PrP <sup>Sc</sup> <i>in vivo</i> <sup>*</sup>	conc. brain [nmol/g]
anle138b				84	78 <sup>a</sup> , 57 <sup>b</sup> , 108 <sup>c</sup>	34.1
sery312b				42	13 <sup>a</sup>	3,6
anle253b				80	59 <sup>a</sup>	2.1
sery384				55	<10 <sup>a</sup>	13,9
sery417				51	<10 <sup>a</sup>	0
anle138c				19	<10 <sup>a</sup>	n.d.
sery338b				46	35 <sup>a</sup>	30.3
sery345				<10	<10 <sup>a</sup>	16.6
sery378b				34	39 <sup>a</sup>	26
anle234b				<10	<10 <sup>a</sup>	32.1
anle186b				48	30 <sup>c</sup>	31.1
sery335b				52	68 <sup>a</sup> , 46 <sup>b</sup>	29.6
anle197b				16	<10 <sup>b</sup>	n.d.
anle236b				<10	12 <sup>a</sup>	39.3
anle232b				26	23 <sup>a</sup>	n.d.

The table summarizes the effect of various compounds in regard to prion propagation *in vitro* (SIFT, PMCA) and *in vivo* in prion-infected mice, as well as compound concentrations achieved in the brain 4 hours after oral application of 1 mg compound in DMSO/peanut butter. For all compounds other than anle138b, only the part of the molecule (R1, R2, or R3) that differs from this lead structure is displayed.

<sup>#</sup> inhibition relative to high control, 10  $\mu$ M compound, RML prion strain.

<sup>\*</sup> relative inhibition of PrP<sup>Sc</sup> accumulation normalized to DMSO-treated group (0% inhibition) and PrP<sup>Sc</sup> level at start of treatment (100% inhibition).

<sup>a</sup> PrP<sup>Sc</sup> level in brain 120 days after i.c. infection and treatment for 40 days with 1

mg compound (oral, in peanut butter).

b PrP<sup>Sc</sup> level in spleen determined 35 days after i.p. infection followed by 34 days of treatment with 1 mg compound (oral, in peanut butter).

c PrP<sup>Sc</sup> level in brain at 106 days after i.c. infection and treatment for 24 days (14 days i.p. (0.84 mg compound); 2 x 5 days oral by gavage (1 mg)).

anle138b [3-(1,3-benzodioxol-5-yl)-5-(3-bromophenyl)-1H-pyrazole] showed the highest anti-prion activity both *in vivo* and *in vitro* (**Figure 9**). Comparison of anle138b with systematic variations of this structure revealed a well-defined structure-activity relationship (SAR). Regarding the 5-phenyl (R3), bromine in meta-position led to the highest inhibitory activity, whereas the change of bromine location to para- or ortho-position in the 5-phenyl ring (R3) reduced or abolished the activity, respectively. Interestingly, substitution in the ortho-position for steric reasons tilts this phenyl ring so that the molecule is no longer planar (Wagner et al, 2013). Testing different halogen atoms in the meta-position revealed a bell-shaped correlation with the size of the substituent. Regarding the central five-membered ring (R2), pyrazole was associated with the highest activity. For the substituent at the 3-phenyl (R1), SAR was more complex, as modifications in this position strongly affected bioavailability in the brain. 1,3-Benzodioxole as in anle138b was associated with the best bioavailability and good inhibitory activity *in vitro*, thus resulting in the highest activity *in vivo*. Notably, when brain levels are taken into account, there is a strong correlation between anti-prion activity *in vitro* and *in vivo* (**Figure 9**), indicating that the therapeutic effect *in vivo* is based on direct targeting of PrP<sup>Sc</sup>.

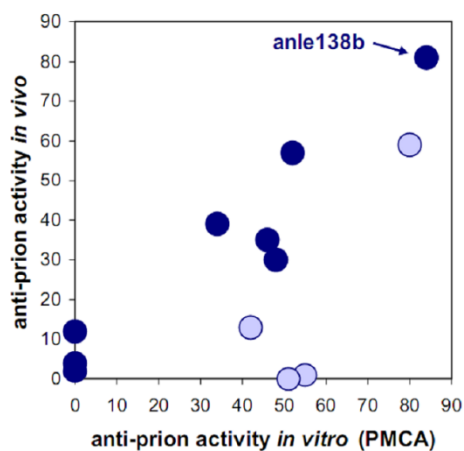


**Figure 9. Correlation between anti-prion activity *in vitro* and *in vivo*.** For compounds shown in Table 1 that reach brain levels 15 nmol/g (indicated by dark blue dots), there is a strong linear correlation ( $R = 0.951$ ) between anti-prion activity *in vitro* and *in vivo*. Those compounds that reach lower brain levels (represented as light blue dots) result in lower *in vivo* activities. No compounds with low anti-prion activity in the PMCA assay *in vitro* are active *in vivo*. Anle138b is the most active compound in both assays. Anti-prion activity is provided as % inhibition.

#### 4.1.2 Efficacy of treatment started after the onset of disease

SAR was primarily investigated through the effect of treatment for 40 days (80-120 dpi) on PrP<sup>Sc</sup> accumulation, which provides rapid and reliable biochemical quantification and thus allowed testing of a large number of compounds *in vivo*. To further investigate the mode of action and therapeutic potency, we chose anle138b, which in our SAR study had the highest therapeutic efficacy *in vivo*. To be useful for treatment in humans, a compound should also be effective when given after signs and symptoms of disease are detectable. Thus, we analysed the effect on clinical outcome (i.e. motor performance, weight loss, and survival) for treatment started at different time points after intracerebral infection (**Figure 10**). Without treatment, at about 80 dpi subtle clinical signs can be observed (Mallucci et al, 2007) and PrPres is detectable in the brain (**Figure 10 c**), at 120 dpi obvious signs of disease are present (**Figure 10 b and c**). Even start of treatment with anle138b after onset of disease at 120 dpi resulted in a substantially prolonged survival and preservation of body weight (**Figure 10 a and b**). To our knowledge, the prolongation of survival obtained with anle138b is the largest that has been found for any drug-like compound tested so far in late-stage treatment experiments (Demaimay et al, 1997; Trevitt and Collinge, 2006; Kawasaki et al, 2007; Colombo et al, 2009). The medicinal chemistry optimization of DPP compounds thus was essential for high *in vivo* efficacy compared to the efficacy observed for the first hit compounds derived from the compound collection used for primary screening (Leidel et al, 2011; Geissen et al, 2011). Analysis of mice at different time points during treatment revealed that anle138b strongly inhibited accumulation of PrP<sup>Sc</sup> (**Figure 10 c and d**) and neuronal cell death (**Figure 10 e**)

even when the start of treatment was in the symptomatic phase. Interestingly, the number of pyknotic nuclei indicating apoptotic neuronal cell death seemed not to depend on the absolute amount of PrP<sup>Sc</sup> but correlated with the rate of PrP<sup>Sc</sup> amplification. This is in line with published data (Collinge, 2001) and provides an explanation for the strong therapeutic effect found also in the late-treatment group.

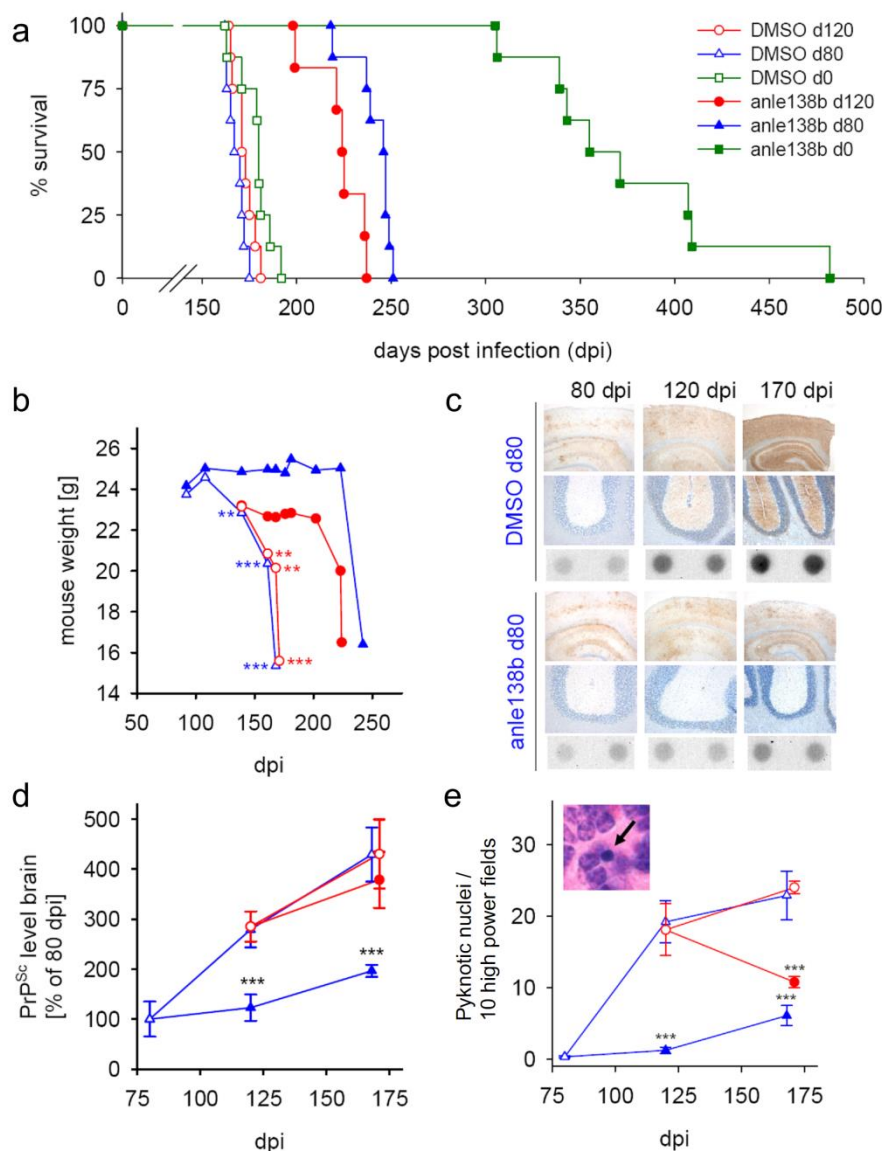


**Figure 10. Influence of daily anle138b treatment on PrP<sup>Sc</sup> accumulation and prion pathology of mice infected with RML scrapie. (a)** Survival curves of mice treated orally with anle138b beginning at 0, 80 or 120 days post i.c. prion infection.

Treatment resulted in prolonged survival, even when started at an advanced disease stage at 120 dpi. **(b)** Control mice showed a progressive weight loss starting after 100 dpi. Treatment with anle138b from 80 dpi onwards prevents weight loss for ~100 days. Treatment from 120 dpi inhibits further weight loss for ~70 days. **(c)** Immunohistochemistry (upper row: cortex/hippocampus, middle row: cerebellum) and dot blot analysis (lower row) showed that anle138b treatment inhibits PrP<sup>Sc</sup> accumulation in comparison to DMSO-treated control animals. **(d)** Quantification of brain PrP<sup>Sc</sup> levels at different time points shows highly significant inhibition of PrP<sup>Sc</sup> accumulation in mice treated from 80 dpi onwards. PrP<sup>Sc</sup> accumulation is also reduced in animals treated from 120 dpi. **(e)** Histological analysis reveals a significantly reduced number of pyknotic nuclei both in mice treated from 80 dpi and 120 dpi onwards. Inset is an example of a pyknotic granule cell nucleus (arrow). Error bars in **(d)** and **(e)** indicate standard error (n = 4), \*\* = p < 0.01, \*\*\* = p < 0.001. The legend shown in **(a)** is also applicable to **(b)**, **(d)** and **(e)**.

#### 4.1.3 Targeting of pathological PrP<sup>Sc</sup> aggregation by anle138b

Regarding the mode of action, these findings in combination with the finding that PrP<sup>C</sup> expression is unaffected by anle138b (Wagner et al, 2013) indicate that anle138b directly blocks PrP<sup>Sc</sup> amplification and reduces neurotoxicity *in vivo*. Notably, we observed a significant change in size distribution of aggregates indicating a modulation of the abundance of different oligomeric species. To characterize oligomer formation *in vivo*, we used sucrose gradient centrifugation, as this method, which is well established in the prion field (Prusiner et al, 1980), has several advantages compared to other methods for analysis of size distribution of aggregates: i) It allows direct analysis of brain homogenates, which would be difficult by gel filtration, ii) there is no purification step, which might modify the aggregation state before analysis, and iii) it allows to detect and quantify all potential particle sizes (i.e. monomers, oligomers, fibrils) simultaneously. Analysis of brain homogenates by sucrose-gradient centrifugation assay reveals a strong reduction of high molecular weight species and also a shift towards smaller oligomer size for low molecular weight oligomers (**Figure 11**). That oligomer modulation - in addition to reduced toxicity - also interferes with

PrP<sup>Sc</sup> amplification is further corroborated by the fact that PrP<sup>Sc</sup> amplification is also blocked in PMCA assay (**Figure 12**). This method provides several key advantages for compound testing. It has been shown that PMCA provides an experimental tool for rapid propagation of authentic infectious prions *in vitro* (Weber et al, 2006) and preserves strain properties (Castilla et al, 2008). Importantly, this approach constitutes the only experimental approach to test the efficacy of compounds in a purely human system (human prions + human brain tissue). Moreover, we found that the results obtained in the PMCA assay are predictive for the effects observed *in vivo* (**Table 1**, **Figure 10**). We tested anle138b using a range of murine (RML, ME7 and 301C (i.e. mouse-adapted BSE)) and human strains (sCJD and vCJD). Anle138b strongly inhibited all prion strains tested including BSE-derived and human prions in a purely human system. Dose-response curves for the RML prion strain used in our animal experiments and for human vCJD were similar ( $EC_{50}$  RML = 7.3  $\mu$ M,  $EC_{50}$  vCJD = 7.1  $\mu$ M), indicating that this compound may also be useful for treatment of human prion disease (**Figure 13**).

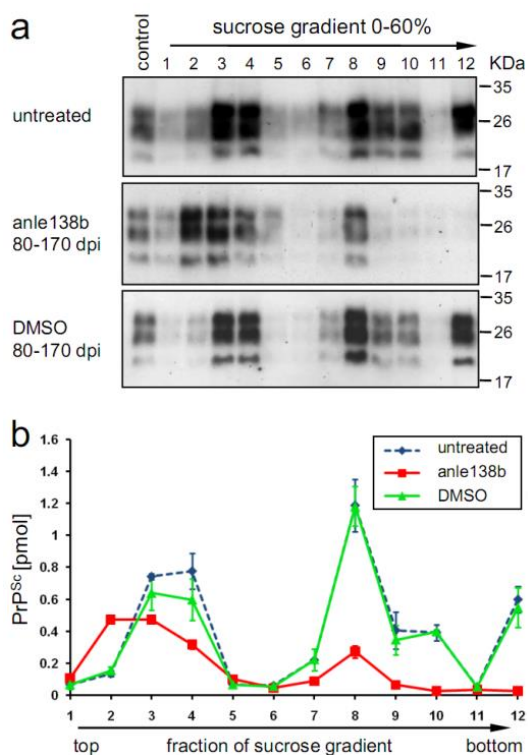


**Figure 11. Size modulation of mouse RML PrP<sup>Sc</sup>/PrPres oligomers by anle138b.**

(a) Size distribution of PrP<sup>Sc</sup> aggregates was analyzed by sucrose gradient centrifugation, PK-digestion and WB. (b) Quantifications of WBs show that mice treated with anle138b show a strong reduction of high molecular weight species (fractions 7-12). Also small molecular weight oligomers (fractions 3-4) are reduced and show a shift towards smaller size (fraction 2) indicating that anle138b blocks aggregation at the level of small oligomers. DMSO-treated mice are indistinguishable from terminally ill untreated mice. Shown are mean  $\pm$  s.e.m.

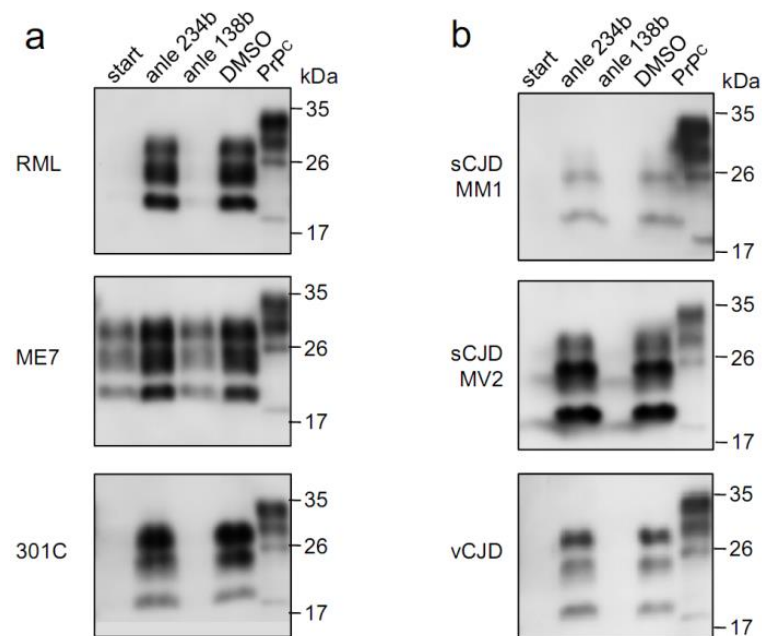


**Figure 12. Inhibition of various human and non-human prion strains in PMCA.**

For PMCA assay, infected brain homogenates were diluted 100-fold by appropriate normal brain homogenates containing compounds (1  $\mu$ l of 10 mM solutions in DMSO) or 1  $\mu$ l of DMSO as control. (a) Mouse-adapted scrapie strains (RML, ME7) and Mouse-adapted BSE (301C) were used as seed in C57BL/6 mouse normal brain homogenates. (b) sCJD and vCJD samples were propagated in non-CJD human brain homogenates. sCJD MM1, the type 1 sCJD whose PrP is methionine/methionine homozygous at codon 129 aa; sCJD MV2, the type 2 sCJD whose PrP is methionine/valine heterozygous at codon 129 aa; vCJD is methionine/methionine homozygous. Non-CJD human brains prepared for PMCA substrates were selected. In all gels, 0.5% (w/v) normal brain homogenates from C57B/L6 and human brain, respectively, were loaded directly in the last lane as a reference without proteolysis

(indicated as PrP<sup>C</sup> on the top). All other samples were treated with 50 µg/ml PK. 'Start' indicates those samples containing infected brain homogenates before PMCA (lane 1 of each gel). Molecular weight markers are indicated on the right. PrP migrates in three different bands due to the presence of unglycosylated, monoglycosylated, and diglycosylated forms, and digestion with Proteinase K results in a shift to lower molecular weights with the unglycosylated band migrating at ~20 kDa. Anle138b shows a strong inhibitory activity in all prion strains tested. As an additional control, the inactive isomer anle234b (see Table 1) was used.

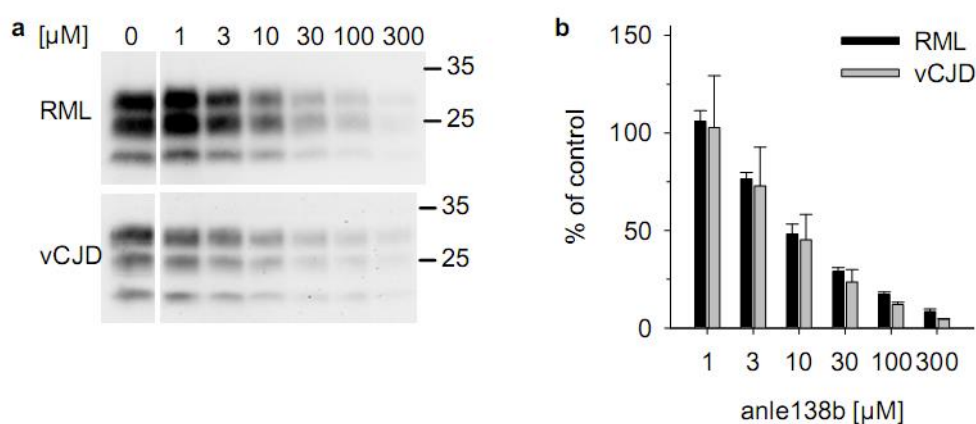


**Figure 13. Inhibition of *in vitro* propagation of different prion strains by anle138b.**

(a) Normal brain homogenates of C57BL/6 mouse and human seeded with a 100-fold dilution of infected brain homogenates respectively were mixed with different concentration of anle138b (0, 1, 3, 10, 30, 100 and 300 µM, final concentration). PMCA reactions were conducted 18 cycles for mouse substrate and 40 cycles for human substrate. The effect of anle138b was dose-dependent. Molecular weight markers are indicated on the right in kDa. (b) The amount of PrP<sup>Sc</sup> was quantified densitometrically and normalized to the control reaction without compound. Similar dose-response curves were obtained for human prions (vCJD) and for the murine prion strain RML that was used in animal experiments. Three independent experiments were carried out. Results are presented as mean ± s.e.m.



#### 4.1.4 Therapeutic efficacy of anle138b in Parkinson disease (PD)

$\alpha$ -Synucleinopathies share molecular features in regard to aggregate structure and seeding with prion diseases (Glabe and Kaye, 2006; Angot et al, 2010; Luk et al, 2012) and are of high clinical importance due to their high prevalence (Forman et al, 2005). Thus, we tested our library of DPP-derivatives with respect to effects on  $\alpha$ -syn oligomer formation and surprisingly found that Anle138b turned out to inhibit  $\alpha$ -syn oligomer formation at the same concentration range that was active in the PMCA anti-prion assay and that was reached in brain tissue (the *in vitro* SIFT assay and *in vivo* survival tests of screening anti-PD compounds were done by Armin Giese, Johannes Levin, Felix Schmidt and Catharina Prix, see ref. Wagner et al, 2013). Similar to the prion mouse model, we found a strong reduction of pathological  $\alpha$ -syn oligomers in the anle138b treated mice (**Figure 14**). The level of total  $\alpha$ -syn was unchanged in anle138b-treated mice (Wagner et al, 2013), indicating that anle138b does not interfere with expression and degradation of  $\alpha$ -syn in these mice but acts as an aggregation inhibitor.

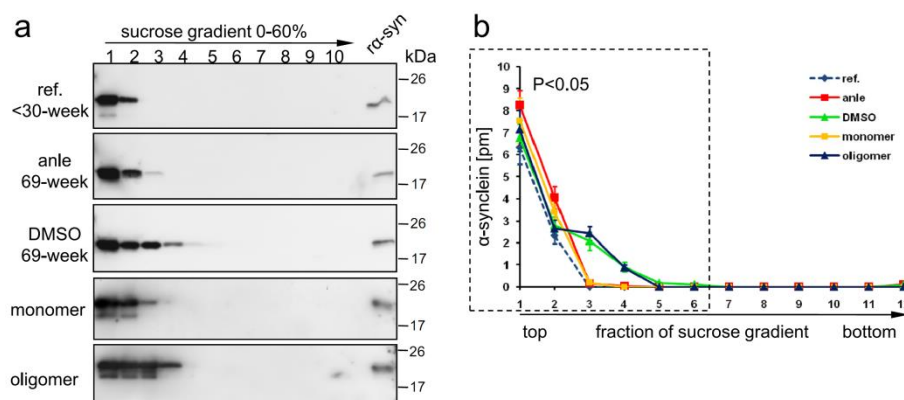


**Figure 14.** (a) Sucrose gradient centrifugation shows that in young transgenic mice  $\alpha$ -syn is found in the same fractions (1-2) as monomeric recombinant  $\alpha$ -syn. In 69-weeks-old placebo-treated mice (DMSO),  $\alpha$ -syn oligomers can be found that show the same size distribution as oligomers derived from recombinant  $\alpha$ -syn by treatment with DMSO/ $\text{Fe}^{3+}$ . Oligomer formation in transgenic mice is inhibited by treatment with anle138b. For the corresponding graph shown in (b), four mice per group were analyzed.

## 4.2 Establishment of RT-QuIC for prion diagnosis

### 4.2.1 Minimum component for prion propagation

PrP<sup>Sc</sup> is an abnormal protein thought to be the only essential component of infectious prion agents. The 'protein-only' hypothesis proposed by S. B. Prusiner (Prusiner, 1998) postulates that both the transmission and infection of prions are only caused by this protein PrP<sup>Sc</sup> and without any other participant. According to this hypothesis, PrP<sup>Sc</sup> should be the only component that can convert normal PrP<sup>C</sup> into abnormal forms both *in vitro* and cause prion diseases *in vivo*. In other words, understanding the conditions of prion transmission and propagation depends on investigating the elements on the side of host tissues but not the side of prion particles. Thus, a 'bottom-up' study can be logically raised: spiking PrP<sup>Sc</sup> into a system that contains as few factors as possible, e.g., only PrP<sup>C</sup>, to see if the PrP<sup>Sc</sup> can still propagate and to test potential cofactors derived from normal cells that may enhance the amplification of PrP<sup>Sc</sup>. Theoretically, this strategy can help to not only investigate the mechanism of prion propagation, but also establish a sensitive amplification system of prion diagnosis that can detect small amount of PrP<sup>Sc</sup> *in vitro*.

Many studies have addressed this strategy by testing many cellular elements that may help the invasion and propagation of prions (Telling et al, 1995; Deleault et al, 2003; Deleault et al, 2007; Atarashi et al, 2007; Wang et al, 2010; Kim et al, 2010). With more potential cofactors to be found, the available evidence indicates a simple truth: prion propagation in affected individuals is rather complex involving many cellular components so that the mechanism of prion propagation has not been settled yet. However, attempts of developing diagnostic techniques for prion diseases have made an achievement that allows efficient prion amplification in a minimal system that contains just bacterially expressed recombinant prion protein (rPrP) substrate and spiked prion seeds without any association with other mammalian cellular cofactors. This technique is termed quaking-induced conversion (QuIC) (**Figure 15**) (Atarashi et al, 2008).

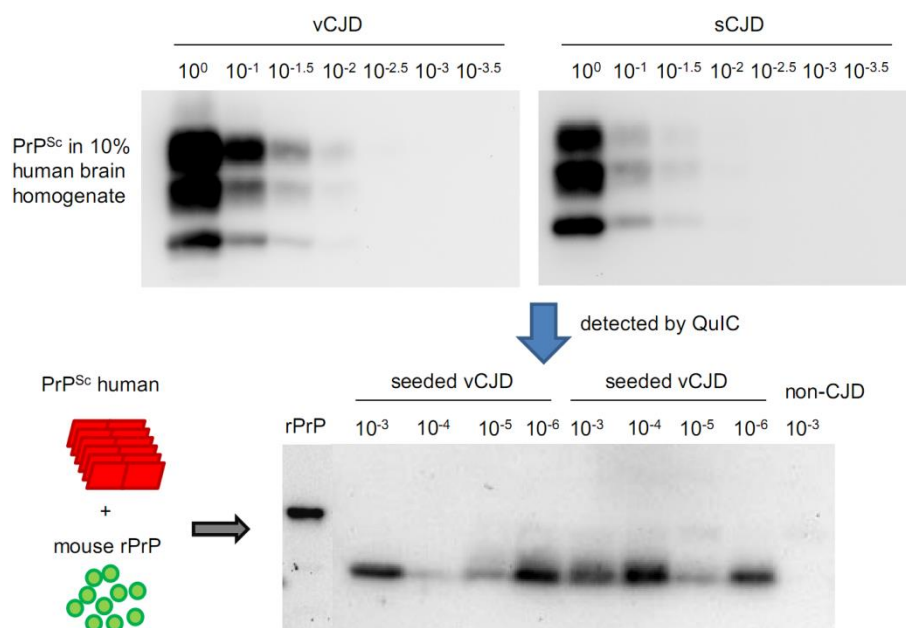


**Figure 15. Detecting PrP<sup>Sc</sup> of human in QuIC reaction.** The classical technique for detecting human PrP<sup>Sc</sup> is to digest the brain homogenates with PK followed by detecting PrPres with WBs (upper panels). This technique is limited by the sensitivities of WB, e.g., PrPres signals of vCJD and sCJD are undetectable in  $\geq 10^{-2.5}$ -diluted brain homogenates. Thus, WB can detect PrPres only in the brains of biopsy or autopsy harvested from the CJD patients of terminal stage. WB cannot fulfill the requirement of early stage diagnosis that is needed to facilitate early (i.e. presymptomatic) anti-prion treatment. QuIC is a prion propagation system that mixing PrP<sup>Sc</sup> and rPrP substrate to amplify PrP<sup>Sc</sup> in vitro. PK-digested QuIC products can be analyzed by WB to detect newly formed rPrPres (lower panel). Reactions seeded by diluted CJD brains ( $10^{-3}$  to  $10^{-6}$ -fold dilution), but not that seeded by diluted non-CJD brain, show positive rPrPres bands in WB, indicated that small amounts of PrP<sup>Sc</sup> which cannot be detected directly by normal WB are amplified to reach the detectable levels by QuIC. Human brain-derived PrP contains 3 glycosylated forms: diglycosylated, monoglycosylated and unglycosylated. Thus, human PrPres shows 3 separated bands in normal WB. In contrast, both bacterially expressed rPrP substrate and PK-digested rPrPres has only one band that lacks glycosylation..

#### 4.2.2 Technique evolution from QuIC to RT-QuIC

By automatically converting rPrP substrate into partially PK-resistant rPrP (rPrPres), PrP<sup>Sc</sup> in seeded sample can be amplified in the QuIC system. Although QuIC has shown its ability of detecting rather small amount of PrP<sup>Sc</sup> through 'prion propagation', the time-span of reaction and the consecutive PK-digestion and Western blotting steps are problematic for a routine diagnostic application. For example, QuIC is still an end-point diagnostic technique so that the reaction must be stopped at a very right time when PrP<sup>Sc</sup> has been amplified but those 'neat' reactions have not caused spontaneous conversion of rPrP to rPrPres yet. Therefore, QuIC technique has to be optimized by employing rPrP substrates of many species and multiple working conditions including temperature, detergent and ion strength (Atarashi et al, 2008). Furthermore, results of tests will not be available before digesting the products with PK of right concentrations and detecting with antibody of right types (monoclonal or polyclonal against the epitopes on PK-resistant pattern of rPrPres) (Atarashi et al, 2007; Atarashi et al, 2008).

A study termed amyloid seeding assay (ASA) showed that the newly formed rPrPres can be detected by fluorescence caused by thioflavin T (ThT)-binding to the  $\beta$ -sheet of rPrPres (Colby et al, 2007). Despite the fact that neither the sensitivity nor specificity of ASA is ideal, it at least suggests a method of using ThT as the detection agent in a well-defined system of prion amplification. Hence, a technique termed real-time QuIC (RT-QuIC) has been developed (Wilham et al, 2010). By adding ThT into the QuIC assay system followed by performing prion amplification in an automated fluorescence reader, the conversion of PrP<sup>Sc</sup> can be observed directly. Thus, a much easier detection can be achieved. RT-QuIC overcomes the shortages of QuIC discussed above and, allows performing multiple reactions at the same time, e.g., in a 96-well or 384-well plate. This is very important because it fulfills the requirement of detecting prions in a high-throughput system.

Based on the both sensitivity and specificity shown in experimental studies, RT-QuIC has been subjected to clinical trials of diagnosis of human prion diseases. Current seeds for human trials are cerebrospinal fluid (CSF) samples obtained from definite CJD (for positive controls and pilot studies) and probable CJD (for case-control and

cohort studies) patients, since both the existence and low infectivity of prion in CSF has been addressed (Brown et al, 1994). A recent study showed 80% sensitivity and 100% specificity of using RT-QuIC to diagnose CJD in CSF (Atarashi et al, 2011), while another study showed these two quotas with 91% and 98% (McGuire et al, 2012), respectively. Both studies showed better sensitivity and specificity, respectively, than detecting 14-3-3 protein, another protein marker widely accepted for diagnosing suspected sCJD in human CSF (Collins et al, 2000; Sanchez-Juan et al, 2006).

4.2.3    Establishment of RT-QuIC for diagnosing human CJD in CSF

The pilot study of RT-QuIC tests was separated in two parts: i) test the sensitivity and specificity of RT-QuIC of detecting PrP<sup>Sc</sup> in diluted human brains and CSF, and ii) test blindly prepared CSF samples of our own collection. As described before, RT-QuIC results of prion amplification can be indicated directly by the ascendant curves of ThT-fluorescence (**Figure 16**). RT-QuIC showed high reliability when detecting PrP<sup>Sc</sup> in diluted human brains and CSF by using human rPrP substrate in reactions (**Figure 17**). I obtained 100% sensitivity and 100% specificity for detecting known CJD samples (**Table 2**). Thereafter, human CSF samples of our own collections were prepared blindly in two batches followed by seeding into RT-QuIC. Again, I obtained 100% reliability of discriminating CJD and non-CJD CSF samples in RT-QuIC (**Table 3**). These results indicate that the RT-QuIC technique in our lab has been established to detect prions.

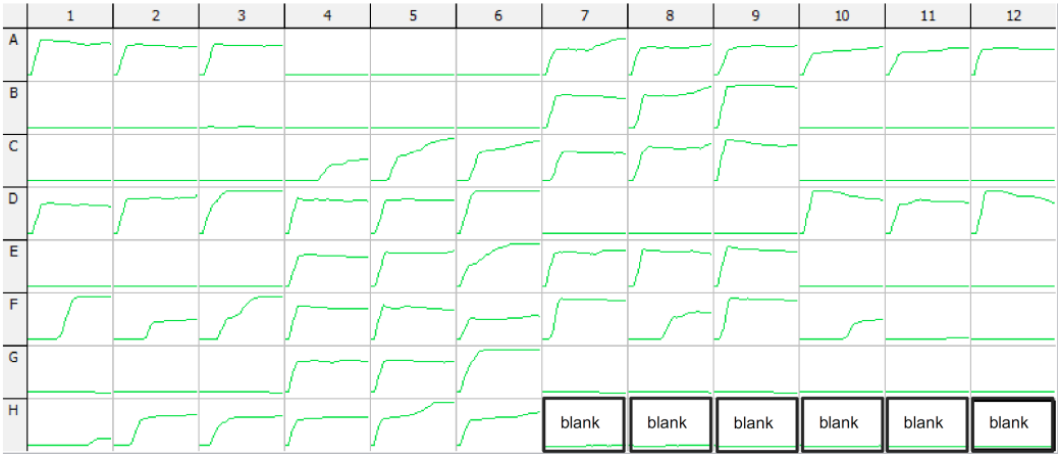


**Figure 16.** One typical read-out of RT-QulC of amplifying PrP<sup>Sc</sup> with a 96-well plate. rPrP substrate was spiked with PrP<sup>Sc</sup> samples or non-prion brain control followed by performing in RT-QulC reactions for several hours (normally 90-96 h). Those rPrP substrates seeded by samples containing PrP<sup>Sc</sup> were converted into  $\beta$ -sheet rich rPrPres which was detected by ThT fluorescence and show ascendant curves in real-time. In this plate, each sample was repeated with triplicate (i.e., wells A1-A3 were seeded by the PrP<sup>Sc</sup> sample coming from one preparation of prion disease, wells B1-B3 were seeded by the control sample coming from one non-prion preparation, etc.). Parallel repeats in RT-QulC are essential because in some cases, the pipetting error causes unstable amplification for detecting PrP<sup>Sc</sup> (e.g., F1-F3 and H1-H3, which wells were all seeded with PrP<sup>Sc</sup> samples), or even false-negativity (e.g., F10-F12). 'blanks' indicated in the bottom row are solutions containing PrP<sup>Sc</sup> but not rPrP substrate for showing that ascendant curves are caused by the growth of rPrPres but not seeds.

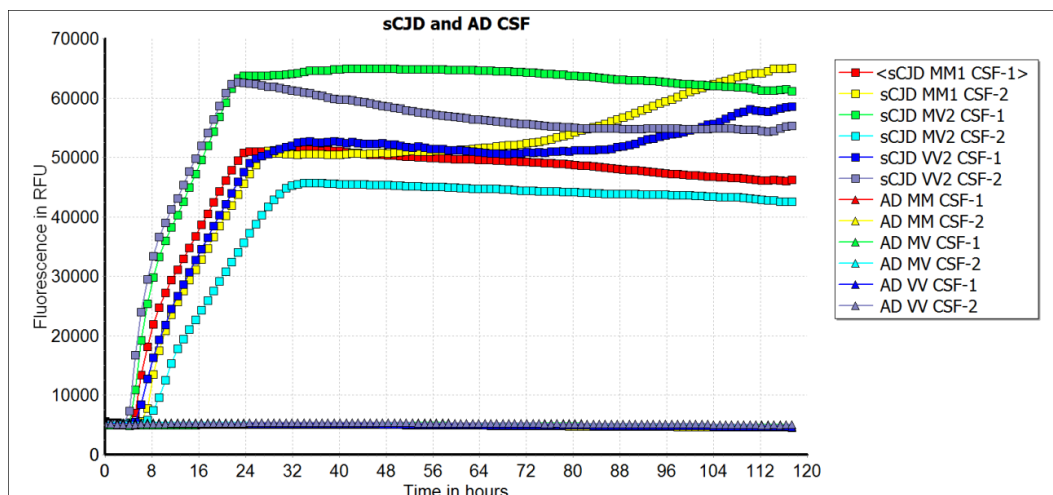


**Figure 17.** Discriminating human sCJD from Alzheimer disease (AD) by amplifying PrP<sup>Sc</sup> of CSF with RT-QulC. CSF samples of definite sCJD and AD were spiked 10  $\mu$ l into RT-QulC reactions containing human rPrP substrate. These reactions were performed for 120 h and the positive reactions were indicated by ascendant curves in read-outs. Human sCJD cases are MM1 (methionine/methionine homozygous type 1), MV2 (methionine/valine heterozygous type 2) and VV2 (valine/valine homozygous type 2). AD CSF samples were chosen corresponding

genotypes (represented as MM, MV and VV, respectively). Each type of CJD and AD has 2 randomly selected cases (indicated as 1 and 2). All CJD cases are positive at ~8 h, and none of AD case shows false-positivity in 120 h, indicating high reliability of RT-QuIC amplification system for detecting PrP<sup>Sc</sup> in human CSF. This result is a combination of zoom-in data coming from several wells of a plate like those shown in Figure 16.

**Table 2. Summary of one batch of pilot study**

	CSF	Replication	positive	negative	sensitivity	specificity
<b>CJD</b>	64	256	64 (256)	0	100%	-
<b>Non-CJD</b>	78	312	0	78 (312)	-	100%

In this batch of pilot study, CSF samples of 64 definite CJD cases and 78 non-CJD cases were tested. RT-QuIC of each case was prepared in 4 parallel reactions. Every RT-QuIC reaction seeded by CJD CSF showed positive (100% sensitivity), and every non-CJD CSF showed negative (100% specificity). Pilot study was done in several batches to test the reliability and reproducibility of using RT-QuIC for the detection of human PrP<sup>Sc</sup>.

**Table 3. Summary of one batch of blind test (BT) by using CSF samples of own collection**

No.	Disease	Type (129 aa)	RT-QuIC	No.	Disease	Type (129 aa)	RT-QuIC
BT2-1	AD	ND	0/3	BT2-17	sCJD	MM1	3/3
BT2-2	sCJD	MM1	2/3	BT2-18	sCJD	MV2	3/3
BT2-3	sCJD	MV2	3/3	BT2-19	AD	ND	0/3
BT2-4	sCJD	MM1	3/3	BT2-20	AD	ND	0/3
BT2-5	AD	ND	0/3	BT2-21	inflammation	ND	0/3
BT2-6	sCJD	VV2	3/3	BT2-22	AD	ND	0/3
BT2-7	sCJD	MM1	3/3	BT2-23	sCJD	MM1	3/3
BT2-8	inflammation	ND	0/3	BT2-24	sCJD	MM2	2/2
BT2-9	PD	ND	0/3	BT2-25	sCJD	MM1	3/3
BT2-10	sCJD	MM1	3/3	BT2-26	AD	ND	0/3
BT2-11	AD	ND	0/3	BT2-27	AD	ND	0/3
BT2-12	sCJD	MM1	3/3	BT2-28	sCJD	MV2	2/2
BT2-13	sCJD	MV2	3/3	BT2-29	PD	ND	0/3
BT2-14	PD	ND	0/3	BT2-30	sCJD	MM1	3/3
BT2-15	sCJD	MV2	3/3	BT2-31	AD	MV	0/3
BT2-16	AD	MM	0/3	BT2-32	sCJD	MM2	2/2
sensitivity	100%						
specificity	100%						

Subject key: sCJD, sporadic Creutzfeldt-Jakob disease; AD, Alzheimer disease; PD, Parkinson disease; inflammation, normal inflammation in the brain without neurodegenerative change. Shown 'RT-QuIC' columns are results indicated with numbers of positive reaction/performed reaction.



#### 4.2.4 Diagnosing human CJD in CSF samples obtained by international collaborations

To test the utility of RT-QuIC in our lab for diagnosing human CJD patients by detecting PrP<sup>Sc</sup> in the CSF, I received two batches of blinded human CSF samples from NCJDRSU (The National CJD Research & Surveillance Unit, University of Edinburgh, UK). After gaining the results, I sent the diagnostic conclusions back to NCJDRSU for judgment. As expected, I observed 100% of both sensitivity and specificity. It is noteworthy that most of these blinded samples are from patients who are still living in the hospital. These results of blinded tests indicate that RT-QuIC is a reliable technique for prion diagnosis is feasible in our lab.

Since I found that the patented human rPrP (Song Shi, Armin Giese and Hans Kretzschmar, Method for the isolation of recombinant prion protein and the use thereof, EP 13182421.1) seemed to be a better substrate for amplifying human CJD in RT-QuIC reactions, I compared this rPrP substrate with hamster rPrP prepared by NCJDRSU and NIH (McGuire et al, 2012; Peden et al, 2012; Wilham et al, 2010). I found that RT-QuIC reactions containing human rPrP gave much shorter lag-phases of amplification than hamster rPrP. More importantly, reactions using human rPrP had better reproducibility than those using hamster rPrP. Furthermore, much higher relative fluorescence unit (RFU) that facilitated to immediately distinguish CJD CSF from those non-CJD cases was observed in reactions containing human rPrP but not hamster rPrP. These results suggest that it may be necessary to prepare rPrP of different species for detecting various prion strains. Details are provided for blinded testing of samples from international collaboration (**Figure 18, 19, 20, 21 and Table 4, 5**).

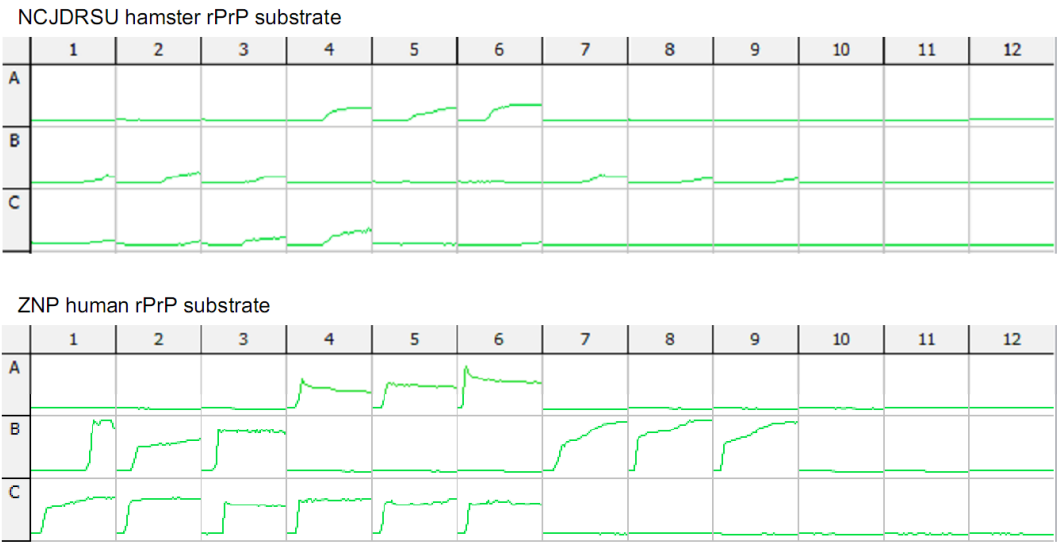


**Figure 18. Reactions using hamster rPrP (NCJDRSU) and human rPrP (ZNP) substrates are seeded with blinded CSF samples from the UK for testing the reliability of RT-QuIC.** Each sample was done with triplication. Results showed that reactions using hamster rPrP produce comparable conclusions with those using human rPrP. However, fluorescence of hamster rPrPres is much lower than that of human rPrPres. For testing of hamster rPrP, each well was seeded with 15  $\mu$ l of CSF into 85  $\mu$ l of substrate preparation containing 100  $\mu$ g/ml rPrP (final concentration). For testing of human rPrP, each well was seeded with 10  $\mu$ l of CSF into 90  $\mu$ l of substrate preparation containing 100  $\mu$ g/ml rPrP (final concentration). The results are summarized in Table 4.

**Table 4. Summary of the first batch of collaborated blind test for diagnosing CJD in CSF**

CSF No.	well	RT-QuIC (hamster rPrP)	RT-QuIC (human rPrP)	conclusion
1818	A1-A3	0 of 3	0 of 3	non-CJD
4531	A4-A6	3 of 3	3 of 3	CJD
4379	A7-A9	0 of 3	0 of 3	non-CJD
4426	A10-A12	0 of 3	0 of 3	non-CJD
4444	B1-B3	3 of 3	3 of 3	CJD
4453	B4-B6	0 of 3	0 of 3	non-CJD
4466	B7-B9	3 of 3	3 of 3	CJD
4510	B10-B12	0 of 3	0 of 3	non-CJD
4572	C1-C3	3 of 3	3 of 3	CJD
4673	C4-C6	2 of 3	3 of 3	CJD
no seed Ctrl.	C7-C9	0 of 3	0 of 3	no spontaneous conversion
no rPrP Ctrl.	C10-C12	0 of 3	0 of 3	no background

These results were confirmed at the NCJDRSU with 100% sensitivity and 100% specificity.

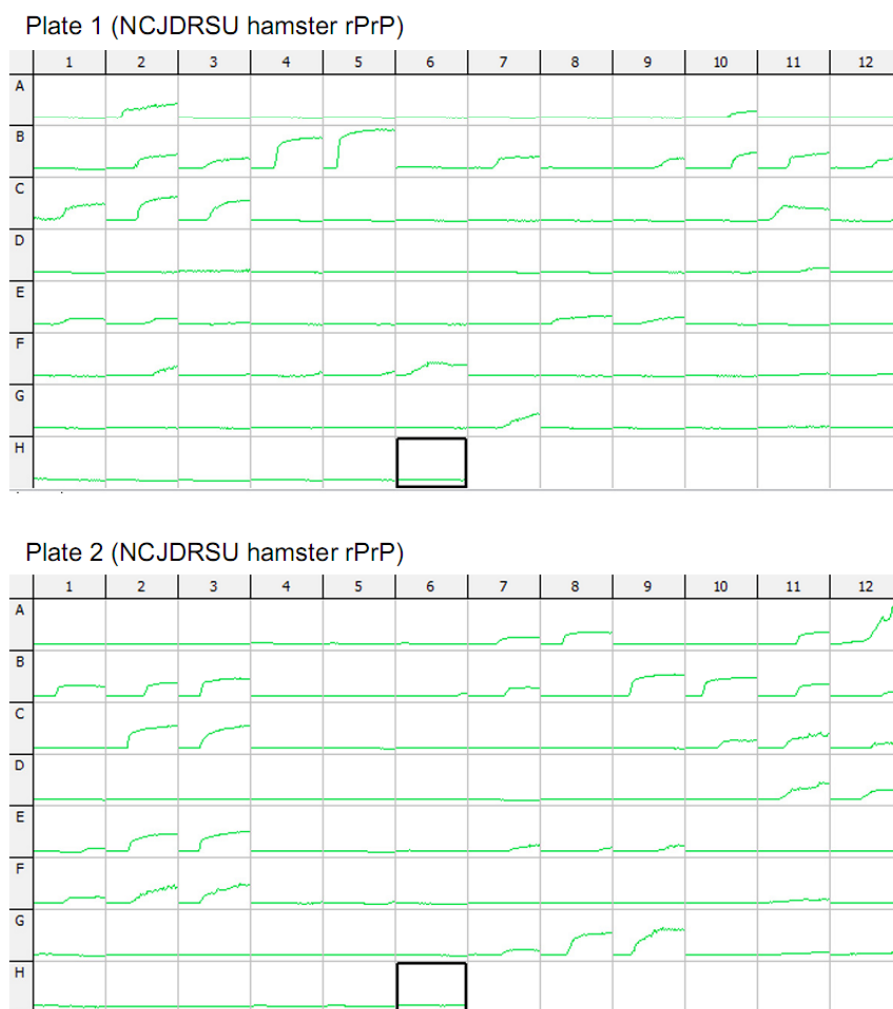


**Figure 19. Testing reliability of RT-QuIC using NCJDRSU supplied hamster rPrP substrate and human CSF for diagnosis of CJD (second round).** Each sample was tested in triplicate and RT-QuIC was performed twice independently (plate 1 and 2). Results of two runs are not fully comparable with each other, e.g., A2 is positive in plate 1 but negative in plate 2, A7 and A8 are negative in plate 1 but positive in plate 2. Each well was seeded with 30  $\mu$ l of CSF into 70  $\mu$ l of substrate preparation containing 100  $\mu$ g/ml hamster rPrP (final concentration). Summary is shown in Table 5.

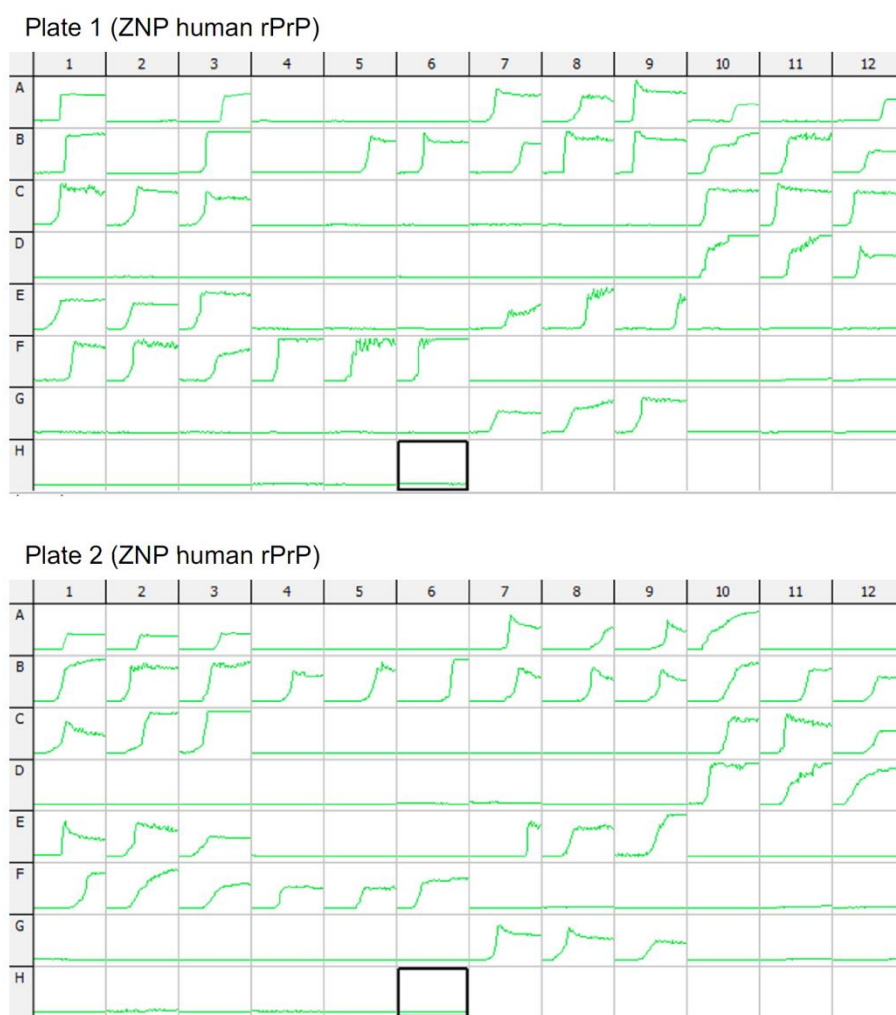


**Figure 20. Testing reliability of RT-QulC using self-prepared human rPrP substrate and human CSF for diagnosis of CJD (second round).** Each sample was tested in triplicate and RT-QulC was performed twice independently (plate 1 and 2). Constantly, fluorescence provided by human rPrPres shows higher performance than that of hamster rPrPres shown in Figure 19, indicating that more  $\beta$ -sheet rich rPrPres is formed in these reactions. It is noteworthy that results of this figure are from 72 h while those in Figure 19 are from 120 h, suggesting that human rPrP substrate is more sensitive to detect human PrP<sup>Sc</sup> in RT-QulC. Each well was seeded with 10  $\mu$ l of CSF into 90  $\mu$ l of substrate preparation containing 100  $\mu$ g/ml human rPrP (final concentration). Comparison of profiles is shown in Figure 19. Summary is shown in table 5.

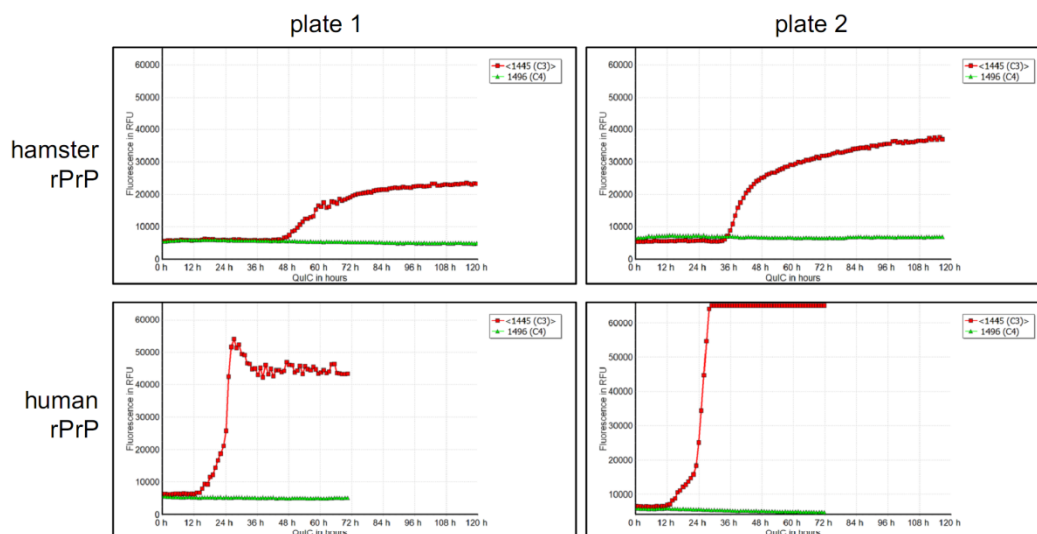


**Figure 21. Zoom-in profiles of RT-QulC result of directly comparing the performance of hamster rPrP substrate to human rPrP.** C3 and C4 wells seeded with identical cases (1445 and 1496) in each plate shown in Figure 19 and 20 were chosen. Positive reactions using hamster rPrP show lag-phases from 30 to 40 h and fluorescence intensities (RFU) from 20 000 to 40 000 which are caused by amplification of PrP<sup>Sc</sup> in 30  $\mu$ l of human CJD CSF. Reactions using human rPrP provide < 24 h of lag-phases and 50 000 to above 60 000 RFU which are caused by only 10  $\mu$ l of human CJD CSF. Due to the high performance of human rPrP substrate, we concluded that it is not essential to run these reactions longer than 72 h.

**Table 5. Summary of the second batch of collaborated blind test (NCJDRSU confirmed results)**

CSF No. (30 cases)	well No. (96-well plate)	NCJDRSU rPrP (positive/3 parallel)			ZNP rPrP (positive/3 parallel)		
		test 1	test 2	diagnosis	test 1	test 2	diagnosis
1180	A1-A3	1/3	0/3	CJD	2/3	3/3	CJD
1187	A4-A6	0/3	0/3	no	0/3	0/3	no
1215	A7-A9	0/3	2/3	CJD	3/3	3/3	CJD
1247	A10-A12	1/3	2/3	CJD	2/3	2/3	CJD
1293	B1-B3	2/3	3/3	CJD	2/3	3/3	CJD
1337	B4-B6	2/3	1/3	CJD	2/3	3/3	CJD
1356	B7-B9	2/3	2/3	CJD	3/3	3/3	CJD
1416	B10-B12	3/3	3/3	CJD	3/3	3/3	CJD
1445	C1-C3	3/3	2/3	CJD	3/3	3/3	CJD
1496	C4-C6	0/3	0/3	no	0/3	0/3	no
1577	C7-C9	0/3	0/3	no	0/3	0/3	no
1929	C10-C12	1/3	3/3	CJD	3/3	3/3	CJD
1974	D1-D3	0/3	0/3	no	0/3	0/3	no
2091	D4-D6	0/3	0/3	no	0/3	0/3	no
2158	D7-D9	0/3	0/3	no	0/3	0/3	no
4051	D10-D12	1/3	2/3	CJD	3/3	3/3	CJD
4060	E1-E3	2/3	3/3	CJD	3/3	3/3	CJD
4384	E4-E6	0/3	0/3	no	0/3	0/3	no
4396	E7-E9	2/3	3/3	CJD	3/3	3/3	CJD
4397	E10-E12	0/3	0/3	no	0/3	0/3	no
4404	F1-F3	1/3	3/3	CJD	3/3	3/3	CJD
4407	F4-F6	3/3	0/3	CJD	3/3	3/3	CJD
4410	F7-F9	0/3	0/3	no	0/3	0/3	no
4412	F10-F12	0/3	0/3	no	0/3	0/3	no
4432	G1-G3	0/3	0/3	no	0/3	0/3	no
4437	G4-G6	0/3	0/3	no	0/3	0/3	no
4454	G7-G9	1/3	3/3	CJD	3/3	3/3	CJD
4545	G10-G12	0/3	0/3	no	0/3	0/3	no
4563	H1-H3	0/3	0/3	no	0/3	0/3	no
4604	H4-H6	0/3	0/3	no	0/3	0/3	no

For those using hamster rPrP from NCJDRSU (red labeled).

- case 1180 (A1-A3), positive in test 1, negative in test 2, diagnose as probable CJD;
- case 1215 (A7-A9), negative in test 1, positive in test 2, diagnose as probable CJD;
- case 4407 (F4-F6), positive in test 1, negative in test 2, diagnose as probable CJD;

For those using ZNP human rPrP (blue labeled).

- cases above are all positive in test 1 and 2, diagnose as definite CJD.

#### 4.2.5 Determining optimal substrates for detection of various prions

I tested for the suitable recombinant prion protein substrates of RT-QuIC to diagnose prion diseases of different types and species. The wild-type full-length recombinant prion proteins of human, hamster, mouse and sheep were purified. These proteins as the substrates were subjected to RT-QuIC reactions seeded by brain samples ( $10^{-8}$  g) of human sCJD (MM1), human vCJD, cattle classic BSE (C-BSE) and cattle low-type BSE (L-BSE), respectively. These reactions were performed at 37°C, 42°C, 50°C and 55°C, respectively (Figure 22).

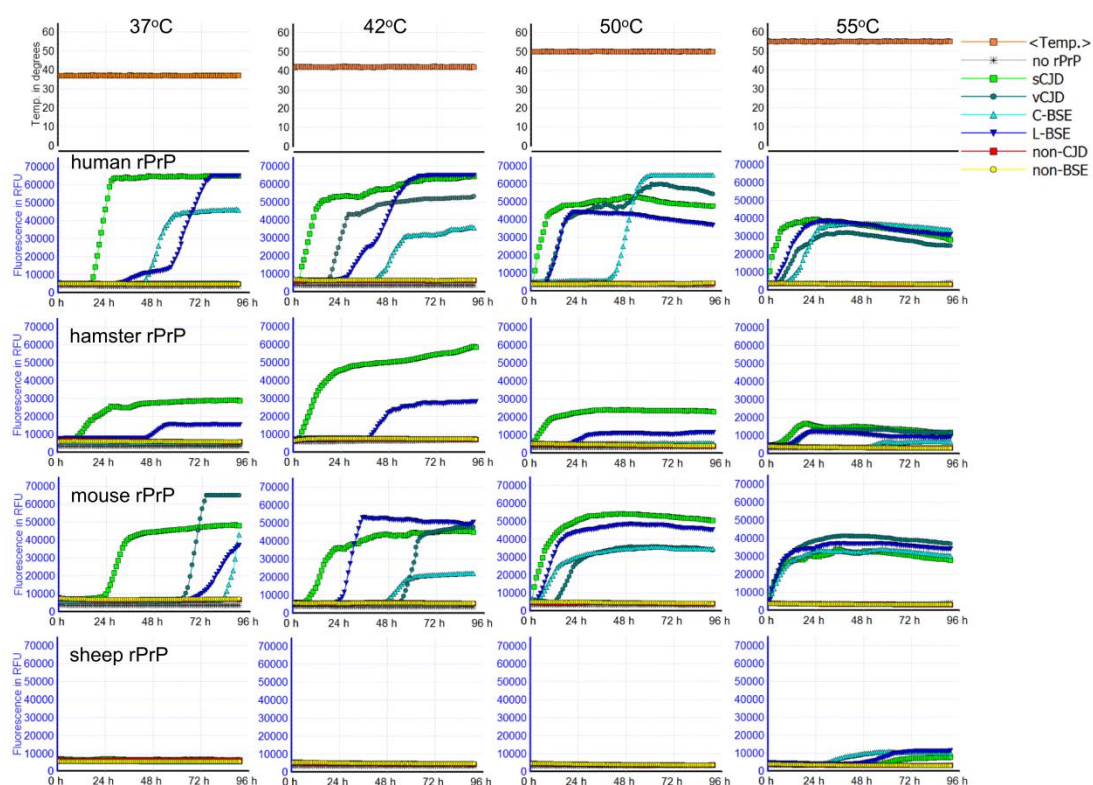


Figure 22. RT-QuIC reactions perform at 37°C, 42°C, 50°C and 55°C by using



**human, hamster, mouse and sheep rPrP, respectively.** These reactions were spiked with  $10^{-8}$  g brain of sCJD (MM1), vCJD, C-BSE and L-BSE for 96 hr of amplification, respectively.  $10^{-8}$  g brain of either non-CJD human or normal cattle was seeded as the negative control. Positive reactions seeded by prion samples result in ascendant curves in RT-QuIC. Neither control seed nor non-rPrP reaction caused false-positive result. Shown are average curve of RT-QuIC curves ( $n = 6$  for each prion type).

I found that human rPrP was suitable to detect all types of prions above at 42°C, 50°C and 55°C with the shortest lag-phases comparing to those reactions using recombinant protein substrates derived from other species. It seemed that reactions seeded with vCJD were not efficient at 37°C. Hamster recombinant prion protein reacted with sCJD and L-BSE seeds, but did not respond to either vCJD or C-BSE. All prion seeds triggered amplifications in the reactions containing mouse recombinant prion protein that has comparable activity with recombinant human prion protein in RT-QuIC. Recombinant sheep prion protein reacted with prion seeds only at 55°C showing low curves, suggesting the insufficient activity of sheep rPrP for RT-QuIC substrate. These results indicate that protein substrates from different species have distinguishable activities of amplifying prions in RT-QuIC. Recombinant prion proteins of human and mouse are converted with higher efficacy than those of the hamster and sheep.

I also tested the activities of recombinant prion proteins derived from 4 species listed above for amplifying relatively low amount of prion ( $10^{-10}$  g of brain) from 3 types of human sCJD (MM1, MV2 and VV2, **Figure 23**) at different temperatures in RT-QuIC. Human recombinant prion protein showed the highest activity at all temperature conditions compared to other species. Human and hamster proteins showed comparable activities of amplifying all types of sCJD prions at 42°C. Mouse recombinant prion protein produced lower curves than those from human and hamster. Sheep protein did not detect low amounts of human sCJD prions. These data indicate that substrates of both human and hamster are suitable for detecting low amounts of sCJD prions, particularly at 42°C. Taking the results of Figure 22 and 23 together, I therefore conclude that recombinant prion proteins of human and hamster are suitable

## Results

to detect human sCJD prions, human and mouse proteins are better to detect human vCJD and cattle BSE, and sheep protein is not suitable to detect human and cattle prions by RT-QulC.

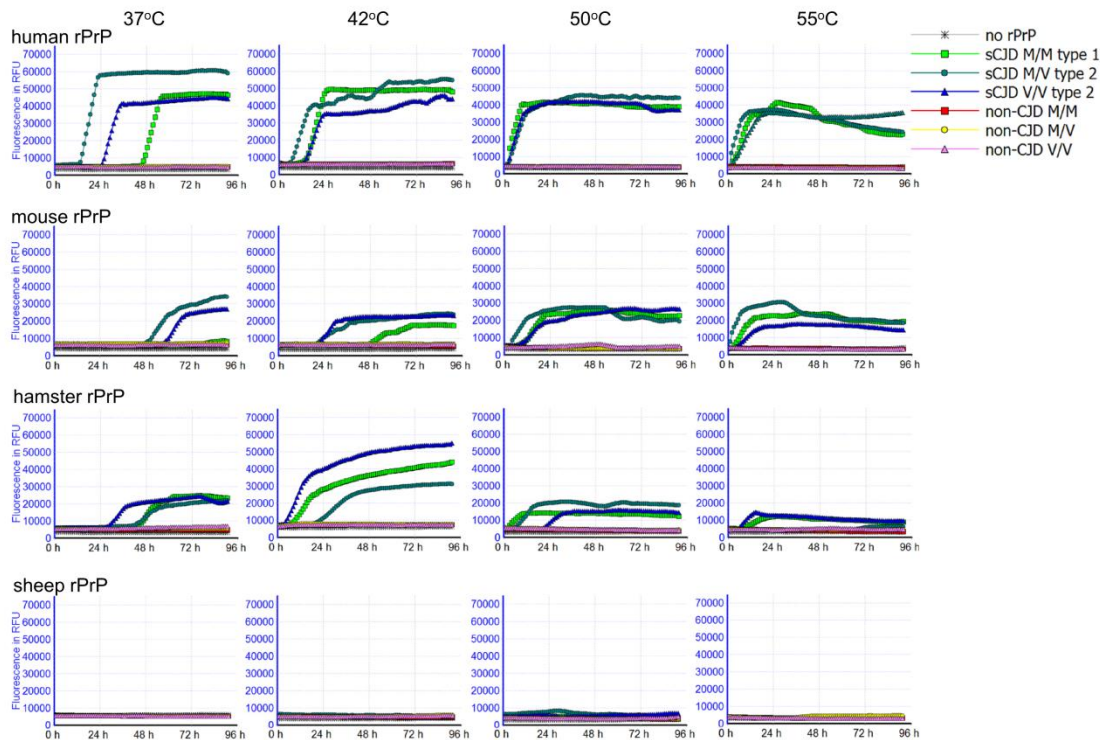


**Figure 23. Detections of CJD prions in the brains ( $10^{-10}$  g of brain) of human sCJD MM1, MV2 and VV2 by using recombinant prion protein substrates of human, mouse, hamster and sheep, respectively.** Reactions were performed at 37°C, 42°C, 50°C and 55°C, respectively.  $10^{-10}$  g brain of genotype-correlated (MM, MV and VV) non-CJD human cases was applied as negative controls in RT-QulC. Neither control seed nor non-rPrP reaction caused false-positive result. Shown are average curve of RT-QulC (n = 6 for each CJD type).

### 4.3 Establishing qRT-QulC for quantification of PrP<sup>Sc</sup> in prion-infected tissues

#### 4.3.1 Establishing quantitative RT-QulC

The mechanism of normal RT-QulC is based upon the conversion of PK-sensitive rPrP into rPrPres conformer, which is rich in  $\beta$ -sheet structures, by seeding the reaction mixture with PrP<sup>Sc</sup> and periodic shaking. The correlation between Thioflavin T (ThT) fluorescence and seeded amount of rPrPres has been shown in **Figure 24** and section 2.2.4. These findings drove me to establish a technique termed quantitative RT-QulC (qRT-QulC).

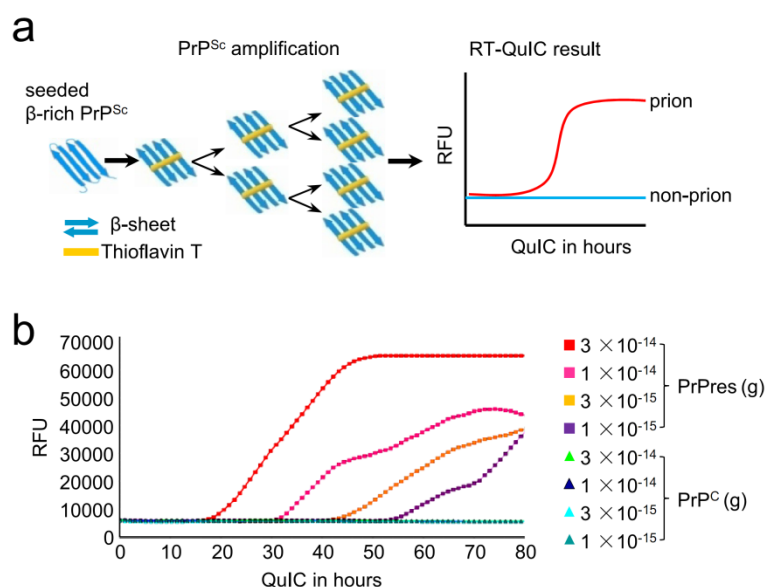


**Figure 24 The basis of amplifying PrP<sup>Sc</sup> with RT-QulC.** (a) Schematic illustration of RT-QulC. PrP<sup>Sc</sup> converts rPrPsen to rPrPres thereby increasing the total amount of  $\beta$ -sheeted PrP. This increase can be demonstrated by the increased ThT-fluorescence. Therefore, the sample containing PrP<sup>Sc</sup> (prion) is distinguished from that without PrP<sup>Sc</sup> (non-prion). RFU, relative fluorescence units. (b) However, it was not the amount of newly formed rPrPres but the lag-time until the steep increase of amplification (ascendant curves) that was related to the seeded quantity of PK-treated PrP<sup>Sc</sup>

(PrPres). Different amounts of purified mouse RML scrapie-prion PrPres and normal mouse PrP<sup>C</sup> were seeded into reactions to perform 80 hours of RT-QuIC. PrP<sup>C</sup> did not cause ascendant curves.

To establish a high-throughput quantification system, PrPres derived from two mouse-adapted scrapie prion strains, RML and ME7, was purified from infected C57BL/6 mouse brains by repeated NaCl precipitation, allowing recovery of 97% of the total PrP<sup>Sc</sup> (Polymenidou et al, 2002). The concentration of PrPres was measured by semi-quantitative Western blotting by comparing band intensities of PrPres to reference samples containing known quantities of rPrP (Saá et al, 2006). To estimate the minimum amount of PrPres equivalent that can start the seeding reaction, I serially diluted PrPres (from  $10^{-8}$  to  $10^{-11.5}$  g) (**Figure 25 a**).  $10^{-9.5}$  g of both RML and ME7 PrPres were visible as a faint band on the WB while  $10^{-10}$  g was not detectable. As the control, PrP<sup>C</sup> from healthy C57BL/6 mouse brain was purified and quantified as above. For controlling the quality of the real-time curve, the ThT-binding fluorescence of both PrPres and PrP<sup>C</sup> was measured (**Figure 25 b**); the results showed that the fluorescence starting from  $10^{-9.5}$  g of PrPres was identical to that of PrP<sup>C</sup> and the blank (no PrP). Since  $10^{-10}$  g of PrPres from both prion strains was undetectable in either WB or ThT-fluorescence, we chose it as the initial seed.

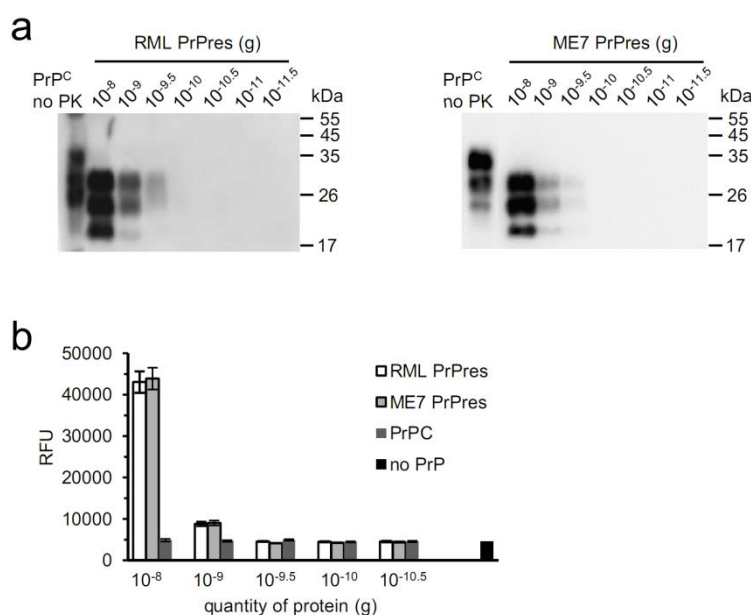


**Figure 25. Directly detecting purified PrPres with WBs and ThT-binding**

**fluorescence.** (a) Purified mouse RML and ME7 scrapie-prion PrPres was serially diluted and detected by immunoblotting. Aliquots were digested with 100 µg/ml Proteinase K (PK) before loading on the gel. Undigested PrP<sup>C</sup> is shown as a migration control. Signals were detected by 4H11 monoclonal antibody. Molecular weights are shown on the right. (b) Fluorescence of purified RML and ME7 PrPres and normal PrP<sup>C</sup> was measured after ThT-binding. The mean and s.e.m. are shown (n=5).

To establish the quantitative RT-QulC (qRT-QulC), the seeds containing  $10^{-10}$  to  $10^{-16}$  g of purified RML and ME7 PrPres and PrP<sup>C</sup> per 10 µl were prepared by serial half-log ( $10^{0.5}$ -fold) dilution (a total of 39 samples). Full-length mouse rPrPsen (amino acids 23-230) was utilized as the substrate. To see if preceding PK-digestion affects the seeding activity of prion seeds in the qRT-QulC reaction, preparations using full-length mouse rPrP (aa 23-231) as substrate were seeded with 1 ng and 0.1 ng of undigested RML-infected brains, and PrPres purified from 1 ng and 0.1 ng of PK-digested brains, followed by qRT-QulC reactions at 37°C for 70 hours (**Figure 26 a**). The results showed practically no differences. In order to maintain comparability of results between qRT-QulC and immunoblotting, we chose PK-digested PrPres as the seed in the experiments presented here if not indicated otherwise. To define the appropriate time-span of qRT-QulC for obtaining reliable results, non-seeded and  $10^{-11}$  g of PrPres seeded qRT-QulC reactions were performed for 140 hours (**Figure 26 b**). This result showed that non-seeded reactions generated spontaneous conversion after 90 hours; this limited the time-span to 90 hours in our study.

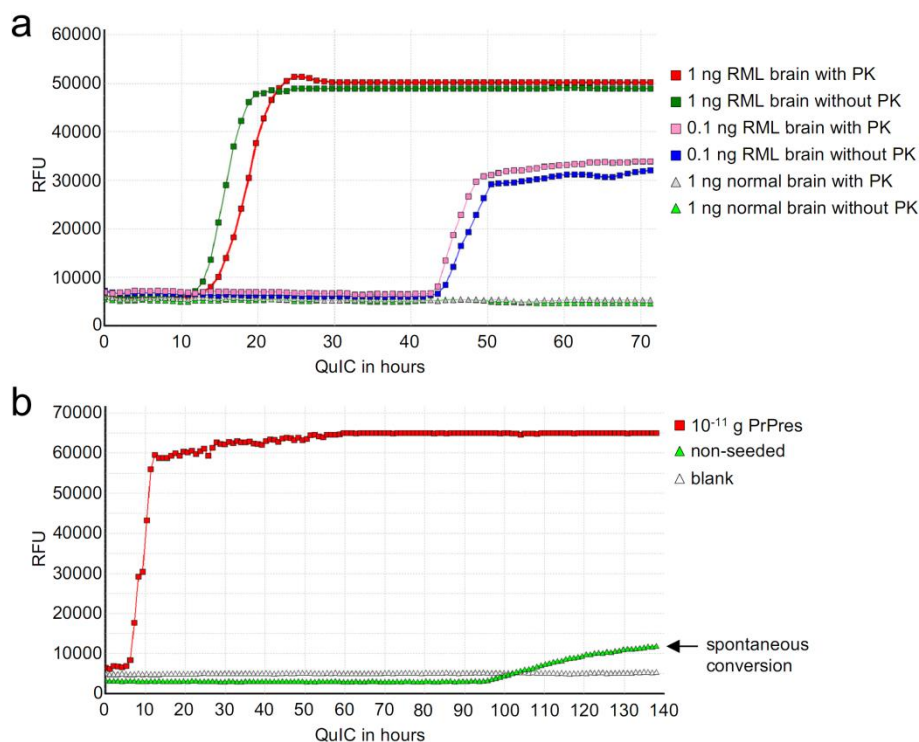


**Figure 26. Determining the seeding activity of PrPres and time span of qRT-QulC.**

(a) Comparing the seeding activity of PK-digested and undigested prion-infected brains. Seeds for RT-QulC were 1 ng and 0.1 ng of original RML brains of terminally ill C57BL/6 mice, or PK-digested PrPres purified from both samples, respectively. PK-digestions were performed at 37°C for 1 h with 20 µg/ml PK followed by sodium chloride precipitation and purification. Reactions seeded by PK-digested and undigested 1 ng of normal C57BL/6 mouse brain were set as controls. (b) RT-QulC reactions with seed ( $10^{-11}$  g of PrPres) and without seed (non-seeded) were performed for 140 hours. The spontaneous conversion of non-seeded reactions is indicated by an arrow. Reactions without seed and substrate (blank) were the control. All profiles represent the means of three parallel reactions. RFU, relative fluorescence unit.

For standardizing the results, a 'positive reaction' of RT-QulC was recorded when the detected intensity of fluorescence was equal or higher than a threshold. The threshold was 3 times the fluorescence of the initial phase (0 h). The corresponding hours required to reach the threshold (Rht) was recorded as the independent variable (x), and the equivalent amount of seeded PrPres was the dependent variable (y), as

shown in **Figure 27 a**. Next, RT-QulC reactions seeded with  $10^{-10}$  to  $10^{-16}$  g of PrPres and PrP<sup>C</sup> were performed up to 90 h (**Figure 27 b**). Five repeats of RT-QulC for each seeded amount of PrPres and PrP<sup>C</sup> equivalents (a total of 260 reactions) were tested. Reactions seeded with  $10^{-10}$  to  $10^{-15.5}$  g of PrPres were positive within 90 h whereas most of those seeded with  $10^{-16}$  g PrPres were negative. Reactions seeded with different amounts of PrP<sup>C</sup> did not show spontaneous conversion up to 90 h. Therefore, the RT-QulC allowed detecting  $10^{-15.5}$  g ( $\approx 0.32$  fg) of PrPres, which was 1 million times more sensitive than the WB shown in **Figure 25 a**. By analyzing the distribution of the required hours mathematically using a standard tool (Microsoft Excel), we obtained calibration curves and derived two formulas for calculating the quantities of seeded RML and ME7 PrPres in the qRT-QulC system (**Figure 27 c**). Details of running dose-response reactions to obtain those Rhts are shown in **Figure 28, 29 and 30**.

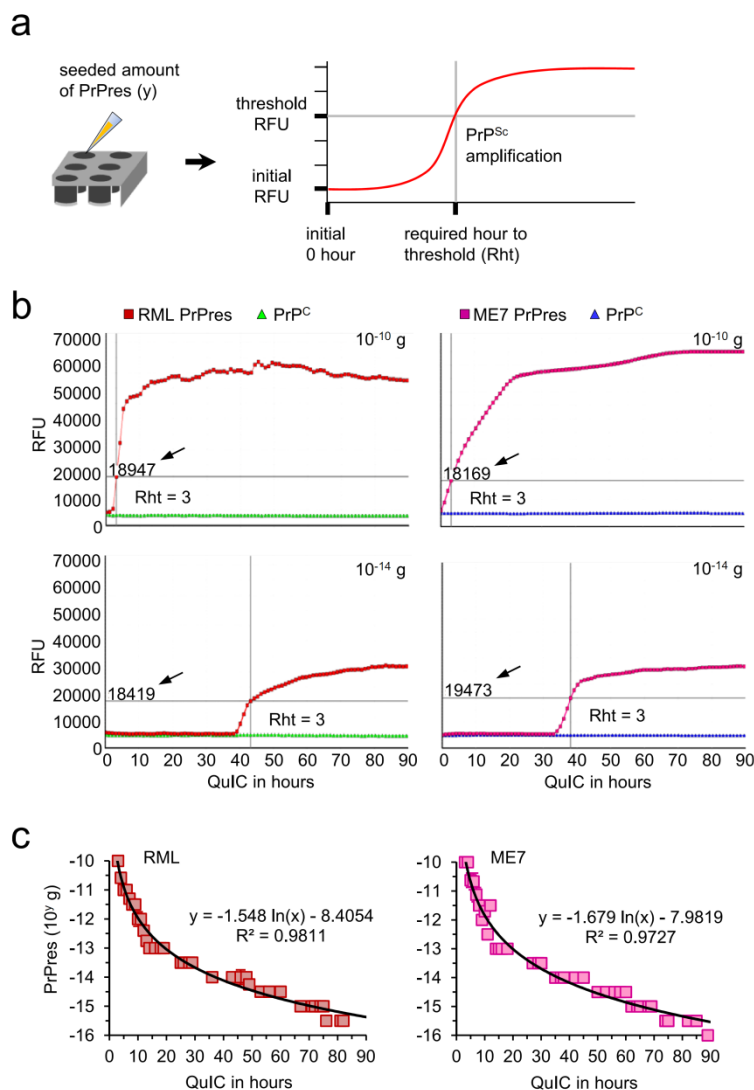


**Figure 27. Establishing the quantitative RT-QulC (qRT-QulC).** (a) Schematic illustration of qRT-QulC. The PrPres propagating duration (hour) required to reach the threshold (Rht) which was at least 3 times the starting fluorescence was set as the independent variable (x), the correlated seeded amount of PrPres was the dependent variable (y). (b) Different amounts of purified PrPres ( $10^{-10}$  to  $10^{-16}$  g with serial  $10^{0.5}$ -fold dilution) were seeded into RT-QulC reactions using mouse rPrP as the substrate. RT-QulC process was followed from 0 to 90 h by showing the number of hours required to reach the threshold (indicated by black arrows and intersecting lines). Purified PrP<sup>C</sup> with identical amounts was seeded in independent RT-QulC reactions as control. Seeded amounts of both PrPres and PrP<sup>C</sup> are indicated on the top right. (c) The results from five repeats of RT-QulC seeded by PrPres were



provided to yield standard calibration curves and formulas for quantification. This relates QuIC time necessary to reach the threshold to the amount of seeded PrPres. The mean and s.e.m. are shown (n=5).

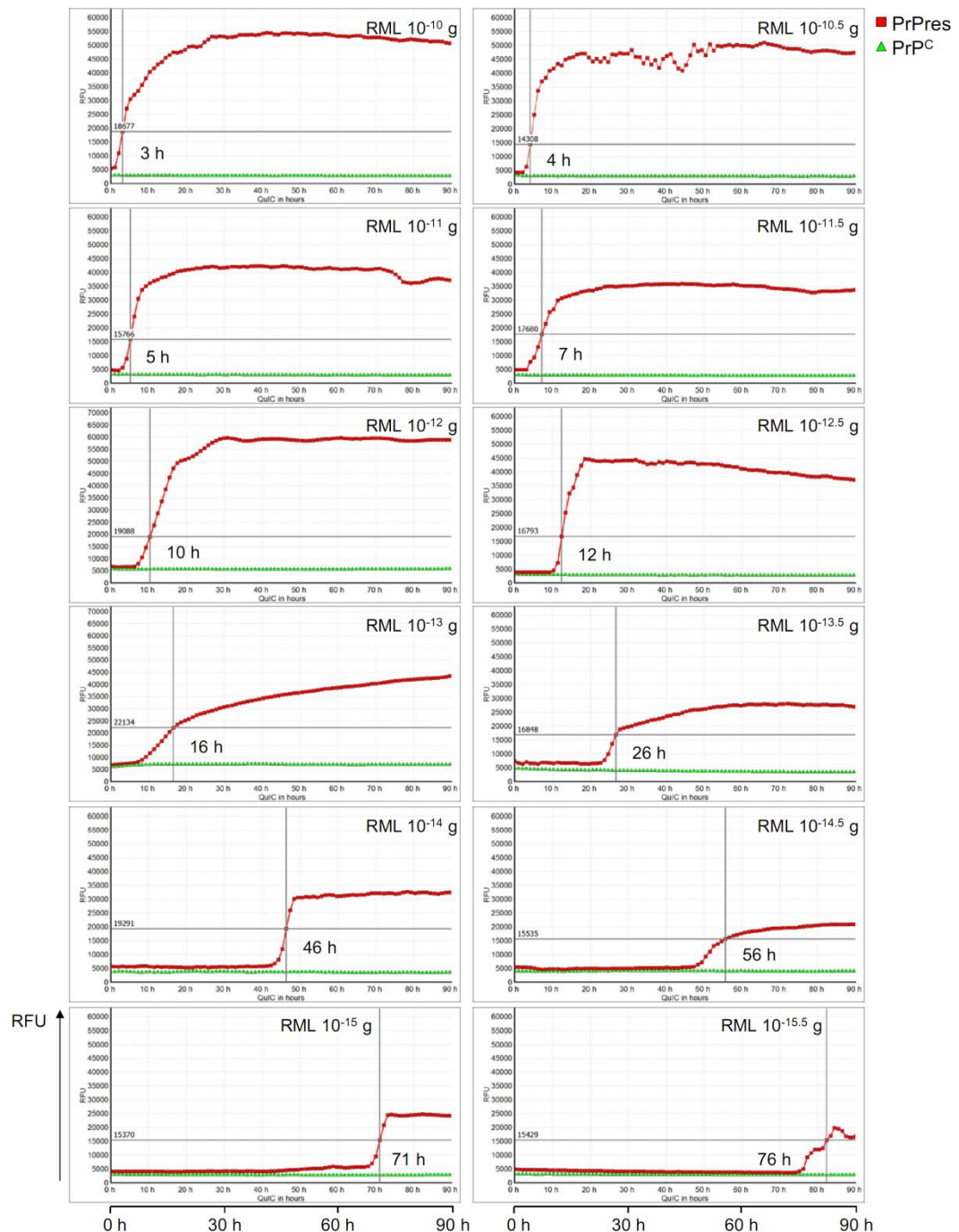


**Figure 28. Detecting seeded RML PrPres with RT-QuIC.** Purified RML PrPres and

## Results

control PrP<sup>C</sup> with the quantities from  $10^{-10}$  to  $10^{-16}$  g were seeded into reactions independently to perform 90 h of RT-QuIC at 37°C.

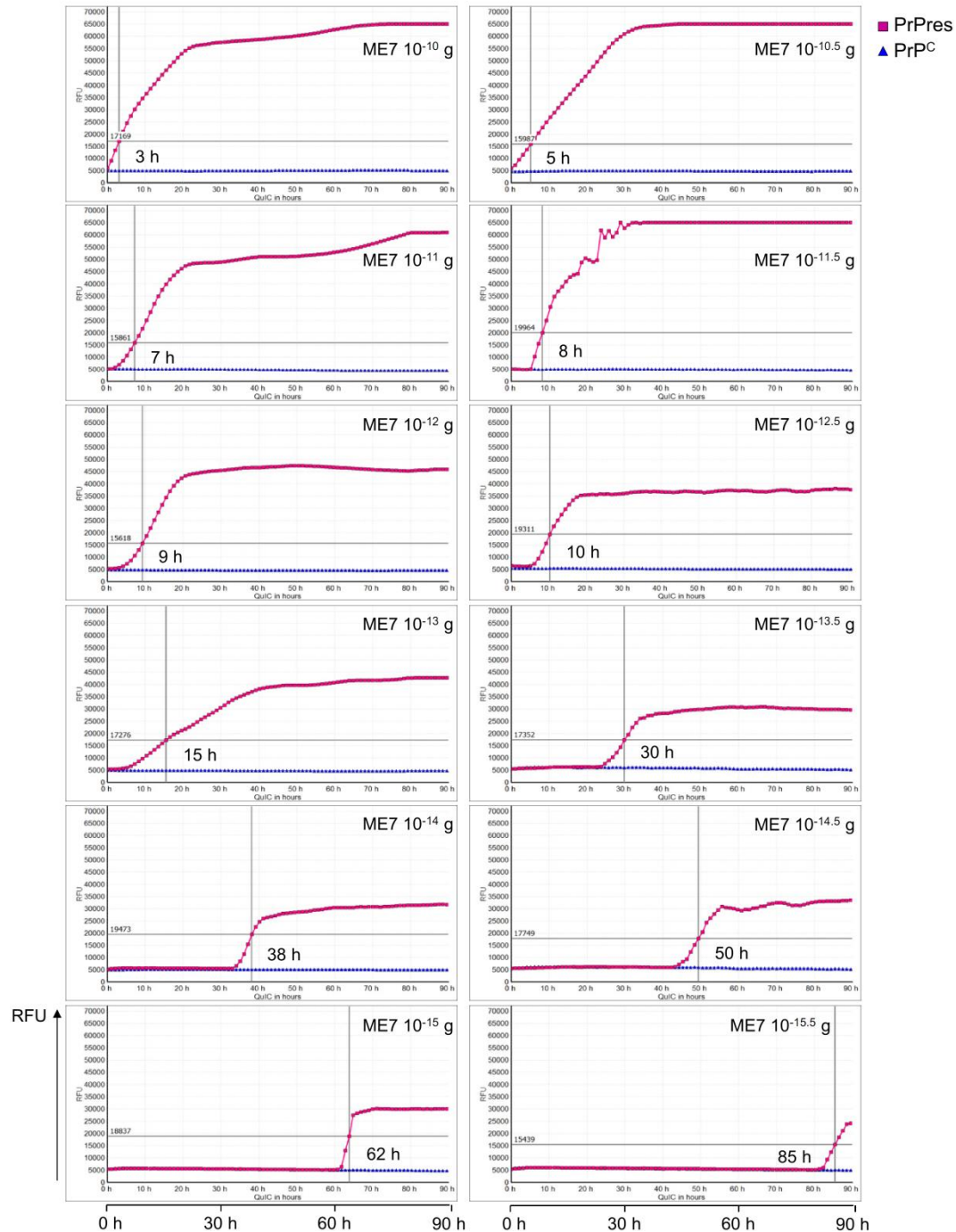


**Figure 29. Detecting seeded ME7 PrPres with RT-QuIC.** Purified ME7 PrPres and control PrP<sup>C</sup> with the quantities from  $10^{-10}$  to  $10^{-16}$  g were seeded into reactions

independently to perform 90 h of RT-QuIC at 37°C.

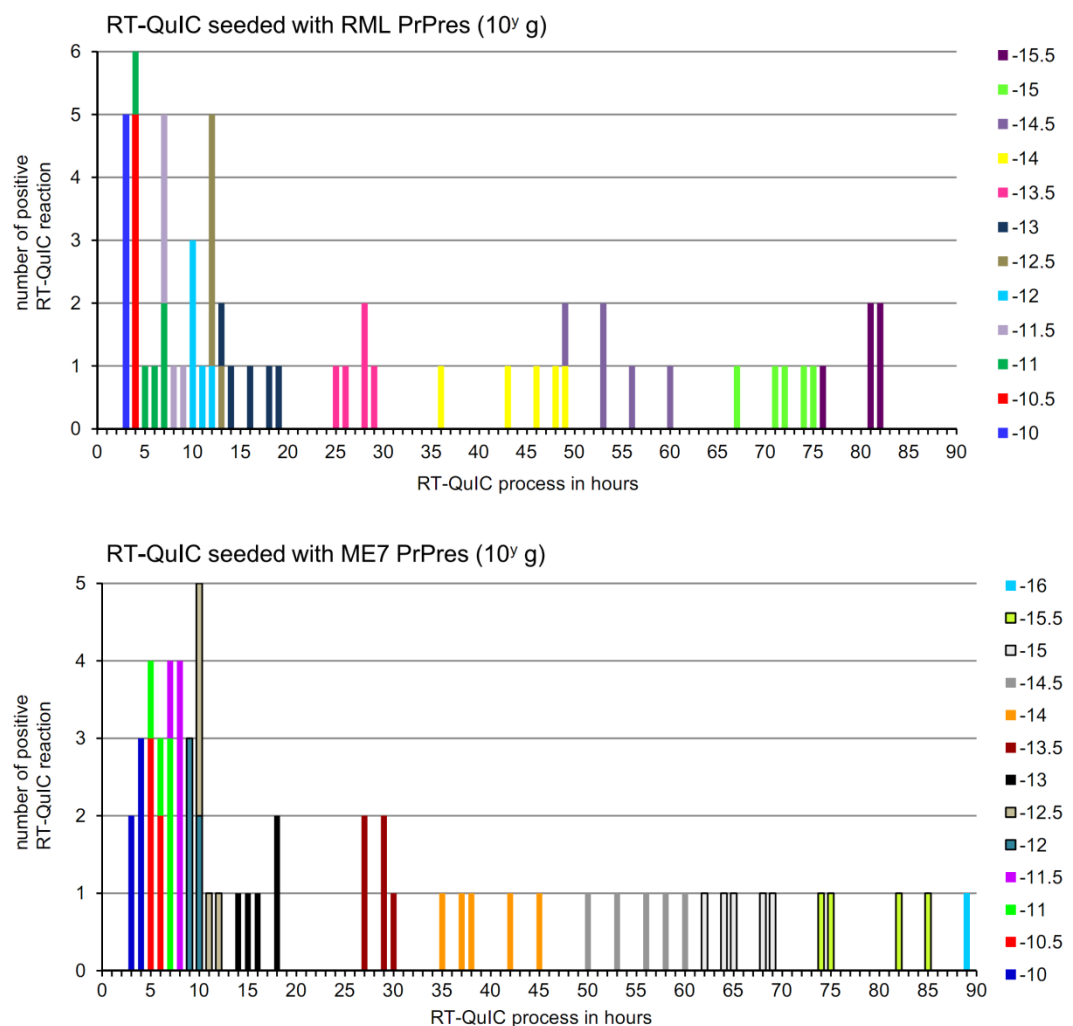


**Figure 30. Positive RT-QuIC reactions seeded with PrPres (10<sup>-10</sup> to 10<sup>-15.5</sup> g for RML and 10<sup>-10</sup> to 10<sup>-16</sup> g for ME7) within 90 h are shown.** Each scale on the Y-axis represents one effective reaction, the X-axis indicates the required hours corresponding to the reaction. The reactions seeded with 10<sup>-16</sup> g of RML PrPres were negative up to 90 h and thus are not shown in the figure.

#### 4.3.2 Quantification of PrPres in peripheral organs

To investigate the feasibility of qRT-QuIC to determine the progression of prion

disease, qRT-QulC was used to measure PrPres at different days post inoculation (dpi). 30, 60, 90, 120, 135, 150 and 170 dpi were chosen for RML, 30 to 150 dpi were chosen for ME7, since 170 dpi denotes the terminal stage of the RML strain while 150 dpi is the terminal stage of the ME7 strain. Groups of each 5 C57BL/6 mice were inoculated intracerebrally and the brains and peripheral tissues (heart, liver, spleen, lung, kidney and hind-limb muscle) were harvested at the dpi indicated above. The tissues of age-related healthy C57BL/6 mice were chosen as controls ( $n = 5$  for each dpi). 10 mg of each tissue were treated with the method of purifying PrPres for obtaining tissue extracts as the seeds of RT-QulC reactions. This purification step was important to remove potential components affecting RT-QulC efficiency. Since the PrPres level is much higher in the brain than in other organs, 1 mg of brain from infected mice of different time-points was first analyzed by Western blotting for obtaining an overview of the presence of PrPres (**Figure 31 a**). By Western blotting, neither in RML nor in ME7 was PrPres detectable at 30 and 60 dpi, in both strains PrPres first appeared at 90 dpi and showed a steady increase to the terminal stage. For the preparation of RT-QulC seeds, the brain extracts of 90 to 170 dpi of the brain were diluted  $10^4$ -fold, and those of the spleen and muscle were diluted 10-fold. Before measuring PrPres concentrations in peripheral organs, a comparison was done to estimate the reliability of qRT-QulC (**Figure 31 b**). The results showed that PrPres concentrations in the brains obtained from qRT-QulC were comparable to those from quantitative Western blottings at different time points after inoculation (**Table 6**), indicating that qRT-QulC is suited to measure the PrPres concentrations.

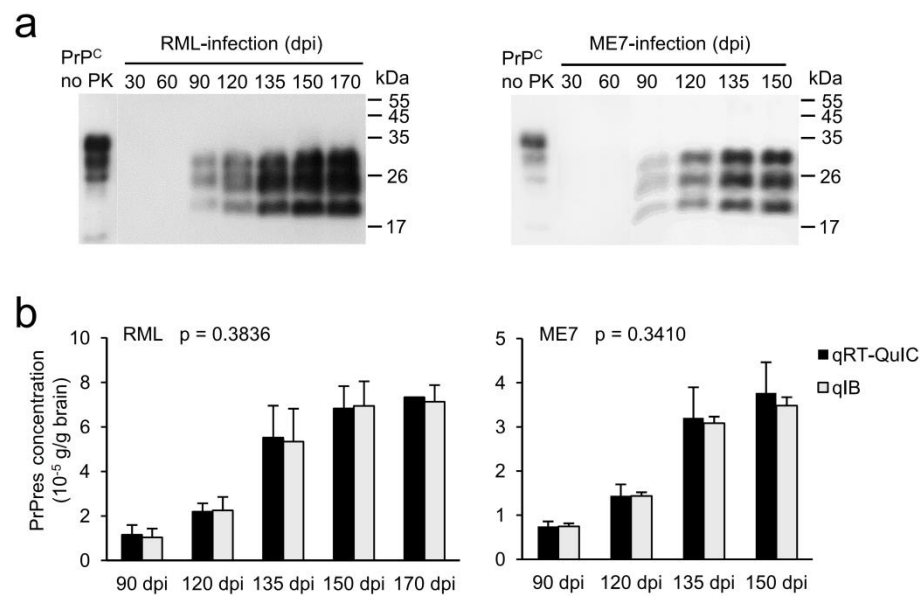


**Figure 31 Quantification of RML and ME7 PrPres in brain at various days post infection (dpi).** (a) 1 mg of brain from scrapie-infected mice at was analyzed by WBs after digestion with 100 µg/ml PK. PrP<sup>C</sup> is shown as a migration control. Signals were detected by 4H11 monoclonal antibody. M<sub>r</sub> is shown on the right. (b) Comparing PrPres concentrations measured by quantitative RT-QuIC and qIB (quantitative Western blot). The brains of RML-inoculated mice 90 dpi to 170 dpi and ME7-inoculated mice 90 to 150 dpi were chosen regarding the capacity of immunoblotting to detect PrPres from the time-point not earlier than 90 dpi. After comparing the quantitations obtained by qRT-QuIC and qIB, the significance (p value) was calculated with two-way ANOVA by using detecting methods and time-points as the variables. Shown data are mean and s.e.m (n = 5).

**Table 1. Comparing PrPres concentrations measured by quantitative RT-QulC and quantitative Western blot.**

		PrPres concentration ( $\times 10^{-5}$ g/g brain)	
		with quantitative RT-QulC (qRT-QulC)	with quantitative Western blot (qIB)
RML	90 dpi	$1.16 \pm 0.44$	$1.4 \pm 0.40$
	120 dpi	$2.19 \pm 0.38$	$2.25 \pm 0.61$
	135 dpi	$5.51 \pm 1.44$	$5.34 \pm 1.48$
	150 dpi	$6.83 \pm 1.00$	$6.94 \pm 1.10$
	170 dpi	7.33	$7.13 \pm 0.75$
ME7	90 dpi	$0.75 \pm 0.11$	$0.75 \pm 0.07$
	120 dpi	$1.44 \pm 0.26$	$1.44 \pm 0.08$
	135 dpi	$3.20 \pm 0.69$	$3.08 \pm 0.15$
	150 dpi	$3.77 \pm 0.69$	$3.48 \pm 0.19$

After 90 h of amplification I calculated the concentration of PrPres equivalents based on the detected seeding activity by using the formulas in **Figure 27 c**. The levels of PrPres equivalents (i.e. seeding activity) in the brain showed the expected increasing tendency (**Figure 32**). In particular, seeding activity reached the highest levels at 170 dpi in the RML strain and 150 dpi in the ME7 strain. The detection of seeding activity from 30 to 90 dpi of both prion strains was negative in the heart and hind-limb muscle, but the signals from the heart started to show at 135 dpi in the RML strain and 120 dpi in the ME7 strain, while those from muscle were positive starting at 120 dpi of the RML strain and 90 dpi of ME7. Interestingly, seeding activity in the liver and kidney in the RML strain was detectable in early stages (30 and 60 dpi), and disappeared during the intermediate stages of infection (90, 120 and 135 dpi), whereas those of ME7-infection were continuously negative until 135 dpi. Seeding activity in the spleen of both prion strains was decreasing at early stages followed by an increase in the intermediate stages. The concentration of PrPres equivalents in all three tissues was increased at late to final stages. No seeding activity was detected in the lungs at any time. Since qRT-QulC was 1 million times more sensitive than normal WB, these results suggest a possibility of using qRT-QulC to track disease progression or analyze prion propagation in various tissues.

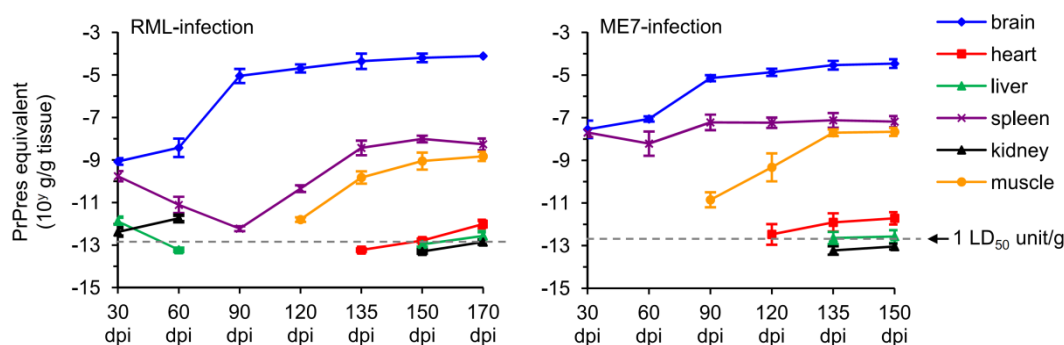


**Figure 32.** Seeding activity (expressed as PrPres equivalents in g/g tissue) in various tissues from different time-points after inoculation was measured by qRT-QulC by using the formulas shown in **Figure 27 c**. The PrPres concentration corresponding to 1 LD<sub>50</sub> units per gram of tissue is represented by a gray broken line. Shown are the mean and s.e.m. (n=5).

To demonstrate the feasibility of qRT-QulC in the assessment of bio-hazard risks, the concentration of PrPres/g tissue (g/g) in various tissues measured by qRT-QulC was compared to the reported half-lethal doses (LD<sub>50</sub>) of both prion strains. The known LD<sub>50</sub> of RML and ME7 are 10<sup>-8.8</sup> and 10<sup>-8.3</sup> g of terminal brains, respectively (Browning et al, 2011). Using the PrPres concentration measured by qRT-QulC, we can roughly extrapolate that 1 LD<sub>50</sub> unit contained 10<sup>-12.93</sup> g of PrPres for RML and 10<sup>-12.72</sup> g for ME7. One LD<sub>50</sub> unit is shown as the gray dotted lines in **Figure 32** to indicate the extent of prion concentration in each gram of tissue (**Table 7** and **8**), suggesting that qRT-QulC can be used for estimating prion contamination in biological materials. As our protocol uses an extraction method for PrPres prior to qRT-QulC that removes potentially interfering factors present in peripheral tissues, the calibration curve obtained for brain-derived PrPres should also provide meaningful results for other tissues from the same species. Moreover, our findings for RML and ME7 indicate that similar assay conditions can be efficient for different strains. However, to ensure optimum sensitivity, the exact conditions of the qRT-QulC assay need to be established for different species and strains.

**Table 7. The concentration of PrPres in 7 tissues from RML scrapie-infected mice of 7 time-points**

	PrPres concentration in tissues (g/g brain)						
	brain	heart	liver	spleen	lung	kidney	muscle
30 dpi	$(9.05 \pm 1.48) \times 10^{-10}$	Neg.	$(1.42 \pm 0.25) \times 10^{-12}$	$(1.98 \pm 0.52) \times 10^{-10}$	Neg.	$(4.50 \pm 0.92) \times 10^{-13}$	Neg.
60 dpi	$(5.21 \pm 1.61) \times 10^{-9}$	Neg.	$^*(6.07 \pm 0.45) \times 10^{-14}$	$(1.05 \pm 0.41) \times 10^{-11}$	Neg.	$(1.89 \pm 0.27) \times 10^{-12}$	Neg.
90 dpi	$(1.16 \pm 0.44) \times 10^{-5}$	Neg.	Neg.	$(6.10 \pm 0.73) \times 10^{-13}$	Neg.	Neg.	Neg.
120 dpi	$(2.19 \pm 0.38) \times 10^{-5}$	Neg.	Neg.	$(4.78 \pm 0.82) \times 10^{-11}$	Neg.	Neg.	$(1.62 \pm 0.17) \times 10^{-12}$
135 dpi	$(5.52 \pm 1.44) \times 10^{-5}$	$^*(5.86 \pm 0.27) \times 10^{-14}$	Neg.	$(4.60 \pm 1.24) \times 10^{-9}$	Neg.	Neg.	$(1.73 \pm 0.35) \times 10^{-10}$
150 dpi	$(6.83 \pm 1.01) \times 10^{-5}$	$(1.64 \pm 0.09) \times 10^{-13}$	$^*(1.13 \pm 0.18) \times 10^{-13}$	$(1.03 \pm 0.15) \times 10^{-8}$	Neg.	$^*(5.38 \pm 0.39) \times 10^{-14}$	$(1.31 \pm 0.64) \times 10^{-9}$
170 dpi	$7.33 \times 10^{-5}$	$(1.07 \pm 0.22) \times 10^{-12}$	$(2.95 \pm 0.57) \times 10^{-13}$	$(6.42 \pm 1.77) \times 10^{-9}$	Neg.	$(1.42 \pm 0.16) \times 10^{-13}$	$(1.63 \pm 0.33) \times 10^{-9}$

Neg indicates the RT-QuIC reaction is negative up to 90 hours. The mean and s.e.m are shown. Concentration of PrPres lower than one LD<sub>50</sub> unit per gram of brain ( $1.16 \times 10^{-13}$  g/g brain) is indicated by sparkle

**Table 8. The concentration of PrPres in 7 tissues from ME7 scrapie-infected mice of 6 time-points**

	PrPres concentration in tissues (g/g brain)						
	brain	heart	liver	spleen	lung	kidney	muscle
30 dpi	$(3.64 \pm 1.97) \times 10^{-8}$	Neg.	Neg.	$(2.20 \pm 1.06) \times 10^{-8}$	Neg.	Neg.	Neg.
60 dpi	$(9.01 \pm 2.31) \times 10^{-8}$	Neg.	Neg.	$(1.34 \pm 1.14) \times 10^{-8}$	Neg.	Neg.	Neg.
90 dpi	$(7.96 \pm 0.78) \times 10^{-6}$	Neg.	Neg.	$(8.20 \pm 5.79) \times 10^{-8}$	Neg.	Neg.	$(1.77 \pm 1.16) \times 10^{-11}$
120 dpi	$(1.51 \pm 0.80) \times 10^{-5}$	$(4.90 \pm 4.62) \times 10^{-13}$	Neg.	$(6.56 \pm 3.48) \times 10^{-8}$	Neg.	Neg.	$(1.18 \pm 1.00) \times 10^{-9}$
135 dpi	$(3.56 \pm 1.88) \times 10^{-5}$	$(1.75 \pm 1.44) \times 10^{-12}$	$(2.67 \pm 1.45) \times 10^{-13}$	$(9.57 \pm 1.70) \times 10^{-8}$	Neg.	$^*(6.45 \pm 2.92) \times 10^{-14}$	$(2.09 \pm 0.79) \times 10^{-8}$
150 dpi	$(3.77 \pm 1.55) \times 10^{-5}$	$(2.23 \pm 1.14) \times 10^{-12}$	$(3.20 \pm 1.85) \times 10^{-13}$	$(7.48 \pm 3.76) \times 10^{-8}$	Neg.	$^*(9.43 \pm 3.00) \times 10^{-14}$	$(2.34 \pm 0.98) \times 10^{-8}$

Neg indicates the RT-QuIC reaction is negative up to 90 hours. The mean and s.e.m are shown. Concentration of PrPres lower than one LD<sub>50</sub> unit per gram of brain ( $1.89 \times 10^{-13}$  g/g brain) is indicated by sparkle.



## 4.4 Monitoring anti-prion treatment by quantifying PrP<sup>Sc</sup> in the urine

As described in the Introduction, an effective anti-prion compound anle138b has been developed for treating prion disease. The common strategy of monitoring PrPres levels in the brains harvested at different time-points of prion incubation period to estimate disease progress and therapeutic efficacy is acceptable for experiments in rodents, but it is not applicable for further clinical tests in humans. For human trials, a safer technique is needed that detects PrPres in samples easily obtained, e.g., urine, to evaluate the treatment. Since the sensitive and specific qRT-QuIC had been established, I chose qRT-QuIC to track progress of prion disease in anle138b-treated mice by quantifying PrPres in the urine.

### 4.4.1 Testing the reliability of quantifying PrPres with qRT-QuIC

To address the reliability of quantification, the standard quantities of RML PrPres purified from 2 mg of infected brains of anle138b-treated and untreated mice of different dpi (80, 120 and 170 dpi, and 250 dpi of treated mice) were separated and detected by Western blottings (**Figure 33a**). 80 dpi was chosen since the PrPres in the brain at this stage was visible in both immunohistochemistry and WB (Wagner et al, 2013). 170 dpi was the terminal stage of untreated mice and 250 dpi was that of treated ones. Quantities of PrPres were calculated by comparing the signal intensities with those of a known amount of rPrP. Results were analyzed statistically to assess deceleration of prion propagation in brains after drug treatment (**Figure 33b**). Concentrations of PrPres in untreated mouse brains increased rapidly to reach high levels at the terminal stage of RML-infection (170 dpi), which was significantly different from the slight increases in treated mice brains ( $p = 0.006$ ). The treated mice reached a terminal stage at 250 dpi presumably due to the accumulative neuronal toxicity of prions although the PrP<sup>Sc</sup> level was lower than in the untreated ones; a similar observation has been reported previously (Kawasaki et al, 2007). These data indicate that anle138b prolongs the incubation period of infection by inhibiting prion propagation in the brain.

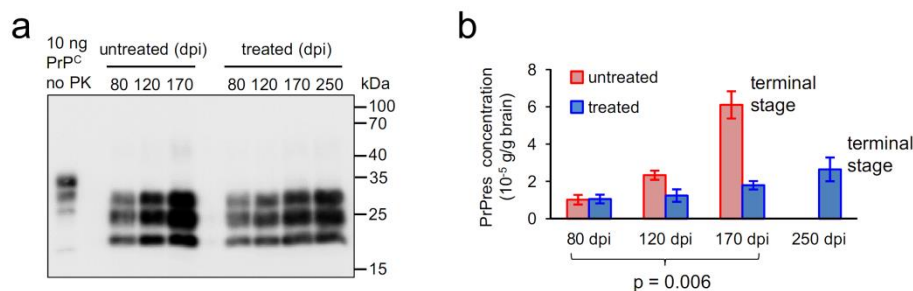


**Figure 33. Western blotting measured PrPres concentrations in the brains of different dpi.** (a) Purified PrPres from 2 mg of brain of different dpi of treated and untreated mice were detected by immunoblotting. PrP<sup>C</sup> is the migration control on the left. Molecular weights are shown on the right. (b) The concentrations of PrPres in the brains (g/g) of 5 mice of each time points were measured by quantitative immunoblotting densitometrically. Significance of comparing PrPres quantitations of treated and untreated mice was calculated with the t-test ( $p = 0.006$ ).

To measure the accuracy of qRT-QulC, PrPres purified from anle138b-treated and untreated mouse brains was serially diluted ( $10^{-7}$ ,  $10^{-8}$ ,  $10^{-9}$  and  $10^{-10}$  g of brains,  $n = 5$ ) followed by seeding into qRT-QulC preparations. Profiles of detecting PrPres in  $10^{-10}$  g brains with qRT-QulC are shown in **Figure 34 a** to demonstrate the number of hours required to initiate reactions seeded with PrPres. Using the formula in **Figure 27 c**, PrPres equivalents were quantified and were converted to PrPres concentrations (g/g brain) with extrapolation to compare with quantities detected by Western blotting (**Figure 34 b**). Quantitation results from two methods did not show significant differences on measuring PrPres concentrations ( $p = 0.1276$  for untreated groups and  $p = 0.5673$  for anle138b-treated groups) indicating that qRT-QulC provided accuracies comparable to Western blotting. Due to the extremely high sensitivity (**Figure 27 a and b**) as well as the reliable quantification, we argued that qRT-QulC was competent to quantify the PrPres in materials containing minimal amounts of PrP<sup>Sc</sup>.

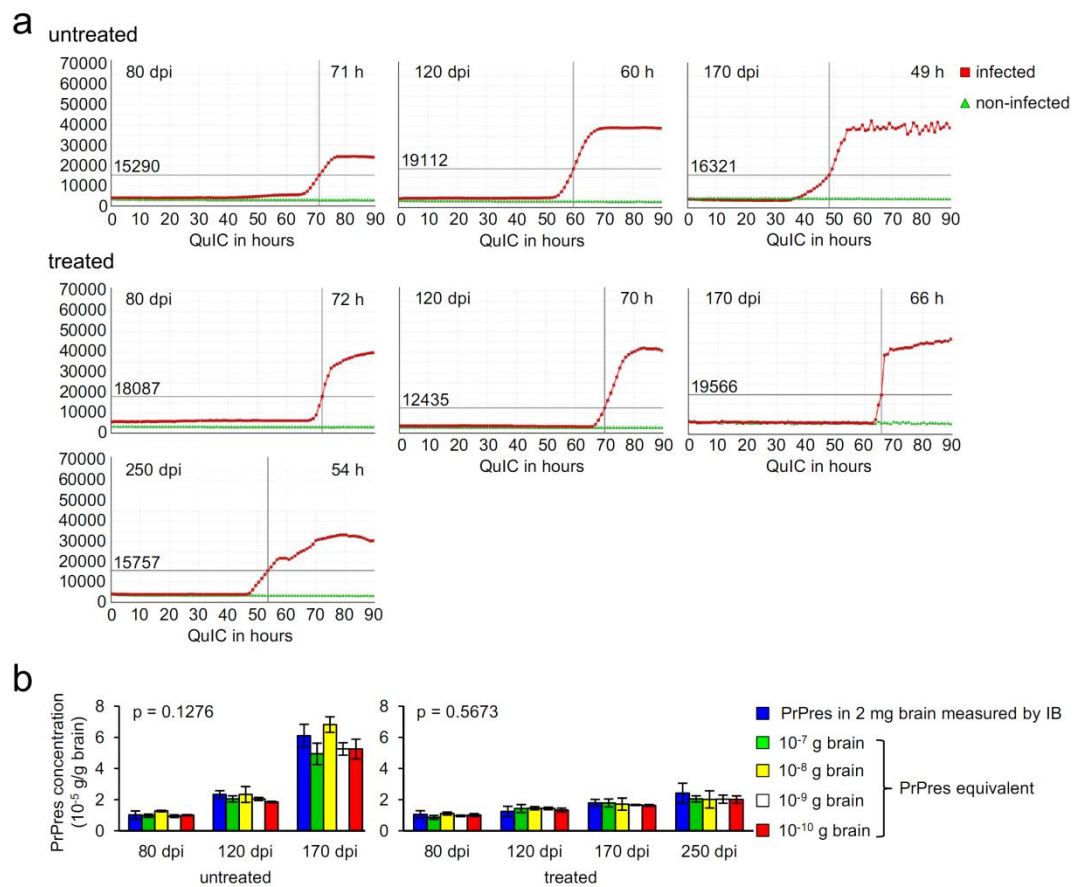


**Figure 34. PrPres concentrations measured by qRT-QuIC are comparable to the results of Western blotting.** (a) PrPres purified from  $10^{-10}$  g of brains of different dpi was measured by qRT-QuIC. The required hours for measuring PrP<sup>Sc</sup> concentrations are indicated on the top right. PK-digested  $10^{-10}$  g of brains from uninfected mice was seeded as controls. (b) The PrPres equivalents from  $10^{-7}$  g to  $10^{-10}$  g of brain of different dpi from treated and untreated mice were measured by performing qRT-QuIC. PrPres concentrations in the brain (g/g) were calculated by extrapolation using the formula in **Figure 27 c**. Results of qRT-QuIC were compared to the results of Western blotting (IB) as shown in **Figure 33 b**. The significances were calculated by two-way ANOVA using the weight of used brains and dpi as the variables ( $p = 0.1276$  for untreated groups and  $p = 0.5673$  for treated groups).

#### 4.4.2 Quantifying PrPres in the urine monitors anti-prion treatment

The urine samples were harvested from the mice shown in **Figure 33 b**. To remove components potentially affecting qRT-QuIC, urine from both anle138b-treated and untreated mice (200  $\mu$ l from each mouse) was purified following the procedure of isolating PrPres described in Material and Methods to receive 'urine extracts' which contains extremely low amount PrPres that was not visible on Western blots. The urine PrPres was seeded into qRT-QuIC reactions (**Figure 35 a**). For untreated mice, results showed that PrPres was detectable in the urine at both 120 and 170 dpi, but not at 80 dpi. Interestingly, for anle138b-treated mice, PrPres was positive in the urine of 170 and 250 dpi, whereas it was negative in 80 or 120 dpi. In particular, reaction seeded by urine extract from untreated mice of 170 dpi showed obviously shorter lag-times than other reactions. After performing 35 independent reactions (5 mice for each dpi), a total of 20 urine extracts were found positive in qRT-QuIC: from untreated mice of 120 and 170 dpi, and from treated mice of 170 and 250 dpi (**Figure 35 b**). In these results, seeding activity of 5 urine extracts of each dpi showed high reproducibility (5/5 and 0/5), indicating high stability of detecting PrPres in the urine of RML-infected mice with qRT-QuIC. PrPres equivalents in urine extracts were quantified with qRT-QuIC formula in **Figure 27 c** followed by mathematical extrapolation to concentrations in the urine (g/ml) (**Figure 35 c**). The results showed that urine extracts from untreated mice of 170 dpi had significantly higher PrPres equivalents than those from untreated 120 dpi ( $p = 0.0007$ ) and treated 170 dpi ( $p = 0.0002$ ), while the later two had similar PrPres equivalents. However, urine extracts from anle138b-treated mice of 250 dpi showed slightly increased PrPres equivalents ( $p = 0.0547$ ) comparing with those of treated 170 dpi. These results indicate that anle138b interrupts not only the PrP<sup>Sc</sup> formation in the brain, but also decreases the PrPres equivalents in the urine of prion-infected mice. This also implies a correlation of PrP<sup>Sc</sup> concentrations of the urine and the brain.

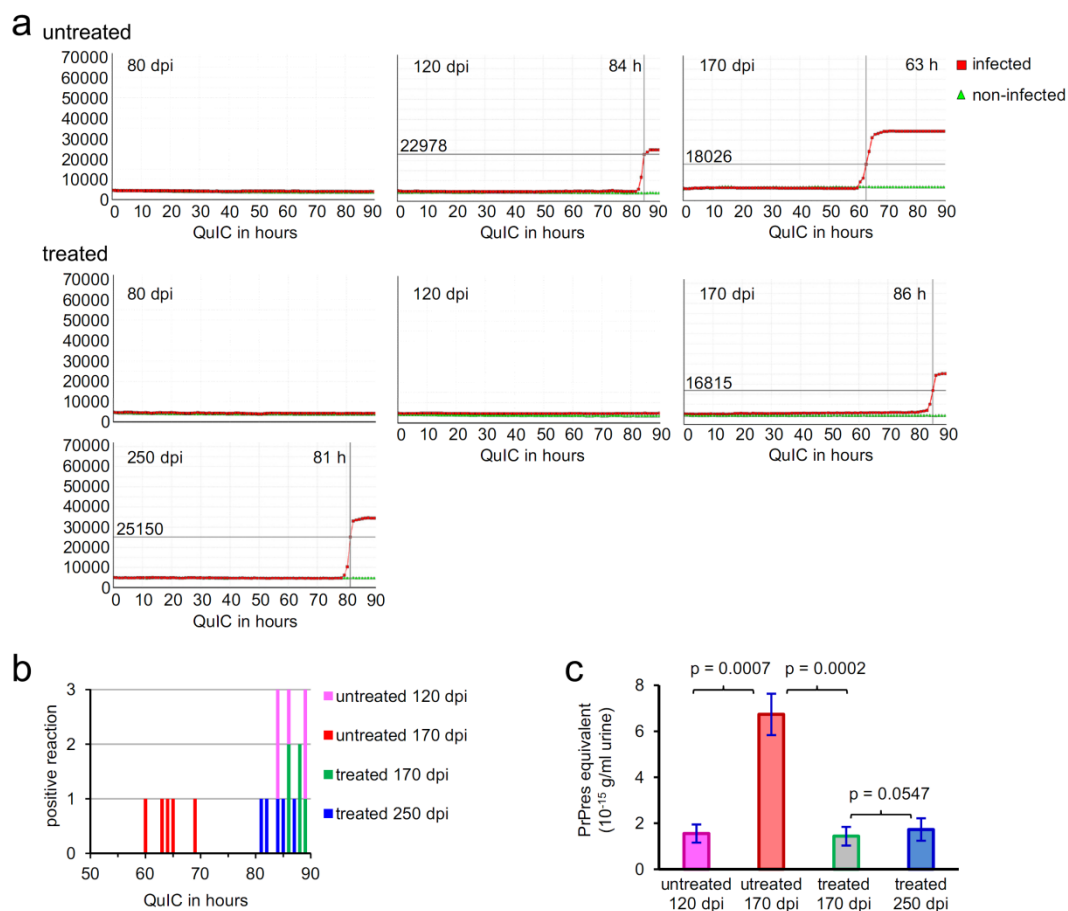


**Figure 35. Quantification of PrPres equivalents in the urine of mice treated with anti-prion compound anle138b and untreated mice.** (a) 200  $\mu$ l of mouse urine from 80, 120, 170 dpi of untreated mice, and 80, 120, 170 and 250 dpi of mice treated with anle 138b were collected followed by preparing PK-treated urine extracts as the seeds for qRT-QuIC. The urine extracts of non-infected mice are the controls. (b) A total of 20 positive reactions were observed while seeding prion-infected urine in qRT-QuIC. Each scale on the Y-axis represents one positive reaction. (c) PrPres equivalents in the urine (g/ml) were calculated by employing the formula in **Figure 27 c**. The significances were calculated using the t-test. Shown are mean and s.e.m. (n = 5).

To see if the changes in the urine corresponded to the changes in the brain, PrPres equivalents of 1 ml of urine were divided by those of  $10^{-10}$  g of brain from corresponding dpi to obtain the ratios (urine/brain, represented as u/b value). Equivalents from 120 and 170 dpi of untreated mice, and those of 170 and 250 dpi of treated mice, were

chosen, since urine extract-seeded qRT-QuIC reactions were positive only in these four groups (**Figure 36**). The u/b values did not show significant differences in either the untreated ( $p = 0.4593$ ) or treated group ( $p = 0.3985$ ), indicating that alterations of PrPres equivalents in the urine are parallel to those in the brain. This corroborates the rationale of measuring PrPres in the urine to demonstrate the therapeutic effect of anti-prion treatment *in vivo*.

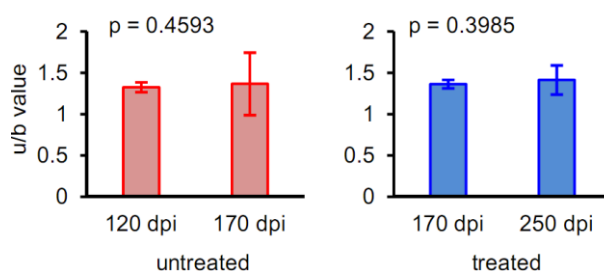


**Figure 36. Changes of PrPres equivalents in the urine corresponded to those in the brain.** For each dpi, PrPres equivalents in 1 ml of urine were divided by the equivalents in  $10^{-10}$  g of brain to obtain a ratio (urine/brain, u/b value). The potential differences of ratios were analyzed using the t test. Shown are mean and s.e.m. ( $n = 5$ )

## 5 Discussion

### 5.1 Utilizing PMCA for screening anti-prion compounds

In the study of screening anti-prion compounds for anti-prion therapy, I employed PMCA as one of the decisive steps before bioassays. The advantages of PMCA are evident from the work: i) it allows directly spiking compounds in a cell-free system to efficiently analyze their anti-prion activities to narrow down the library of candidates and indicate those promising options before time- and cost-consuming *in vivo* studies, ii) PMCA utilizes original brain homogenates as the substrates containing most of ingredients in brain, e.g., protein supply, small chemicals and lipids (Deleault et al, 2003; Wang et al, 2010), which are reported to be the essential factors of prion propagation *in vivo*, thus, not only the inhibition performed by PMCA is in line with those by animal model, even the EC<sub>50</sub> of compounds observed from PMCA assay is also comparable with that *in vivo*, iii) PMCA is adapted to prions of various species and strains (Castilla et al, 2008), thus it can estimate anti-prion efficacies for different strains and hosts, which is important for developing treatments for human patients, as clinical trials in humans are very time-consuming and limited by the low number of patients available for clinical trials. It is noteworthy that, the third advantage of PMCA may be the most important one. To my knowledge, the cell culture model of prion infectivity has only been established for the mouse-adapted scrapie prions. A cellular model for human prion, however, is not available so far. Transgenic mouse models of expressing human PrP<sup>C</sup> have been established. Human prion incubation periods in these models are from 200 to 300 days (Wadsworth et al, 2008). Therefore, using PMCA to test the anti-prion ability of those drug-like candidates before animal and human tests is necessary.

### 5.2 Tests of inhibiting prion propagation *in vivo* are essential

Regarding treatment of prion diseases in humans, DPP-derivatives and specifically anle138b represent a new lead structure with several favorable features according to the *in vivo* assays. They are small molecules that have an excellent oral bioavailability and blood-brain-barrier penetration without signs of toxicity at therapeutic doses. To

the best of our knowledge, the prolongation of survival even in late-stage treatment experiments obtained in prion-infected mice is by far the largest that has been discovered for any drug-like compound tested so far. I did not observe a selection and over-representation of PrP<sup>Sc</sup> species in treated animals indicating that there is no development of new resistant strains. However, none of these observations above can be addressed by *in vitro* studies. Several studies aiming at the development of new therapeutic anti-prion compounds could show anti-prion activity only in cell culture but lack data in animal models or compounds were found to be inefficient *in vivo* (Ghaemmaghami et al, 2010; Gallardo-Godoy et al, 2011; Thompson et al, 2011). For example, quinacrine was reported to exhibit a strong anti-prion activity in cell-culture (Korth et al, 2001). However, *in vivo* studies in mice and humans were unsuccessful (Collinge et al, 2009) as this compound does not reach sufficient concentrations in the brain (Gayraud et al, 2005), which underlines the importance of systematic and timely *in vivo* testing to optimize therapeutic efficacy of synthesized compounds not only *in vitro* but *in vivo*.

### 5.3 RT-QuIC for diagnosing prion diseases

The established RT-QuIC for diagnosing human CJD in CSF had received 100% sensitivity and 100% specificity. The results of blind tests were better than the data of published studies (Atarashi et al, 2011; McGuire et al, 2012). Further tests using different rPrP species to amplify various prion strains showed that one rPrP substrate may effectively amplify only a subset of PrP<sup>Sc</sup>, suggesting that selecting optimal rPrP substrate before performing clinical diagnosis of prion diseases is required.

In previous tests from other laboratories, it was concluded that vCJD seed was not suitable in RT-QuIC since only hamster rPrP was used in these studies (Orrú et al, 2009; Peden et al, 2012). Although human rPrP has been used for detecting human sCJD (Atarashi et al, 2011) but not vCJD, to gain 80% sensitivity from detecting 30 blindly prepared human CSF, it was concluded that those RT-QuIC reactions containing human rPrP could only be monitored for 48 h due to the false-positive problem in these tests. One solution is to use serial RT-QuIC (oral presentation in JPND-Demtest meeting, 2012, Hannover, Germany), which involved serially



transferring RT-QulC products from reactions of 48 h into freshly prepared human rPrP substrates similar to the principle of sPMCA mentioned in section 2.2.2 and Figure 3. Serial RT-QulC may help to increase both the sensitivity and specificity. However, it will also retain the shortages of sPMCA, such as increasing the risks of cross-contamination and spreading the human prions with aerosol. I solved this issue of detecting vCJD PrP<sup>Sc</sup> by inventing a new preparation of human rPrP and increasing the quality of mouse rPrP. My data indicate that reliable RT-QulC substrates were developed for detecting human CJD and cattle BSE that may help to solve the threats for public health.

Cautiously, given the large number of cases that needs to be diagnosed as prion diseases or other neurodegenerative disorders, we only picked up a tiny part of prion cases to establish this diagnostic technique. A greater number of cases, especially those cases with co-existence of prion disease with other fatal disease such as Alzheimer disease (AD), Parkinson disease and dementia with Lewy Body (DLB) that may lead to diagnostic problems, should be tested. Furthermore, more samples from livestock should be subjected to RT-QulC in the future to gain a better understanding of how to apply this technique for not only human clinical validation but also safety assessments of food and other animal products.

#### 5.4 qRT-QulC for quantifying PrP<sup>Sc</sup> in prion-infected tissues

I have developed quantitative RT-QulC (qRT-QulC) to quantify with high accuracy minute amounts of PrP<sup>Sc</sup> in the brain and various peripheral tissues at levels far below detection by *in vivo* transmission. qRT-QulC is based upon the quantitative correlation between the seeded amount of PrPres and the lag time to the start of the conversion reaction detected by RT-QulC. By seeding known amounts of PrPres quantified by immunoblot into qRT-QulC a standard calibration curve can be obtained. Using this calibration curve, seeded undetermined amounts of PrPres can be directly calculated. The qRT-QulC allows quantifying PrPres concentrations at extremely low levels as low as  $10^{-15.5}$  g PrPres, which corresponds to 0.001 LD<sub>50</sub> units obtained by *in vivo* i.c. transmission studies. I have find that PrPres concentration increases steadily in the brain after inoculation and can be detected at various time points during the incubation

period in peripheral organs (spleen, heart, muscle, liver, kidney) in two experimental scrapie strains (RML, ME7) in the mouse.

In a recent study, Wilham and colleagues (Wilham et al, 2010) used SD50 (50% seeding dose) to quantify seeding activity in the RT-QuIC. SD50 was defined as minimum seeded amount causing 50% of RT-QuIC reactions to be positive. Using end-point titration in a dilution series for quantification, SD50 was shown to correlate with the infectivity of 263K strains in hamster. To obtain SD50 values for one prion strain in RT-QuIC, serially diluted standard sample are required, e.g., serially diluted prion-infected reference brain homogenate and serially diluted undetermined materials. Thus, this approach requires multiple repetitions to yield the percentage of positive reactions for every dilution. In contrast, qRT-QuIC is a lag time-based assay and the amount of PrPres equivalents in suspected materials can be directly calculated and quantified with much fewer repetitions based on the calibration curve. The respective advantages and disadvantages of end-point titration and lag time assays are well known from assays of prion infection *in vivo*. End-point titration provides an accurate measure of infectious units. However, end-point *in vivo* assay also requires multiple repetitions for each dilution of seeds to obtain the titration of one prion strain, whereas the incubation time *in vivo* assay is more commonly used for prion quantification as much less animals are required. These drive to conclude that the qRT-QuIC assay is more suitable than SD50 measurements for quantitative detection and high-throughput assay for prion diagnosis.

## **5.5 Monitoring anti-prion treatment by quantifying PrP<sup>Sc</sup> in the urine**

Two strategies were normally applied to test anti-prion efficacy of drugs in previous studies: i) Tracking the progress of disease by measuring the PrP<sup>Sc</sup> concentration in the brain at different dpi, ii) observing the survival time; a combination of i) and ii) is often applied. However, these methods require large numbers of animals for analyzing PrPres in the brain plus long-term experiments spanning the entire prion-incubation period. Furthermore, these strategies are impossible or difficult to apply in clinical trials of human prion disease. A recent study (Collinge et al, 2009) testing quinacrine for

anti-prion activity in humans showed 2 years of monitoring clinical features of treated patients without identifying the PrP<sup>Sc</sup> states in materials, e.g., CSF, due to the lack of sensitive detection and quantification techniques to verify the appropriate concentration of drugs and to track the progression of disease for assessing anti-prion therapeutic effects.

The sensitive and reliable qRT-QulC enabling to monitor the efficacy of anti-prion treatment in living animals by using urine samples has been developed. By collecting urine for qRT-QulC to monitor treatment instead of harvesting brains for WB during the prion-incubation period, two advantages can be seen: i) the required number of experimental animals for one treatment can be decreased significantly (**Figure 37**), which helps to minimize the costs and animal suffering; This advantage will be much more obvious when assessing anti-prion therapy in big animals (e.g., primates, elk, cattle and sheep). ii) qRT-QulC as a rapid, sensitive and specific diagnostic method can provide a reliable assessment of anti-prion therapy in vivo that can be applied in humans. In addition, since the presence of prions has been identified in the CSF, blood, urine, saliva and feces of certain species (Brown et al, 1994; Saá et al, 2006; Mathiason et al, 2006; Tamgüney et al, 2009), these biological materials provide more options of seeds to monitor anti-prion therapy by quantifying PrPres, or PrP<sup>Sc</sup>, with the qRT-QulC technique.

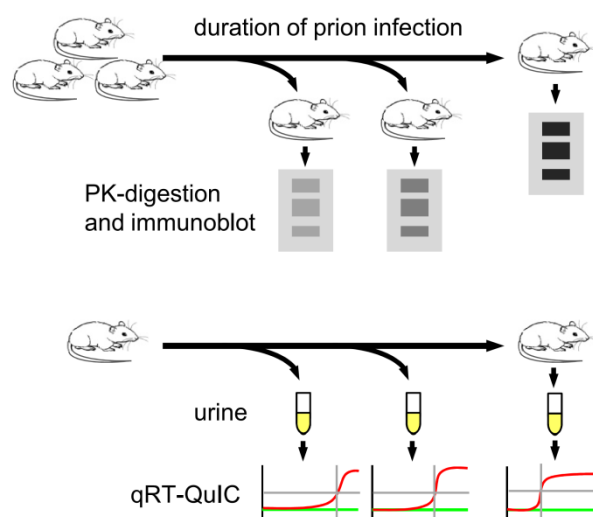


**Figure 37. The advantage of using qRT-QulC to monitor the anti-prion treatment**

***in vivo***. The common strategy is to harvest brains from experimental animals (mice) at several time-points for tracking changes of PrPres concentrations with, e.g., immunoblotting, for evaluation of anti-prion treatments. These experiments have to be performed with many groups of mice. Gray rectangles represent PrPres bands of diglycosylated, monoglycosylated and unglycosylated PrP, respectively, after PK-digestion and immunoblotting. Densities of PrPres bands correspond to increases of PrPres concentration in disease progression. However, using qRT-QuIC as the diagnostic tool to quantify PrPres equivalents in the urine, prion progression can be monitored in the living animals. Thus, the required number of experimental animals is much smaller than those in the top panel of the schematic. Thus, qRT-QuIC increases the efficiency of monitoring the progress of prion-infection and estimating therapeutic effects. The amplification of PrPres in the qRT-QuIC reaction is represented by red curves, the controls are depicted by green curves.

Gabizon's group was the first to report PrP<sup>Sc</sup> in the urine of CJD patients and scrapie-infected hamster (Shaked et al, 2001), but their findings could not be reproduced by other groups by simply following the published protocol (Serban et al, 2004; Furukawa et al, 2004; Head et al, 2005). However, scrapie could be transmitted by inoculating mice and sheep with urine of nephritic animals (Seeger et al, 2005) and with highly enriched urinary proteins from symptomatic prion-infected humans and animals (Haley et al, 2009; Notari et al, 2012). This suggested the authentic existence of prions, or PrP<sup>Sc</sup>, in the urine of scrapie or CJD-affected individuals, particularly those with simultaneous inflammatory kidney disease. However, the mechanism of PrP<sup>Sc</sup> amplification in the urinary system or shedding into the urine of animals is not understood at the moment.

The time-span of qRT-QuIC in our experiments was fixed at 90 hours since longer duration may cause false positivity. A previous study has shown that RT-QuIC is stable up to 120 hours (McGuire, 2012) when choosing hamster rPrP to amplify CJD PrP<sup>Sc</sup> in human CSF, since hamster rPrP is thought to be a suitable substrate for amplifying human PrP<sup>Sc</sup> in QuIC (Orrú et al, 2009). In contrast, I used mouse rPrP as the substrate for quantifying mouse prion PrPres, since I found that mouse rPrP responded

rapidly to the triggered amplification by mouse PrPres. It is possible that using rPrP of other species may necessitate comparable or longer reaction times.

In conclusion, I have utilized qRT-QulC to monitor the treatment of the anti-prion compound anle138b by measuring the PrPres equivalents in the urine of prion-infected mice. Furthermore, qRT-QulC can help to not only decrease the number of experimental animals, but also provide a technical improvement of assessing treatment in humans. Many more studies will be necessary before the understanding of the pathophysiology of PrP<sup>Sc</sup> shedding into the urine. The technique may have drawbacks, e.g., it may be slow to visualize a trend such as prion amplification that is quick in the CNS, it may differ from species to species etc. Be that as it may, qRT-QulC will open up a whole new avenue of anti-prion drug testing in the near future.

## 5.6 Perspectives

The presented studies have demonstrated that autocatalytic prion amplification *in vitro* can be utilized for the screening of anti-prion drug candidates, sensitive diagnosis of prion diseases, tracking disease progression and monitoring therapeutic effect of prions. Freshly prepared brain homogenates containing most of the brain-derived essential elements for the propagation of spiked prion in PMCA allow the elucidation of anti-prion activities of compounds, which provides an effective tool for drug testing before clinical trials in human. Meanwhile, highly efficient amplification of prion in RT-QulC and qRT-QulC allow for the rapid diagnosis and accurate quantification using small samples, which fulfills the need for measuring of disease progression with minimal injury on the individual. Based on the presented findings on PMCA, RT-QulC and qRT-QulC, two major lines of forthcoming research can be considered. On one hand, an investigation of the possibility of translating the achievement from the mouse model to human clinical trials should be performed. While the clinical validation is started, the CSF, blood and urine of the patient should be periodically collected for prion detection and quantification, the latter can serve to indicate disease progression and to monitor treatment response in case/control studies. Even without knowing the pharmacokinetic of the drug in human brain, qRT-QulC can still assist the physicians to get a better assessment of therapeutic efficacy in prion-infected patients. The second

type of studies is related to enable drug screening in the context of basic and preclinical research. Although anle138b has demonstrated to be highly active for inhibition of prion propagation both *in vitro* and *in vivo*, the ultimate neutralization and cure of the disease is not settled. Developing new drugs based on anle138b will not only contribute to prion research, also provide manifold references to other protein disorder related diseases.

Findings presented here suggest a suitable systematic procedure of prion treatment: first, selecting the most promising candidates with PMCA; second, using much fewer mice for *in vivo* test through monitoring therapeutic efficacy by quantifying urinary PrP<sup>Sc</sup> with qRT-QuIC; third, rapidly discriminating prion-infected patient at early clinical stage with RT-QuIC; four, treating patient with newly developed drug combined with estimating prion levels in samples easily obtained, e.g., urine, with qRT-QuIC. This procedure should significantly increase the efficiency of treatment development for prion disease both at the preclinical and at the clinical level.

## 6 References

- Angot E, Steiner JA, Hansen C, Li JY, Brundin P (2010). Are synucleinopathies prion-like disorders? *Lancet Neurol* 9, 1128-1138.
- Atarashi R, Moore RA, Sim VL, Hughson AG, Dorward DW, Onwubiko HA, Priola SA, Caughey B. (2007). Ultrasensitive detection of scrapie prion protein using seeded conversion of recombinant prion protein. *Nat Methods* 4, 645-650.
- Atarashi R, Wilham JM, Christensen L, Hughson AG, Moore RA, Johnson LM, Onwubiko HA, Priola SA, Caughey B (2008). Simplified ultrasensitive prion detection by recombinant PrP conversion with shaking. *Nat Methods* 5, 211-212.
- Atarashi R, Satoh K, Sano K, Fuse T, Yamaguchi N, Ishibashi D, Matsubara T, Nakagaki T, Yamanaka H, Shirabe S, Yamada M, Mizusawa H, Kitamoto T, Klug G, McGlade A, Collins SJ, Nishida N (2011). Ultrasensitive human prion detection in cerebrospinal fluid by real-time quaking-induced conversion. *Nat Med* 17, 175-178.
- Atarashi R, Sano K, Satoh K, Nishida N (2011). Real-time quaking-induced conversion: a highly sensitive assay for prion detection. *Prion* 5, 150-153.
- Barria MA, Mukherjee A, Gonzalez-Romero D, Morales R, Soto C. (2009) De novo generation of infectious prions in vitro produces a new disease phenotype. *PLoS Pathog* 5, e1000421.
- Bertsch U, Winklhofer KF, Hirschberger T, Bieschke J, Weber P, Hartl FU, Tavan P, Tatzelt J, Kretzschmar H, Giese A (2005). Systematic identification of antiprion drugs by high-throughput screening based on scanning for intensely fluorescent targets. *J Virol* 79, 7785-7791.
- Bieschke J, Giese A, Schulz-Schaeffer W, Zerr I, Poser S, Eigen M, Kretzschmar H (2000). Ultrasensitive detection of pathological prion protein aggregates by dual-color scanning for intensely fluorescent targets. *Proc Natl Acad Sci U S A* 97, 5468-5473.
- Bieschke J, Weber P, Sarafoff N, Beekes M, Giese A and Kretzschmar H (2004). Autocatalytic self-propagation of misfolded prion protein. *Proc Natl Acad Sci USA* 101, 12207-12211.
- Browning S, Baker CA, Smith E, Mahal SP, Herva ME, Demczyk CA, Li J, Weissmann

- C (2011). Abrogation of complex glycosylation by swainsonine results in strain- and cell-specific inhibition of prion replication. *J Biol Chem* 286, 40962-40973.
- Brown P, Wolff A, Gajdusek, DC (1990). A simple and effective method for inactivating virus infectivity in formalin-fixed tissue samples from patients with Creutzfeldt-Jakob disease. *Neurology* 40, 887-890.
- Brown P, Gibbs CJ Jr, Rodgers-Johnson P, Asher DM, Sulima MP, Bacote A, Goldfarb LG, Gajdusek DC (1994). Human spongiform encephalopathy: the National Institutes of Health series of 300 cases of experimentally transmitted disease. *Ann Neurol* 35: 513-529.
- Casalone C, Zanusso G, Acutis P, Ferrari S, Capucci L, Tagliavini F, Monaco S, Caramelli M (2004) Identification of a second bovine amyloidotic spongiform encephalopathy- molecular similarities with sporadic Creutzfeldt-Jakob disease. *Proc Natl Acad Sci USA* 101, 3065-3070.
- Castilla J, Saá P, Soto C. (2005) Detection of prions in blood. *Nat Med* 11, 982-985.
- Castilla J, Saa´ P, Hetz C and Soto C (2005). In vitro generation of infectious scrapie prions. *Cell* 121, 195–206.
- Castilla J, Morales R, Saá P, Barria M, Gambetti P, Soto C (2008) Cell-free propagation of prion strains. *EMBO J* 27, 2557-2566.
- Caughey B, Raymond GJ, Ernst D, Race RE (1997). N-terminal truncation of the scrapie-associated form of PrP by lysosomal protease(s): implications regarding the site of conversion of PrP to the protease-resistant state. *J Virol* 65, 6597-6603.
- Caughey, B. (2000) Formation of Protease-Resistant Prion Protein in Cell-Free Systems. *Curr Issues Mol Biol* 2, 95-101.
- Chen B, Morales R, Barria MA, Soto C (2010). Estimating prion concentration in fluids and tissues by quantitative PMCA. *Nat Methods* 7, 519-520.
- Clark DE (2003). In silico prediction of blood-brain barrier permeation. *Drug Discov Today* 8, 927-933.
- Colby DW, Zhang Q, Wang S, Groth D, Legname G, Riesner D, Prusiner SB (2007). Prion detection by an amyloid seeding assay. *Proc Natl Acad Sci USA* 104, 20914-20919.
- Colombo L, Piovesan P, Ghirardi O, Salmona M, Forloni G (2009). ST1859 reduces prion infectivity and increase survival in experimental scrapie. *Arch Virol* 154, 1539-1544.



- Collins S, Boyd A, Fletcher A, Gonzales M, McLean CA, Byron K, Masters CL (2000). Creutzfeldt-Jakob disease: diagnostic utility of 14-3-3 protein immunodetection in cerebrospinal fluid. *J Clin Neurosci* 7, 203-208.
- Collinge J, Whitfield J, McKintosh E, Beck J, Mead S, Thomas DJ, Alpers MP (2006). Kuru in the 21st century—an acquired human prion disease with very long incubation periods. *Lancet* 367, 2068–2074.
- Collinge J (2001). Prion diseases of humans and animals: their causes and molecular basis. *Annu. Rev. Neurosci* 24, 519-550.
- Collinge J, Gorham M, Hudson F, Kennedy A, Keogh G, Pal S, Rossor M, Rudge P, Siddique D, Spyer M, Thomas D, Walker S, Webb T, Wroe S, Darbyshire J (2009). Safety and efficacy of quinacrine in human prion disease (PRION-1 study): a patient-preference trial. *Lancet Neurol* 8, 334-344.
- Demaimay R, Adjou KT, Beringue V, Demart S, Lasmezas CI, Deslys JP, Seman M, Dormont D (1997). Late treatment with polyene antibiotics can prolong the survival time of scrapie-infected animals. *J Virol* 71, 9685-9689.
- Deleault NR, Lucassen RW, Supattapone S. (2003) RNA molecules stimulate prion protein conversion. *Nature* 425, 717-720.
- Deleault NR, Harris BT, Rees JR, Supattapone S. (2007) Formation of native prions from minimal components in vitro. *Proc Natl Acad Sci USA* 104, 9741-9746.
- Doh-ura K, Ishikawa K, Murakami-Kubo I, Sasaki K, Mohri S, Race R, Iwaki T (2004). Treatment of transmissible spongiform encephalopathy by intraventricular drug infusion in animal models. *J Virol* 78, 4999-5006.
- Forman MS, Lee VM, Trojanowski JQ (2005). Nosology of Parkinson's disease: looking for the way out of a quagmire. *Neuron* 47, 479-482.
- Furukawa H, Doh-ura K, Okuwaki R, Shirabe S, Yamamoto K, Udon H, Ito T, Katamine S, Niwa M (2004). A pitfall in diagnosis of human prion diseases using detection of protease-resistant prion protein in urine. Contamination with bacterial outer membrane proteins. *J Biol Chem* 279, 23661-23667.
- Gallardo-Godoy A, Gever J, Fife KL, Silber BM, Prusiner SB, Renslo AR (2011). 2-Aminothiazoles as therapeutic leads for prion diseases. *J Med Chem* 54, 1010-1021.
- Gayrard V, Picard-Hagen N, Viguie C, Laroute V, Andreoletti O, Toutain PL (2005). A possible pharmacological explanation for quinacrine failure to treat prion diseases: pharmacokinetic investigations in a ovine model of scrapie. *Br J*

- Pharmacol 144. 386-393.
- Geissen M, Leidel F, Eiden M, Hirschberger T, Fast C, Bertsch U, Tavan P, Giese A, Kretzschmar H, Schatzl HM, Groschup MH (2011). From high-throughput cell culture screening to mouse model: identification of new inhibitor classes against prion disease. *Chem Med Chem* 6, 1928-1937.
- Ghaemmaghami S, May BC, Renslo AR, Prusiner SB (2010). Discovery of 2-aminothiazoles as potent antiprion compounds. *J Virol* 84, 3408-3412.
- Gill ON, Spencer Y, Richard-Loendt A, Kelly C, Dabaghian R, Boyes L, Linehan J, Simmons M, Webb P, Bellerby P, Andrews N, Hilton DA, Ironside JW, Beck J, Poulter M, Mead S, Brandner S (2013). Prevalent abnormal prion protein in human appendixes after bovine spongiform encephalopathy epizootic: large scale survey. *BMJ* 347, f5675.
- Giese A, Groschup MH, Hess B, Kretzschmar H (1995). Neuronal cell death in scrapie-infected mice is due to apoptosis. *Brain Pathol* 5, 213-221.
- Glabe CG and Kaye R (2006). Common structure and toxic function of amyloid oligomers implies a common mechanism of pathogenesis. *Neurology* 66, S74-S78.
- Gonzalez-Romero D, Barria MA, Leon P, Morales R, Soto C (2008). Detection of infectious prions in urine. *FEBS Lett* 582, 3161-3166.
- Haley NJ, Seelig DM, Zabel MD, Telling GC, Hoover EA (2009). Detection of CWD prions in urine and saliva of deer by transgenic mouse bioassay. *PLoS One* 4, e4848.
- Harrison C (2013). Neurodegenerative disease: A PERK for the therapy of prion disease. *Nat Rev Drug Discov* 12, 906.
- Head MW, Kouverianou E, Taylor L, Green A, Knight R (2005). Evaluation of urinary PrP<sup>Sc</sup> as a diagnostic test for sporadic, variant, and familial CJD. *Neurology* 64, 1794-1796.
- Herms J, Tings T, Gall S, Madlung A, Giese A, Siebert H, Schürmann P, Windl O, Brose N, Kretzschmar H (1999). Evidence of presynaptic location and function of the prion protein. *J Neurosci* 19, 8866-8875.
- Kawasaki Y, Kawagoe K, Chen CJ, Teruya K, Sakasegawa Y, Doh-ura K (2007). Orally administered amyloidophilic compound is effective in prolonging the incubation periods of animals orally infected with prion diseases in a prion strain-dependent manner. *J Virol* 81, 12889-12898.

- Kim JI, Cali I, Surewicz K, Kong Q, Raymond GJ, Atarashi R, Race B, Qing L, Gambetti P, Caughey B, Surewicz WK. (2010) Mammalian prions generated from bacterially expressed prion protein in the absence of any mammalian cofactors. *J Biol Chem* 285, 14083-14087.
- Korth C, May BC, Cohen FE, Prusiner SB (2001). Acridine and phenothiazine derivatives as pharmacotherapeutics for prion disease. *Proc Natl Acad Sci U S A* 98, 9836-9841.
- Leidel F, Eiden M, Geissen M, Kretzschmar H, Giese A, Hirschberger T, Tavan P, Schatzl HM, Groschup MH (2011). Diphenylpyrazole-derived compounds increase survival time of mice after prion infection. *Antimicrob. Agents Chemother* 55, 4774-4781.
- Lipinski CA, Lombardo F, Dominy BW, Feeney PJ (2001). Experimental and computational approaches to estimate solubility and permeability in drug discovery and development settings. *Adv Drug Deliv Rev* 46, 3-26.
- Luk KC, Kehm VM, Zhang B, O'Brien P, Trojanowski JQ, Lee VM (2012). Intracerebral inoculation of pathological alpha-synuclein initiates a rapidly progressive neurodegenerative alpha-synucleinopathy in mice. *J Exp Med* 209, 975-986.
- Mallucci GR, Collinge J (2005). Rational targeting for prion therapeutics. *Nat Rev Neurosci* 6, 23-34.
- Mallucci GR, White MD, Farmer M, Dickinson A, Khatun H, Powell AD, Brandner S, Jefferys JG, Collinge J (2007). Targeting cellular prion protein reverses early cognitive deficits and neurophysiological dysfunction in prion-infected mice. *Neuron* 53, 325-335.
- Mathiason CK, Powers JG, Dahmes SJ, Osborn DA, Miller KV, Warren RJ, Mason GL, Hays SA, Hayes-Klug J, Seelig DM, Wild MA, Wolfe LL, Spraker TR, Miller MW, Sigurdson CJ, Telling GC, Hoover EA (2006). Infectious prions in the saliva and blood of deer with chronic wasting disease. *Science* 6, 133-136.
- McGuire LI, Peden AH, Orrú CD, Wilham JM, Appleford NE, Mallinson G, Andrews M, Head MW, Caughey B, Will RG, Knight RS, Green AJ (2012) Real time quaking-induced conversion analysis of cerebrospinal fluid in sporadic Creutzfeldt-Jakob disease. *Ann Neurol* 72, 278-285.
- Morales R, Duran-Aniotz C, Diaz-Espinoza R, Camacho MV, Soto C (2012). Protein misfolding cyclic amplification of infectious prions. *Nat Protoc* 7, 1397-1409.
- Notari S, Qing L, Pocchiari M, Dagdanova A, Hatcher K, Dogterom A, Groisman JF,

## References

- Lumholtz IB, Puopolo M, Lasmezas C, Chen SG, Kong Q, Gambetti P (2012). Assessing prion infectivity of human urine in sporadic Creutzfeldt-Jakob disease. *Emerg Infect Dis* 18: 21-28.
- Orrú CD, Wilham JM, Hughson AG, Raymond LD, McNally KL, Bossers A, Ligios C, Caughey B (2009). Human variant Creutzfeldt-Jakob disease and sheep scrapie PrP(res) detection using seeded conversion of recombinant prion protein. *Protein Eng Des Sel* 22, 515-521.
- Orrú CD, Hughson AG, Race B, Raymond GJ, Caughey B (2012) Time course of prion seeding activity in cerebrospinal fluid of scrapie-infected hamsters after intratongue and intracerebral inoculations. *J Clin Microbiol* 50, 1464-1466.
- Pan KM, Baldwin M, Nguyen J, Gasset M, Serban A, Groth D, Mehlhorn I, Huang Z, Fletterick RJ, Cohen FE (1993). Conversion of alpha-helices into beta-sheets features in the formation of the scrapie prion proteins. *Proc Natl Acad Sci USA* 90, 10962-10966.
- Peden AH, McGuire LI, Appleford NE, Mallinson G, Wilham JM, Orrú CD, Caughey B, Ironside JW, Knight RS, Will RG, Green AJ, Head MW (2012). Sensitive and specific detection of sporadic Creutzfeldt-Jakob disease brain prion protein using real-time quaking-induced conversion. *J Gen Virol* 93, 438-449.
- Pfeifer A, Eigenbrod S, Al Khadra S, Hofmann A, Mitteregger G, Moser M, Bertsch U, Kretzschmar H (2006). Lentivector-mediated RNAi efficiently suppresses prion protein prolongs survival of scrapie-infected mice. *J Clin Invest* 116, 3204-3210.
- Polymenidou M, Verghese-Nikolakaki S, Groschup M, Chaplin MJ, Stack MJ, Plaitakis A, Sklaviadis T (2002). A short purification process for quantitative isolation of PrP<sup>Sc</sup> from naturally occurring and experimental transmissible spongiform encephalopathies. *BMC Infect Dis* 2, 23.
- Prusiner SB, Garfin DE, Cochran SP, McKinley MP, Groth DF, Hadlow WJ, Race RE, Eklund CM (1980). Experimental scrapie in the mouse: electrophoretic and sedimentation properties of the partially purified agent. *J Neurochem* 35, 574-582.
- Prusiner SB (1982). Novel proteinaceous infectious particles cause scrapie. *Science* 216, 136-144.
- Prusiner SB (1998) Prions. *Proc Natl Acad Sci USA* 95, 13363-13383.
- Radonić A, Thulke S, Mackay IM, Landt O, Siebert W, Nitsche A (2004). Guideline to reference gene selection for quantitative real-time PCR. *Biochem Biophys Res*

- Commun 313, 856-862.
- Saborio GP, Permanne B, Soto C. (2001) Sensitive detection of pathological prion protein by cyclic amplification of protein misfolding. *Nature* 411, 810-813.
- Safar J, Wille H, Itri V, Groth D, Serban H, Torchia M, Cohen FE, Prusiner SB (1998). Eight prion strains have PrP(Sc) molecules with different conformations. *Nat Med* 4, 1157-1165.
- Saá P, Castilla J, Soto C (2006) Presymptomatic detection of prions in blood. *Science* 7, 92-94.
- Saá P, Castilla J, Soto C (2006) Ultra-efficient replication of infectious prions by automated protein misfolding cyclic amplification. *J Biol Chem* 281, 35245-35252.
- Sanchez-Juan P, Green A, Ladogana A, Cuadrado-Corrales N, Sáánchez-Valle R, Mitrováa E, Stoeck K, Sklaviadis T, Kulczycki J, Hess K, Bodemer M, Slivarichová D, Saiz A, Calero M, Ingrosso L, Knight R, Janssens AC, van Duijn CM, Zerr I (2006). CSF tests in the differential diagnosis of Creutzfeldt-Jakob disease. *Neurology* 67, 637-643.
- Schmittgen TD, Zakrajsek BA, Mills AG, Gorn V, Singer MJ, Reed MW (2000). Quantitative reverse transcription-polymerase chain reaction to study mRNA decay: comparison of endpoint and real-time methods. *Anal Biochem* 285, 194-204.
- Seeger H, Heikenwalder M, Zeller N, Kranich J, Schwarz P, Gaspert A, Seifert B, Miele G, Aguzzi A (2005). Coincident scrapie infection and nephritis lead to urinary prion excretion. *Science* 310: 324-326.
- Serban A, Legname G, Hansen K, Kovaleva N, Prusiner SB (2004) Immunoglobulins in urine of hamsters with scrapie. *J Biol Chem* 279, 48817-48820.
- Shaked Y, Kariv-Inbal Z, Halimi M, Avraham I, Gabizon R (2001). A protease-resistant prion protein isoform is present in urine of animals and humans affected with prion diseases. *J Biol Chem* 276, 31479-31482.
- Shi S, Mitteregger-Kretzschmar G, Giese A, Kretzschmar H (2013). Establishing quantitative real-time quaking-induced conversion (qRT-QuIC) for highly sensitive detection and quantification of PrP<sup>Sc</sup> in prion-infected tissues. *Acta Neuropathol Commun* 1, 44.
- Tamgüney G, Miller MW, Wolfe LL, Sirochman TM, Glidden DV, Palmer C, Lemus A, DeArmond SJ, Prusiner SB (2009). Asymptomatic deer excrete infectious prions in faeces. *Nature* 24, 529-532.

- Telling GC, Scott M, Mastrianni J, Gabizon R, Torchia M, Cohen FE, DeArmond SJ, Prusiner SB (1995) Prion propagation in mice expressing human and chimeric PrP transgenes implicates the interaction of cellular PrP with another protein. *Cell* 83, 79-90.
- Thompson MJ, Louth JC, Ferrara S, Jackson MP, Sorrell FJ, Cochrane EJ, Gever J, Baxendale S, Silber BM, Roehl HH, Chen B (2011). Discovery of 6-substituted indole-3-glyoxylamides as lead antiprion agents with enhanced cell line activity, improved microsomal stability and low toxicity. *Eur J Med Chem* 46, 4125-4132.
- Trevitt CR, Collinge J (2006). A systematic review of prion therapeutics in experimental models. *Brain* 129, 2241-2265.
- Tzaban S, Friedlander G, Schonberger O, Horonchik L, Yedidia Y, Shaked G, Gabizon R, Taraboulos A (2002). Protease-sensitive scrapie prion protein in aggregates of heterogeneous sizes. *Biochemistry* 41, 12868-12875.
- Vascellari S, Orrù CD, Hughson AG, King D, Barron R, Wilham JM, Baron GS, Race B, Pani A, Caughey B (2012). Prion seeding activities of mouse scrapie strains with divergent PrP<sup>Sc</sup> protease sensitivities and amyloid plaque content using RT-QuIC and eQuIC. *PLoS One* 7, e48969.
- Veber DF, Johnson SR, Cheng HY, Smith BR, Ward KW, Kopple KD (2002). Molecular properties that influence the oral bioavailability of drug candidates. *J Med Chem* 45, 2615-2623.
- Wadsworth JD, Joiner S, Hill AF, Campbell TA, Desbruslais M, Luthert PJ, Collinge J (2001). Tissue distribution of protease resistant prion protein in variant Creutzfeldt-Jakob disease using a highly sensitive immunoblotting assay. *Lancet* 358, 171-180.
- Wadsworth JD, Joiner S, Linehan JM, Desbruslais M, Fox K, Cooper S, Cronier S, Asante EA, Mead S, Brandner S, Hill AF, Collinge J (2008). Kuru prions and sporadic Creutzfeldt-Jakob disease prions have equivalent transmission properties in transgenic and wild-type mice. *Proc Natl Acad Sci U S A* 105, 3885-3890.
- Wagner J, Ryazanov S, Leonov A, Levin J, Shi S, Schmidt F, Prix C, Pan-Montojo F, Bertsch U, Mitteregger-Kretzschmar G, Geissen M, Eiden M, Leidel F, Hirschberger T, Deeg AA, Krauth JJ, Zinth W, Tavan P, Pilger J, Zweckstetter M, Frank T, Bähr M, Weishaupt JH, Uhr M, Urlaub H, Teichmann U, Samwer M, Bötzel K, Groschup M, Kretzschmar H, Griesinger C, Giese A (2013). Anle138b: a

- novel oligomer modulator for disease-modifying therapy of neurodegenerative diseases such as prion and Parkinson's disease. *Acta Neuropathol* 19, DOI 10.1007/s00401-013-1114-9.
- Wang F, Wang X, Yuan CG, Ma J. (2010) Generating a prion with bacterially expressed recombinant prion protein. *Science* 327, 1132-1135.
- Weber P, Giese A, Piening N, Mitteregger G, Thomzig A, Beekes M, Kretzschmar H (2006). Cell-free formation of misfolded prion protein with authentic prion infectivity. *Proc Natl Acad Sci USA* 103, 15818-15823.
- Weber P, Reznicek L, Mitteregger G, Kretzschmar H, Giese A (2008). Differential effects of prion particle size on infectivity in vivo and in vitro. *Biochem Biophys Res Commun* 369, 924-928.
- White AR, Enever P, Tayebi M, Mushens R, Linehan J, Brandner S, Anstee D, Collinge J, Hawke S (2003). Monoclonal antibodies inhibit prion replication and delay the development of prion disease. *Nature* 422, 80-83.
- Wilham JM, Orrú CD, Bessen RA, Atarashi R, Sano K, Race B, Meade-White KD, Taubner LM, Timmes A, Caughey B (2010). Rapid end-point quantitation of prion seeding activity with sensitivity comparable to bioassays. *PLoS Pathog* 6, e1001217.
- Wong, C., Xiong, L. W., Horiuchi, M., Raymond, L., Wehrly, K., Chesebro, B. and Caughey, B. (2001) Sulfated glycans and elevated temperature stimulate PrP<sup>Sc</sup>-dependent cell-free formation of protease-resistant prion protein. *EMBO J* 20, 377-386.

## References



## 7 Abbreviations

AD	Alzheimer disease
ASA	amyloid seeding assay
BSE	bovine spongiform encephalopathy
C-BSE	classical type bovine spongiform encephalopathy
CJD	Creutzfeldt-Jakob disease
CNS	central nervous system
CWD	chronic wasting disease
CSF	cerebrospinal fluid
DLB	dementia with Lewy Body
DMSO	Dimethyl sulfoxide
dpi	day post inoculation
DPP	3,5-diphenyl-pyrazole
fCJD	familiar Creutzfeldt-Jakob disease
EC <sub>50</sub>	half maximal effective concentration
FFI	fatal familial insomnia
IPTG	Isopropyl $\beta$ -D-1-thiogalactopyranoside
L-BSE	low type bovine spongiform encephalopathy
LD <sub>50</sub>	half lethal dose
MM	methionine/methionine homozygous at codon 129 aa of prion protein
MM1	classified human case of Creutzfeldt-Jakob disease type 1 whose prion protein is methionine/methionine homozygous at codon 129 aa
MV	methionine/valine heterozygous at codon 129 aa of prion protein
MV2	classified human case of Creutzfeldt-Jakob disease type 2 whose prion protein is methionine/valine heterozygous at codon 129 aa
NBB	N-benzylidene-benzohydrazide
NIH	national institute of health
NTA	Nitrilotriacetic acid
OD	optical density
PCR	polymerase chain reaction
PD	Parkinson disease
PK	proteinase K

## Abbreviations

PMCA	protein misfolding cyclic amplification
PrP	prion protein
PrP <sup>C</sup>	normal cellular prion protein
PrP <sup>Sc</sup>	abnormal scrapie-like prion protein
PrPres	proteinase K-resistant prion protein
PVDF	polyvinylidene fluoride
qRT-QuIC	quantitative real-time quaking-induced conversion
QuIC	quaking-induced conversion
rPrP	recombinant prion protein
rPrPres	proteinase K-resistant recombinant prion protein
RFU	relative fluorescence unit
RT-QuIC	real-time quaking-induced conversion
SAR	structure-activity relationship
sCJD	sporadic Creutzfeldt-Jakob disease
SDS	sodium dodecyl sulfate
SIFT	scanning for intensely fluorescent targets
sPMCA	serial protein misfolding cyclic amplification
ThT	thioflavin T
TSEs	Transmissible spongiform encephalopathies
vCJD	variant Creutzfeldt-Jakob disease
VV	valine/valine homozygous at codon 129 aa of prion protein
VV2	classified human case of Creutzfeldt-Jakob disease type 2 whose prion protein is valine/valine heterozygous at codon 129 aa
WB	Western blot

## 8 Acknowledgements

This dissertation would not have been possible without support and encouragement from many people near and far.

I would like to thank Prof. Dr. Thomas Cremer for supervising my doctoral thesis and making this project possible.

,I would like to gratefully and sincerely thank Prof. Dr. Hans. A. Kretzschmar for giving me the opportunity to pursue the experimental work of my Ph.D. study in his institute. Thanks to Prof. Kretzschmar for his supervision, understanding, patience, help, and most importantly, friendship during my stay with his group. I appreciate the freedom he always has given me in my academic research and his constructive suggestions. His faith and energetic attitude in science have influenced me greatly and will continue to do so in the future.

Next, I would like to take the opportunity to thank Prof. Armin Giese, whose intelligent design of compound, optimistic attitude in science and smart insight in protein conformation made this thesis possible. I would like to thank all my colleagues and friends in Prof. Kretzschmar's research group. Thanks to Jens Wagner for being such a wonderful co-worker on this project and for sharing so much joy and pain. I am thankful to Prof. Christian Griesinger, Sergey Ryazanov, Andrei Leonov in Max Planck Institute for Biophysical Chemistry their expertise in drug synthesis, and I am also grateful to our technician, Janina Mielke, whose constant technique support and pleasant way of laboratory management made my studies stable.

It gives me great pleasure to thank the people in Prof. Giese's group, especially Felix Schmidt, Martin Bartels and Dr. Johannes Levin who provided so much generous help on this project.

Finally, and most importantly, I owe my deepest gratitude to my beloved parents and wife in China. Without their love, concern, support, and strength, I would not have been able to complete this thesis.



## 9 Curriculum Vitae

Name: Shi, Song

Gender: Male

Nationality: P.R.China

Date of Birth: 26-02-1982

Place of Birth: Chongqing, China

### Education

2008 - present	PhD student Department of Biology II Ludwig-Maximilians-Universität München, Germany
2005 - 2008	M. Sc. (Immunology) Institute for Viral Disease Control and Prevention Centre for Disease Control and Prevention, China.
2000 - 2004	B. Sc. (Agriculture) School of Animal Science Huazhong Agricultural University, China.

### Professional employment

2009 - present	Ph.D. student Zentrum für Neuropathologie und Prionforschung, LMU, Prof. Dr. Dr. Hans. A. Kretzschmar
2008 - 2009	Ph.D. student Max-Planck-Institute of Psychiatry Neuroendocrine (AG Spengler)

## Patent

**Shi S**, Giese A and Kretzschmar H, Method for the isolation of recombinant prion protein and the use thereof, EP 13182421.1

## Publications

1. **Shi S**, Mitteregger-Kretzschmar G, Giese A, Kretzschmar H (2013). Establishing quantitative real-time quaking-induced conversion (qRT-QuIC) for highly sensitive detection and quantification of PrP<sup>Sc</sup> in prion-infected tissues. *Acta Neuropathol Commun* 1, 44.
2. Wagner J, Ryazanov S, Leonov A, Levin J, **Shi S**, Schmidt F, Prix C, Pan-Montojo F, Bertsch U, Mitteregger-Kretzschmar G, Geissen M, Eiden M, Leidel F, Hirschberger T, Deeg AA, Krauth JJ, Zinth W, Tavan P, Pilger J, Zweckstetter M, Frank T, Bähr M, Weishaupt JH, Uhr M, Urlaub H, Teichmann U, Samwer M, Bötzel K, Groschup M, Kretzschmar H, Griesinger C, Giese A (2013). Anle138b: a novel oligomer modulator for disease-modifying therapy of neurodegenerative diseases such as prion and Parkinson's disease. *Acta Neuropathol* 19, DOI 10.1007/s00401-013-1114-9.
3. **Shi S**, Colla R, Giese A, Kretzschmar H. Prion strains encrypted in monomeric PrP<sup>Sc</sup>. (under review)
4. **Shi S**, Wagner J, Mitteregger-Kretzschmar G, Ryazanov S, Leonov A, Griesinger C, Giese A, Kretzschmar H. Monitoring treatment of experimental scrapie by quantitative real-time quaking-induced conversion (qRT-QuIC) of PrP<sup>Sc</sup> in the urine. (Submitted)
5. **Shi S**, Colla R, Giese A, Kretzschmar H. Catalytic and templated propagation of prions. (In preparation)
6. **Shi S**, Wagner J, Colla R, Giese A, Kretzschmar H. Recombinant prion protein forms different subtypes in purification. (In preparation)
7. **Shi S**, Schmidt F, Wagner J, Giese A, Kretzschmar H. Diagnosing Alzheimer's disease by simply amplifying A-beta aggregates. (In preparation)
8. **Shi S**, Giese A, Kretzschmar H. Determining the valid substrates for *in vitro* detection of various prions of human and livestock. (In preparation)
9. **Shi S**, Dong CF, Wang GR, Wang X, An R, Chen JM, Shan B, Zhang BY, Xu K, Shi Q, Tian C, Gao C, Han J, Dong XP. (2009) PrP<sup>Sc</sup> of scrapie 263K propagates efficiently in spleen and muscle tissues with protein misfolding cyclic amplification.

Virus Res 141: 26-33.

10. **Shi S**, Dong CF, Tian C, Zhou RM, Xu K, Zhang BY, Gao C, Han J, Dong XP. (2009) The propagation of hamster-adapted scrapie PrP<sup>Sc</sup> can be enhanced by reduced pyridine nucleotide *in vitro*. FEBS J. 276:1536-45.
11. Dong CF, **Shi S**, Wang XF, An R, Li P, Chen JM, Wang X, Wang GR, Shan B, Zhang BY, Han J, Dong XP. (2008) The N-terminus of PrP is responsible for interacting with tubulin and fCJD related PrP mutants possess stronger inhibitive effect on microtubule assembly *in vitro*. Arch. Biochem. Biophys. 470: 83-92.
12. Dong CF, Wang XF, Wang X, **Shi S**, Wang GR, Shan B, An R, Li XL, Zhang BY, Han J, Dong XP. (2008) Molecular interaction between prion protein and GFAP both in native and recombinant forms *in vitro*. Med. Microbiol. Immunol. 197:361-8.
13. Wang GR, **Shi S**, Gao C, Zhang BY, Tian C, Dong CF, Zhou RM, Li XL, Chen C, Han J, Dong XP. (2010) Changes of tau profiles in brains of the hamsters infected with scrapie strains 263 K or 139 A possibly associated with the alteration of phosphate kinases. BMC Infect Dis.
14. Li X, Dong C, **Shi S**, Wang G, Li Y, Wang X, Shi Q, Tian C, Zhou R, Gao C, Dong X. (2009) The octarepeat region of hamster PrP (PrP<sup>51-91</sup>) enhances the formation of microtubule and antagonize Cu(2+)-induced microtubule-disrupting activity. Acta Biochim Biophys Sin. 41: 927-37.
15. Shi XH, Han J, Zhang J, Shi Q, Chen JM, Xia SL, Xie ZQ, Shen XJ, Shan B, Lei YJ, **Shi S**, Zhou W, Zhang BY, Gao C, Liu YH, Song J, Guo YJ, Wang DX, Xu BL, Dong XP. (2010) Clinical, histopathological and genetic studies in a family with fatal familial insomnia. Infect Genet Evol 10: 292-7.
16. Wang X, Dong CF, Shi Q, **Shi S**, Wang GR, Lei YJ, Xu K, An R, Chen JM, Jiang HY, Tian C, Gao C, Zhao YJ, Han J, Dong XP. (2009) Cytosolic Prion Protein Induces Apoptosis via Mitochondrial Disruption Pathway in Human Neuronal SH-SY5Y Cells. BMB Rep 42:444-9.